Collective fish swimming in altered environment

Baptiste Lafoux

THÈSE DE DOCTORAT
D'UNIVERSITÉ PARIS CITÉ

Spécialité
Physique

École doctorale n°564
Physique en Île-de-France

Réalisée au **Laboratoire de Physique et Mécanique des Milieux Hétérogènes**

Sous la direction de
Benjamin Thiria et **Ramiro Godoy-Diana**

Présentée par

Baptiste Lafoux

pour obtenir le grade de
DOCTEUR D'UNIVERSITÉ PARIS CITÉ

Dynamiques de nage collective de poissons en environnement altéré

Collective fish swimming in altered environment

présentée et soutenue publiquement le
13 décembre 2023

Devant un jury composé de

Aurélie Dupont - Chargée de recherche	Université Grenoble Alpes	Rapportrice
Fernando Peruani - Professeur	CY Cergy Paris Université	Rapporteur
Agnese Seminara - Chargée de recherche	Université Côte d'Azur	Examinatrice
Olivier Dauchot - Directeur de recherche	ESPCI Paris - PSL	Examinateur
Guy Theraulaz - Directeur de recherche	Université Paul Sabatier	Invité
Benjamin Thiria - Professeur	Université Paris Cité	Directeur
Ramiro Godoy-Diana - Directeur de recherche	ESPCI Paris - PSL	Directeur

Université Paris Cité

Baptiste Lafoux: *Collective fish swimming in altered environments*, October 2023

SUPERVISORS
Benjamin Thiria
Ramiro Godoy-Diana

COLLECTIVE FISH SWIMMING IN ALTERED ENVIRONMENTS

BAPTISTE LAFOUX

À mes grands-parents
À Ibrahima "Diderot" Koné

FOREWORD

Coordinated motion of animals have always captivated the imagination of observers, poets, and scientists alike. Whether it is the graceful ballet of starlings, the precise social organization of ants, or the untamed power of a human crowd, there emerges a fundamental question: how can a collection of similar agents, each of which exhibiting rather straightforward actions when considered in isolation, give rise to intricate structures that manifest on temporal and spatial scales far beyond that of any single individual?

The present report focuses on schools of fish, as a framework for tackling the question of collective motion. In particular, its objective is to understand how collective patterns are altered when the environment in which fish move is disrupted; how factors such as illumination (Chapter 2), confinement (Chapter 3) or flow (Chapter 4) influence organisation within a group of fish. We have chosen an approach based on simplified and highly controlled laboratory experiments: they enable us to operate at a middle ground, without getting caught up either in the intricacies of the natural world, or in pure mathematical abstraction.

This document opens with an introductory chapter describing its background and context (Chapter 1), and closes with some conclusions and perspectives (Chapter 5). The appendices provide details of the experimental setup and additional informations (Appendix A and Appendix B). The reader is invited to progress linearly through the dissertation, although Chapter 4 can be understood independently of the two preceding.

CONTENTS

1

STATE OF THE ART AND CONTEXT

Et si je ne pus observer ni miralets, ni balistes, ni tétrodons, ni hippocampes, ni jouans, ni centrisques, ni blennies, ni surmulets, ni labres, ni éperlans, ni exocets, ni anchois, ni pagels, ni bogues, ni orphes, ni tous ces principaux représentants de l'ordre des pleuronectes, les limandes, les flez, les plies, les soles, les carrelets, communs à l'Atlantique et à la Méditerranée, il faut en accuser la vertigineuse vitesse qui emportait le Nautilus à travers ces eaux opulentes.

— *Vingt Mille Lieues sous les mers* - Chapitre VII (1869), Jules Verne

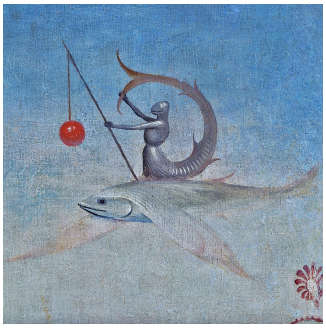

This introductory chapter aims to provide an overview of the scientific context in which this thesis is set. Firstly (Section 1.1), it addresses the topic of collective motion, providing a concise summary of the diverse approaches, models and challenges involved in this vast discipline. Section 1.2 outlines the questions related to fish assemblies (or schools) in particular. Section 1.3 is centred on the model organism used in this work, *Hemigrammus rhodostomus*. The final Section 1.4 details the contents of this manuscript and the objectives pursued in each chapter.

1.1 COLLECTIVE MOTION: AN OVERVIEW

Defining the notion of collective motion is in itself a challenge. As the founder of the discipline in its modern form, Tamas Vicsek nevertheless ventured to do so by providing the following proposition (Vicsek and Zafeiris, 2012): it is the study of displacement in a system consisting of many similar units (or individuals, or agents) interacting through simple "social" rules. These rules can exist in the physical space, or in a underlying network connecting the agents. One of the key characteristics of collective motions is that the behavior of an individual unit is predominantly controlled by the impact of the "others" — causing the unit to exhibit a significantly distinct behavior from what it would display if it was moving alone.

We can see immediately that this statement paves the way for many other questions : What are those rules? What does "many", or "similar" really mean? However, the first issue that we would like to address here is "is this really a problem for physicists?". The study of collective movements is indeed a highly interdisciplinary field, occupying experts in many different areas[1].

1.1.1 *Fields of study of collective motions*

BIOLOGICAL PERSPECTIVE Biology and zoology form the basis of research on collective motion. Scientists have traditionally approached this topic by studying the intriguing motions of animal populations. The flocks of migratory birds (Bajec and Heppner, 2009; Hemelrijk and Hildenbrandt, 2012), the organised movements of insects (Buhl et al., 2006; Dyson et al., 2015) and schools of fish (Parrish, Viscido, and Grünbaum, 2002; Shaw, 1962) are among the most studied systems by ethologists, who are interested in the behavior of animals in their natural environment. From a biological point of view, there is particular interest in the physiological nature of the interactions between individuals that lead to the emergence of synchronized motion at the scale of the group. Among numerous examples, the role of pheromones in the emergence of threads in ants, or the comparative role of vision, olfaction and the sensation of flow in fish (Partridge and Pitcher, 1980; Pavlov and Kasumyan, 2000), are questions that still interest biologists of collective motion.

1 Moussaïd (2010) offers an interesting review of what the study of collective movements borrows from different branches of research on his Youtube Channel Fouloscopie (2019). His video has inspired the following summary.

These are macroscopic groups, but the biological dimension of collective motion can also focus on microscopic systems. The emergence of coordinated patterns can be seen in the movements of bacteria (Gachelin et al., 2014; Zhang et al., 2010) and cells (Arboleda-Estudillo et al., 2010; Poujade et al., 2007), among many others: the interactions underlying these motions are quite different from those among animals, and these specific features are a growing source of interest for experimental biologists (Méhes and Vicsek, 2014).

HUMAN CROWDS AND SOCIAL SCIENCES Among animals capable of collective motions, there is one that particularly fascinates scientists: the human being, whose behaviour can be studied through the prism of crowds. Crowds can display a very wide range of collective structures, which in some cases are reminiscent of the motion of animal groups. For example, it is common to see phenomena of social contagion in panic movements (Lorenz et al., 2011). Here, as in the case of ethology studies, the mathematical representation of interactions between pedestrians makes it possible to understand well-known everyday phenomena, such as the formation of two-way lanes in the street (Moussaïd, Helbing, and Theraulaz, 2011). Interestingly, in certain species of ants or termites, the two-way traffic that is established between the nest and a food source is similarly organised in queues (Couzin and Franks, 2003). A better understanding of interactions within human groups and the study and modelling of crowd dynamics can provide quantitative guidelines for crowd management in order to better anticipate deadly disasters.

PHYSICS PERSPECTIVE Although it is not strictly speaking a case of collective motion, the synergy between physics and collective behaviour can be traced back to the Ising model (Ising, 1925). This is a statistical physics model used to characterise the behaviour of a set of two-state particles interacting with each other. This model shows that a set of simple rules can give rise to complex behaviour when the number of interacting particles becomes large. Subsequently, inspired by the innovative work of Vicsek et al. (1995) and his numerical model of self-propelled particles, physicists have become increasingly involved in the study of collective motion since the 1990s. In the Vicsek model, simple alignment interactions between self-propelled particles lead to the emergence of organised collective motions, reminiscent of the movements of groups of animals. Whether or not these collective states appear depends on the parameters of the simulation, in particular the density of the agents and the intrinsic noise level of their orientation. Based on these numerical observations, a great deal of research over the last three decades has attempted to use the well-known equations governing the behaviour

of matter, whether granular, liquid or solid, to model collective motion. This analogy has its limitations, since there are many differences between the interactions in a group on the move and those between the constituent elements of matter, which we will describe in more detail later. However, this approach allows to use the methodology and powerful mathematical tools offered by physics to study the emergence of order. It has proved effective in many cases, including for instance the study of transitions between collective states (Buhl et al., 2006).

It is interesting to note that this abundant interdisciplinarity allows the emergence of shared ideas between these major fields, which then feed off each other. One example is the faster-is-slower effect: paradoxically, it is quicker for a group of people to evacuate a room if they do not hurry. This counter-intuitive observation can be explained by a physical analogy with granular flows, which create jams when they pass through restrictions too quickly. One solution, already commonly used for evacuating groups of animals (particularly sheep) is to place an obstacle near the exit, which prevents clogging during emergency exit (Garcimartín et al., 2014; Helbing, Farkas, and Vicsek, 2000).

1.1.2 *Statistical physics models for collective motion*

By implementing the statistical physics approach to study collective motions, the objective is to use scaling, modelling, and simulation tools to reach a general understanding of collective motion at all scales. To achieve this, various hypotheses must be formulated to set up the theoretical framework of what we call a system in collective motion. Drawing inspiration from Vicsek and Zafeiris (2012), we can suggest the subsequent guidelines for the component units of such a system:

- They are capable of self-propulsion through internal energy consumption or energy input from their environment
- They can change direction by interacting with neighbors
- There is some inherent noise associated with their motion

Starting from these basic hypothesis, numerous numerical models have been developed with the shared aim of providing a universal description of collective behaviour, using a minimal set of simple equations of motion. We present in the following paragraphs the three models that are most commonly used today.

THE VICSEK MODEL This model (or class of models) was a precursor in the study of collective motion. It describes the motion of an individual i, with a constant

velocity norm v_0. Each individual has an absolute orientation $\theta_i(t)$ and absolute position $\mathbf{r}_i(t)$ at time t. The motion is set by the following two equations describing the evolution of orientation and position between each time step δt in two dimensions:

$$\theta_i(t+\delta t) = \langle \theta_j(t) \rangle_{|r_i(t)-r_j(t)|<R} + \eta_i(t) \tag{1.1}$$

$$\mathbf{r}_i(t+\delta t) = \mathbf{r}_i(t) + v_0 \delta t \mathbf{e}_{\theta_i} \tag{1.2}$$

with $\mathbf{e}_{\theta_i} = (\cos\theta_i, \sin\theta_i)$. These equations can be interpreted as follows. Equation 1.1 expresses the fact that each individual aligns its orientation with the average orientation of the neighbors within a distance R. The orientation is also subject to a noise η_i (drawn from an uniform distribution in the original model). From Equation 1.2, individuals simply move to their new position according to their updated orientation. This model exhibits a very rich phenomenology, with a transition between a disorganised state and a large-scale organised motion, depending on density (agents per unit area) and noise parameters. The model has been extensively studied (see for example CHATÉ et al., 2008) and remains one of the standards in the field.

CUCKER-SMALE MODEL The Cucker-Smale model has been first proposed in 2007 (CUCKER and SMALE, 2007). The main difference between the Vicsek model and the Cucker-Smale model is that in the latter, the velocity vector of the agents can vary instead of only their orientation. The model postulates that every agent updates its velocity by averaging the opposite of the relative velocities of its neighbors within a given distance. For a group of N agents, the velocity of the i-th agent $\mathbf{v}_i$ can be expressed by the following equation:

$$\mathbf{v}_i(t+\delta t) = \mathbf{v}_i(t) + \frac{\delta t}{N} \sum_j K_{ij}(\mathbf{v}_j(t) - \mathbf{v}_i(t)) \tag{1.3}$$

Figure 1.1a illustrates this mechanism. Here K_{ij} is an adjacency matrix that quantifies the way the agents influence each other. In the original paper, it is assumed that the intensity of the interaction decreases with the relative distance between agent, namely:

$$K_{ij} = \frac{1}{(1+|\mathbf{r}_i - \mathbf{r}_j|^2)^\beta} \tag{1.4}$$

AOKI-COUZIN MODEL In the Aoki-Couzin model (Aoki, 1982; Couzin et al., 2002), the initial version of which was developed in the early 1980s by the Japanese biologist Ichiro Aoki, individual behavioral rules of avoidance, alignment and attraction reproduce certain characteristics of collective animal movements. The field of view of each agent is divided in three circular zones that correspond to those rules (see Figure 1.1b). Like in the Vicsek model, the velocity of the agents is a constant. At each time step, the orientation is updated according to the following rules, where $\tilde{\cdot}$ denotes the normalization operator ($\tilde{\mathbf{x}} = \mathbf{x}/|\mathbf{x}|$) :

- Individuals move away from the n_r neighbors that are located in their zone of repulsion (zor):

$$\theta_{\mathrm{r},i}(t+\delta t) = -\sum_{j\neq i}^{n_\mathrm{r}} \widetilde{\mathbf{r}_i - \mathbf{r}_j} \tag{1.5}$$

- Individuals align with the n_o neighbors that are located in their zone of orientation (zoo):

$$\theta_{\mathrm{o},i}(t+\delta t) = \sum_{j\neq i}^{n_\mathrm{o}} \widetilde{\mathbf{v}}_j \tag{1.6}$$

- Individuals move toward the n_a neighbors that are located in their zone of attraction (zoa): :

$$\theta_{\mathrm{a},i}(t+\delta t) = \sum_{j\neq i}^{n_\mathrm{a}} \widetilde{\mathbf{r}_i - \mathbf{r}_j} \tag{1.7}$$

The orientation is the sum of these three contributions: $\theta = \theta_{\mathrm{r},i} + \theta_{\mathrm{o},i} + \theta_{\mathrm{a},i}$. A blind angle can be implemented, to prescribe a zone in which their is no social interaction (see Figure 1.1b).

NEIGHBORS AND INTERACTION DISTANCE The most intuitive approach is to suppose that interactions depend on the metric distance between individuals, but experimental evidence tends to show that the topological distance is the one chosen by the animals during collective movements. Early research on starling flocks showed that each animal interacts with a fixed number of nearest neighbours (6 or 7), rather than all neighbours within a given range (Ballerini et al., 2008). This subtlety is crucial in numerical simulations of collective behaviour. Simulations have, for instance, demonstrated that interacting with one or two neighbours is sufficient to generate complex collective behaviour (Wang et al., 2022). Another option, which is a variation of the topological distance, is to consider that the

influential neighbours are those located in the adjacent cells of the Voronoi diagram (the set of points in the plane closer to the focal individual than to any other individual, see Figure 1.1c) (CALOVI et al., 2015; FILELLA et al., 2018).

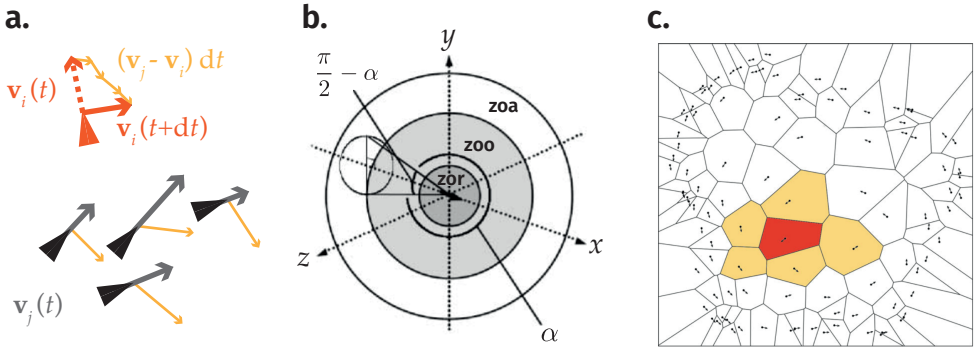

Figure 1.1: **a.** Visual illustration of the governing equation of the Cucker-Smale model **b.** Zones of repulsion (zor), orientation (zoo) and alignment (zoa) around a fish, and representation of its blind angle α in COUZIN et al. (2002). **c.** A school of numerical fish from CALOVI et al. (2014). The areas depicted here are the cells of the Voronoi diagram whose seeds are the fish positions, *i.e* the are the set sets of points that are closest to a given fish than to any other. In red is the cell of the focal fish and in orange those of its Voronoi neighbours (individuals located in cells sharing a border with the focal fish's cell).

DIFFERENCE BETWEEN STATISTICAL PHYSICS AND COLLECTIVE MOTION PHYSICS

Even if a large number of strong analogies can be established between collective phenomena as described by standard statistical physics and those existing in biological systems, there are essential differences between these two approaches.

The first of these is the non-symmetry of interactions between agents. In a classical Newtonian system, two particles interact with each other symmetrically: the force of A on B is the opposite of the force of B on A. Clearly, this assertion cannot be true in the case of social forces, since there is no a priori reason why an individual A should influence B in the same way as B influences A. These interactions may depend, for example, on the relative orientation of the two agents, their velocity vectors, or even internal rules. Another way of considering this difference is to observe that the system's energy is not conserved during "collisions", i.e. interactions between agents leading to a change in their state (typically, their velocity). Here again, this dissipation of energy contradicts the classical principles adopted by statistical physics.

Phase transitions in statistical physics are only described rigorously in the theoretical limit of a number of particles that tends towards infinity. This hypothesis is relatively well validated for many microscopic physical systems, where the number of interacting particles is typically 10^{23}. In contrast, biological systems in general are made up of between 10 and 1000 individuals, with rare extreme cases of 10^6 individuals (Romanczuk and Daniels, 2022). This finite size hinders the classical theoretical approach and challenges the classical predictions of statistical physics, for instance on the behaviour of the system close to criticality.

Another consequence of the 'small' size of biological systems is the role of the boundaries of the domain in which the system evolves. Necessarily, this role sometimes becomes significant in systems with a limited number of interacting agents, whereas statistical physics generally considers it to be negligible.

1.1.3 *State transitions*

We have seen that one of the characteristics of collective motion is the emergence of particular group structures during movement, in other words, a large-scale organisation of the displacement of individuals. These structures, also known as collective states, are characterised by synchronised motion at the scale of the group, which appear through self-organisation: they are not caused by the decisions of each individual, but rather by short-range interactions between a large number of agents.

Self-organisation This emergence of collective patterns organised at the level of a group on the move is generally referred to as self-organisation. It is indeed interesting to note that this synchronisation is not generally due to the presence of a "leader" to guide collective decisions (Romanczuk and Daniels, 2022; Shaw, 1978). Furthermore, even if there are examples of groups of animals with one or more dominant individuals in highly hierarchical societies (such as bees or ants), behaviour at group level is never determined solely by the decisions of the leader (Bonabeau et al., 1997; Wild et al., 2021).

Classification of collective motions In nature, collective states present highly different geometries. They can exist in one dimension (like the lines of ants or humans), two dimensions (in the motions of flocks of sheep or swarms of marching locusts for example) or be three-dimensional (in most schools of fish or

swarms of birds or insects). Research in collective motion usually classifies these states into three main categories:

- **swarming states**: these are essentially disorganised collective motions, where the speeds and directions of movement of each agent are uncorrelated or only weakly correlated. The members of the group move in all directions in space without favouring a common direction.
- **polarised states**: the whole group moves in a coordinated fashion in a preferred direction. The speeds are aligned and the centre of mass of the group thus moves at a speed close to the average speed of the individuals.
- **milling states**: in such structures, individuals move by rotating around the group's centre of mass, in two or three dimensions of space. The speed of each individual is perpendicular to the vector linking its position and the centre of mass.

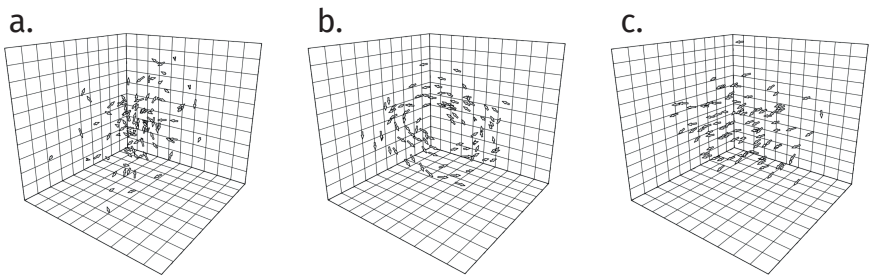

Figure 1.2: The three typical collective states exhibited by the Couzin numerical model in 3D, for 100 self-propelled particles (from Couzin et al. (2002)). a. swarming, b. milling, c. polarized state.

These structures exist in systems in their natural state, in laboratory experiments or can be observed in numerical simulations. Figure 1.2 shows some examples from a numerical simulations. More complex collective movements exist in nature (rotation around a point other than the centre of mass, for example), but these categories provide a basis for describing the geometry of the organisation of collective movements, since all structures can be considered linear combinations of these three main states.

PHASE TRANSITION A phase transition is the process during which a large number of elements constituting a system - often atoms - change their organisation

on a global scale, as a result of a variation of an external physical parameter. A well-known example is the phase transition from a disorganised liquid state to an organised solid state when temperature decreases. By observing the similarity between the collective states described above and the phases of matter as described by statistical physics (gas, solid, liquid), it has been suggested that a parallel can be drawn between transitions between collective states and phase transitions in thermodynamical systems (Becco et al., 2006; Bialek et al., 2012; Giannini and Puckett, 2020).

In fact, it is possible to observe transitions between collective states when the external parameters of a group of moving individuals are modified. These changes in the environment can alter the nature or intensity of interactions between individuals: for example, variations in luminosity change the ability of individuals to see their neighbours. Another type of parameter that can trigger changes the in collective state are environmental constraints, such as the presence of obstacles or predators in the case of groups of animals (Klamser and Romanczuk, 2021; Ryer and Olla, 1998). In some cases, intrinsic noise in the orientation of the individual can also lead to the emergence of collective motion or to transitions between states (Biancalani, Dyson, and McKane, 2014; Calovi et al., 2015; Jhawar et al., 2020). Finally, the number of individuals in the group is knows to trigger collective state transitions in both live (Tunstrøm et al., 2013) and numerically simulated systems (Cambuí and Rosas, 2012). Even if, as mentioned in Section 1.1.2, there are considerable differences between thermodynamic systems and groups in collective motion, this parallel opens interesting avenues for studying complex biological systems by providing powerful pre-existing theoretical tools.

1.2 FISH SCHOOLING

1.2.1 *Advantages of schooling*

Fish provide a typical example of self-organization, with a natural tendency to form ordered groups, known as swarms or schools (Shaw, 1978). More than 50% of fish species exhibit schooling motion during their lifetime (Pitcher, Greenberg, and Haraway, 1998), and this type of behaviour is a strategy that has been adopted for millions of years, as shown by fossils found in Arizona (see Mizumoto, Miyata, and Pratt, 2019 and Figure 1.3). Collective behaviour in fish provides many benefits and plays an important role in their behavioural ecology. Here we propose a summary of the main identified advantages of schooling.

Figure 1.3: Fossil of a school of 259 juvenile fish (*Erismatopterus levatus*) found in the Green River Formation (Arizona, USA). The fossil is dated to around 50 million years ago.

MIGRATION In nature, fish populations migrate over hundreds or thousands of kilometers to find suitable foraging areas, spawning sites or mating partners. Migration is often directly linked to collective behaviour. For instance, shoals of migrating fish spreading on 5 to 10 kilometers and containing millions of individuals have been monitored in the northern Atlantic by ocean acoustic waveguide remote sensing (OAWRS), a technique allowing for instantaneous sampling of fish density over large areas (Makris et al., 2006). In the context of migration, schooling is believed to increase the accuracy of the route chosen by the group. This hypothesis is based on evidence indicating that a larger number of individuals in a group contribute to improved assessment of gradients of environmental cues, such as salinity or water temperature (Berdahl et al., 2013; Pitcher, 1986).

FORAGING Collective foraging strategies are used by both grazing and predatory fish spieces. Experiments on zebrafish have shown that interactions in groups of 3 to 6 individuals enable near-optimal foraging strategies by combining individual and social information (i.e. information shared within the group) (Harpaz and Schneidman, 2020). Conversely, certain predators also employ collective strategies to hunt, utilizing specific formations to separate sub-groups from the shoal of prey (Schmitt and Strand, 1982). Cooperative hunting strategies are observed in both closely-knit and usually solitary species, such as sailfish (Herbert-Read et al., 2016).

PREDATOR AVOIDANCE During encounters with predators, schooling behavior has many advantages for prey fish. This is one of the most commonly cited benefits of schooling behaviour. Firstly, studies have shown that group vigilance is increased when schools are larger. For example, larger schools of minnows detect an artificial predator more quicly than smaller schools (Magurran, Oulton, and Pitcher, 1985). This highlights a form of division of labour, where certain individuals specialize while others can focus on other tasks, such as foraging (Ward

et al., 2011). On the other hand, the transfer of information is improved by the high level of synchronisation in the school. This allows for an assessment of the danger and a rapid reaction speed without each fish needing to confirm independently the nature or distance of the predator (Magurran, 1990). In the case of direct attacks on schools of gobies, individuals benefiting from social information respond even more quickly than individuals exposed directly to the threat (Webb, 1980). Finally, schooling can be an evasion strategy in the event of an attack. The capture rate is lower for a group of fish operating close to a critical point, i.e. in a state where multiple behavioural patterns coexist (Klamser and Romanczuk, 2021). Numerical studies show that a collective strategy is more effective than a selfish escape (Zheng et al., 2005).

ENERGY SAVING Energetic advantages of schooling have been first hypothesized by Breder (1965) and subsequently explored through a theoretical model developed by Weihs (1973) for a two-dimensional school of fish that swim synchronously in a single plane (see Figure 1.4 a.). He argued that it is advantageous for a fish to position itself behind and midway between two adjacent fish, in a diamond-like configuration. In this location, the follower could take advantage of the vortices in the Von Karman street produced by its predecessors. In an infinite school, individual are also believed to profit from a channeling effect induced by their lateral neighbors (Fish, 1999; Liao, 2007). However, this swimming configuration is rarely observed in schools of fish in their natural habitat (Partridge and Pitcher, 1979). Experimentally, two metrics are employed to evaluate the energy consumption of fish. Firstly, assessing the quantity of dissolved oxygen in the water offers a direct evaluation of the metabolic rate, i.e. the energy consummed during swimming. Additionally, the frequency of tail beats serves as an indicator of the 'transport cost'. By combining these two measurements in a swimming tunnel (flume), a study on grey mullets showed that the fish saved energy by swimming in a group rather than alone, regardless of their position in a shoal of eight individuals (Marras et al., 2015). An experiment on *Hemigrammus rhodostomus* swimming in a tunnel, based on kinematic measurements, revealed that the fish chose a phalanx structure (aligned perpendicular to the flow, see Figure 1.4 b.) when the incident velocity was high, in contrast to the Weihs model (Ashraf et al., 2017). In this position, the tail beats are synchronised, suggesting that vortex phase matching can be an energy-saving mechanism (see also Figure 1.4 c. and Li et al., 2020). A recent numerical study of a minimal two-fish school suggests that this structure may results from a trade-off between the classically considered wake vortex har-

vesting strategy and the avoidance of zones that are energetically detrimental (Li et al., 2019).

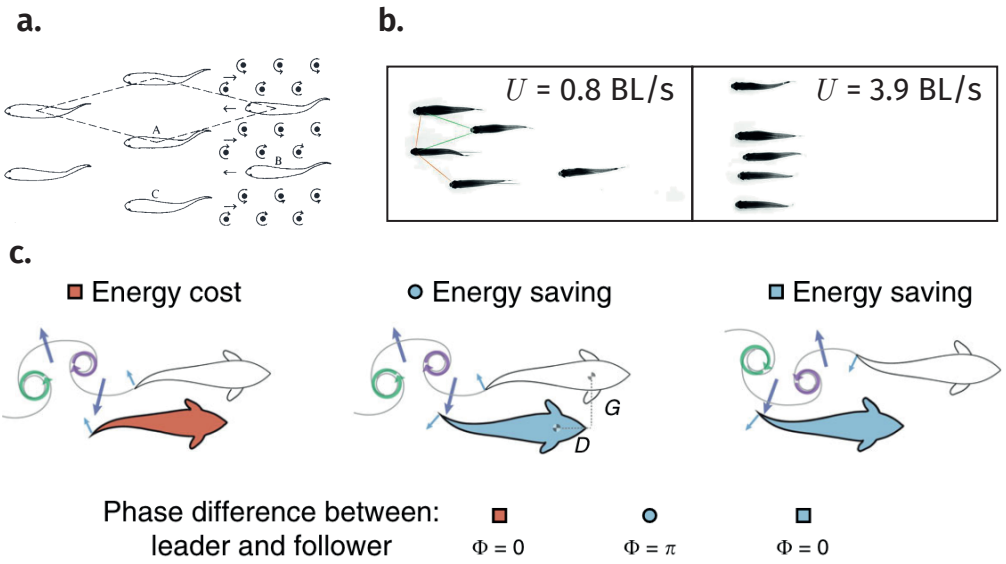

Figure 1.4: **a.** Original schematic from Weihs (1973) showing the diamond-shaped school. Black dots represent the vortices in the wake of predecessor fish, with their rotation direction. **b.** Experimental snapshots from Ashraf et al. (2017) showing diamond-shaped schooling at low speed and the phalanx structure at high speed. The fish swim in a water flume with a flow from left to right. Flow speeds are given in fish Body Length (BL) per second. **c.** Spatial configuration of a pair of fish illustrating the voretx phase matching strategy: energy saving is possible if the two fish synchronize their tailbeat in-phase or out-of-phase, depending on the streamwise distance between the individual (Li et al., 2020).

1.2.2 *Sensory mechanisms of fish*

To interact with their neighbours or their environment in order to swim in schools, fish need to collect information about their surroundings. In particular, knowledge of the distance and relative orientation of neighbours is an essential component in the spontaneous emergence of collective movements (Calovi et al., 2018). This kinematic input enables a given fish to synchronise with its neighbours and is transmitted within the group from close to close. The sum of this information, known as social information, enables each individual to make decisions without necessarily having access to all the environmental cues available. To acquire this information, fish use all the sensory mechanisms that enable them to interact with

their environment. We report here a summary of these sensory systems, inspired by that proposed by Pavlov and Kasumyan (2000).

VISION In fish, vision functions in a similar way to terrestrial mammals or birds: most fish species have a retina with cones and rods that enable them to see colours and, in some cases, to be sensitive to ultraviolet light (Bone and Moore, 2008). the visual sensory modality is crucial in regulating the behavior schooling of fish, and plays a central role in maintaining school cohesion (Pavlov and Kasumyan, 2000). Several experiments have consistently demonstrated the significance of the visual system in schooling behavior. Early studies, such as those by Parr in the 1920s (Parr, 1927, 1931), revealed that fish with impaired vision were unable to participate in schools, and their ability to school was restored when their vision was recovered. Similar findings were observed in various fish species, emphasizing the critical role of the visual system in schooling (Breder, 1959). Fish spiecies exhibiting stronger schooling tendencies were more inclined to respond to their mirror image (Spooner, 1931). One specificity of the vision sensory mechanism is that it allows individuals to access information about their conspecifics in a quasi-instantaneous manner, which makes it preponderant in the realisation of rapid group movements with a high degree of synchronicity.

HYDRODYNAMIC SENSING Most aquatic fish and amphibians have the ability to sense fluctuations of velocity and pressure in the water surrounding them. This sensory ability is mediated by a sensory system (or organ) called the lateral line. This is a line, continuous or not, that generally runs from the animal's nose to its tail along its lateral sides. It is made up of neuromasts (10-100 μm), which are a collection of up to 150 hair cells set in motion by the flow of water around the fish's body (Bleckmann and Zelick, 2009). It is this movement, thanks to the mechano-electrical properties of the hair cells, that produces the sensory signal integrated by the animal's central nervous system. These neuromasts can either be located on the surface of the animals skin, in which case they are known as superficial neuromasts (SN), or at the end of a fluid-filled

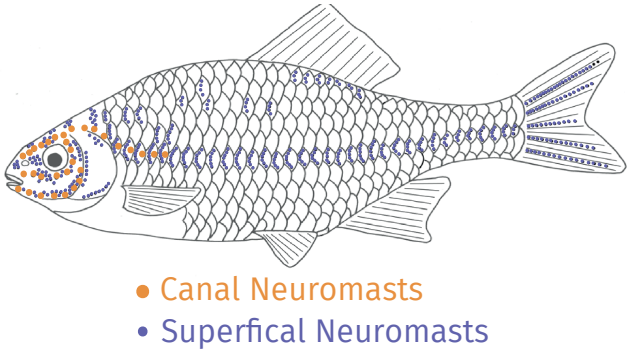

Figure 1.5: Lateral line system of the bitterling *Rhodeus sericeus amarus*. (adapted from Bleckmann and Zelick (2009))

channel (canal Neuromat, CN). Although the lateral line may not be the primary mechanism for the emergence of schooling behaviour, there is experimental evidence that this non-visual system still plays an important role. For instance, in *Abramis brama* (Pitcher and Partridge, 1979), even after removal of the lateral line by mechanical manipulation, modified individuals maintain group behaviour by following healthy individuals. The respective roles of the lateral line and vision in the formation and stability of collective structures in fish remains an open question and is the subject of numerous recent studies (Kulpa, Bak-Coleman, and Coombs, 2015; McKee, 2020; Mekdara et al., 2018; Van Trump and McHenry, 2013).

OTHER SENSORY MECHANISMS Fish have a rich range of sensory abilities that are not limited to the two modalities mentioned above and that enable them to interact with their conspecifics, other animals or their environment. For example, many fish possess a sense of hearing, even though poorly developped (Popper et al., 2019). Olfactory capacities are also important: one example is *Schreckstoff*, which is a chemical alarm signal released passively when an individual suffers an injury. This signal results, for example, in a change in the distances between nearest neighbours in shoals of minnows (Krause, 1993). However, these sensory capacities are either too limited (hearing) or transport information too slowly (olfaction) to be considered as the main interactions enabling collective movement in fish.

1.3 A MODEL FISH FOR COLLECTIVE STUDIES: *HEMIGRAMMUS RHODOSTOMUS*

1.3.1 *Biology overview*

Rummy-nose tetras or red-nose tetra (*Hemigrammus rhodostomus*) is a species member of the Characinae, the main familly of characiform fish; it has been first described by Ahl in 1924 (Burgess, 2004). The species is originating from Brazil and Venezuela, in the lower Amazon basin, in Pará State and Orinoco River, and reaches a standard length of 3 to 5 cm. The red-nose tetra has a silvery body with a bright red spot that extends across the head to the gills (see Figure 1.6). *Hemigrammus rhodostomus* are commonly found in river sections where obstacles such as decaying leaf litter on the riverbed or present, giving it a dark appearance known as "blackwaters". These fish tend to swim in the middle or lower part of the water column (Küchler, Miekeley, and Forsberg, 2000). They also show a preference for

darker areas, likely due to their eggs and fry being sensitive to light. These fish are a very common species found in the aquarium trade due to their bright colors and because they are small, easy to maintain and breed in an artificial environment.

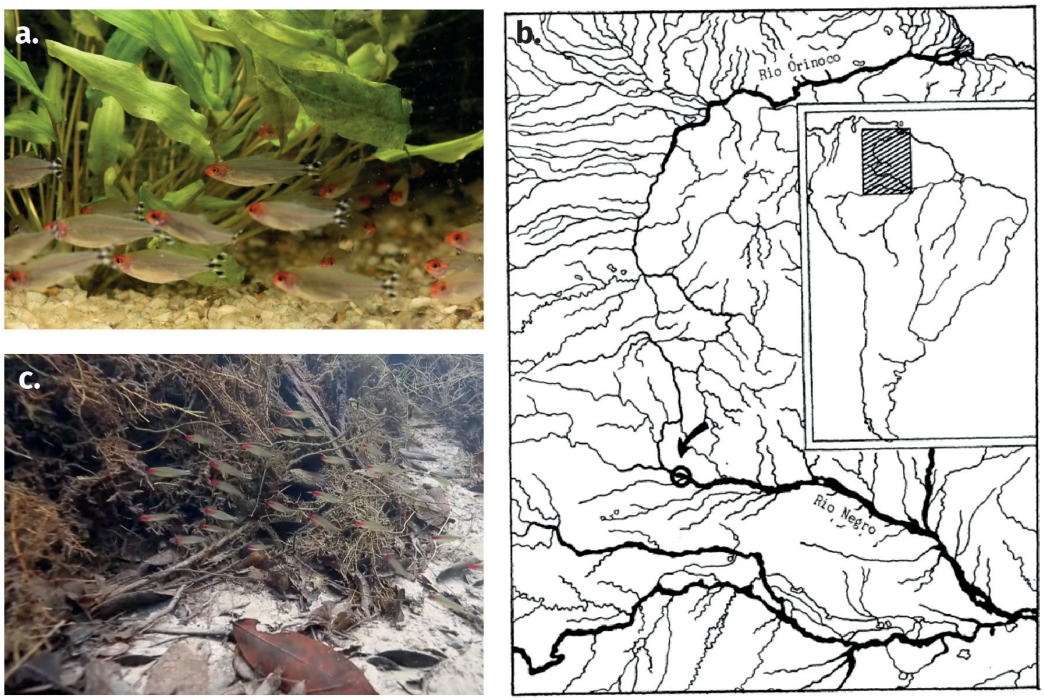

Figure 1.6: **a.** *Hemigrammus rhodostomus* schooling in the lab **b.** Region of origin of *Hemigrammus rhodostomus* in the lower Amazon basin (from Böhlke, 1955). **c.** *Hemigrammus rhodostomus* schooling in their natural habitat (credit: Below Water YouTube channel)

The rummy-nose tetra, in its natural habitat, exhibits a social and cohesive behavior, often forming groups known as schools. These schools can consist of anywhere from about 6 to more than 30 fish. Rummy-nose tetras groups are known to be able to navigate in noisy environments. Interestingly, when introduced to the same environment, different species of *Hemigrammus* will shoal together. Due to their gregarious nature and propensity to form schools, *Hemigrammus rhodostomus* (or its close relative *Hemigrammus bleheri*) has been extensively used in collective motion experimental studies since approximately 2010 (Faucher et al., 2010; Giannini and Puckett, 2020; Jiang et al., 2017; Mekdara et al., 2018). Additionally, their preference for darker areas has made them valuable subjects for experimental studies on collective phototaxis, involving movement in response to light gradients (Berdahl et al., 2013; Puckett, Pokhrel, and Giannini, 2018).

1.3.2 *Swimming gait characteristics*

Hemigrammus rhodostomus is a fish that swim using the body and caudal fin (BCF) propulsion, according to the canonical classification by Breder, 1926. When they swim, individuals of the species always alternate between propulsive "kicks" and gliding phases: this is called the burst-and-coast swimming. This gait involves a two-step process wherein the fish first execute an active phase, generating propulsive force and chosing a new orientation, and then transitions into an inertial, passive phase, gliding or "coasting" in its previous direction without muscular effort. An exemple of the resulting trajectory is provided in Figure 1.7. This type of intermittent locomotion is ubiquitous in Nature at all scales, ranging from bacteria's run-and-tumble (Berg, 2004; Tailleur and Cates, 2008) to birds flap-glide gait (Tobalske, 2001) and is even investigated in order to optimize marine propulsion (Aurégan, 2023). It can be observed as a permanent part of an animal's locomotion, as an exploration strategy, or during short periods of time -typically during high-speed prey escapes- (Domenici, 2001; Domenici and Blake, 1997).

The biomechanics community has extensively studied burst and coast over the past decades (Blake, 1983; Drucker, 1996; Fish, Fegely, and Xanthopoulos, 1991; Li et al., 2021; Paoletti and Mahadevan, 2014; Videler and Weihs, 1982), often focusing on its association with optimizing locomotion costs. Starting with early research by Weihs, 1973, these studies have primarily explored the effects of burst-and-coast on swimming efficiency compared to continuous undulatory mechanisms (Ashraf, Van Wassenbergh, and Verma, 2020).

This type of intermittent locomotion also plays an important role in the species' ability to achieve collective displacement. Indeed, like many other organisms, *Hemigrammus rhodostomus* rely on vision among other mechanisms to estimate the kinematics of neighbours in a group (Collignon, Séguret, and Halloy, 2016; Hemmings, 1966; Pavlov and Kasumyan, 2000; Pita et al., 2015). This visual interaction is essential for the emergence of synchronisation and coordination in groups. However, time is needed for an individual to examine its visual field and, in the presence of motion, the likelihood of detecting critical information in a complex and evolving scene decreases. The ability to slow down from time to time enhances attention to the visual field and thus the ability to process the positions and directions of neighbours (Kramer and McLaughlin, 2001).

Another important feature of intermittent locomotion, which plays a key role in collective movement, is the reduction of perturbations of the sensory system. For example, for fish that use hydrodynamic sensing (measurement of flow around the

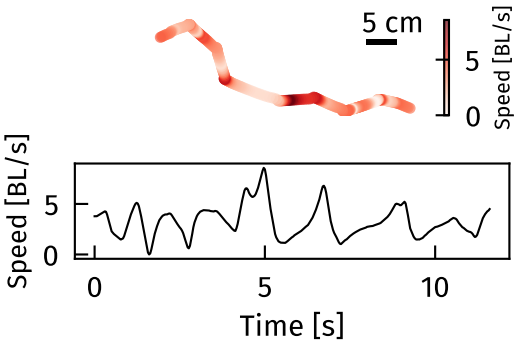

Figure 1.7: **top.** Typical discrete trajectory of a *Hemigrammus rhodostomus* swimming alone in a large tank for a few seconds. The color represents the instantaneous speed, given here in Body Length -BL- per second (1 BL $\sim$ 3.2 cm). The acquisition rate is 30 images per second. Note the sharp changes in direction followed by strong acceleration. **bottom.** Speed of the fish with respect to time, clearly displaying the bursts (acceleration) and coasts (deceleration after a peak of speed).

body) to achieve schooling (Faucher et al., 2010), stopping periods can be beneficial to evaluate surrounding obstacles or neighbours (Kramer and McLaughlin, 2001).

1.3.3 *Breeding and experimental facilities*

To carry out collective motion experiments, adult rummy-nose tetra, with a body length (BL) of 3.92 $\pm$ 0.42 cm were purchased from a professional supplier, EFV group. The fish were kept in a 120L tank on a 14:10 hour photoperiod (day/night), similar to that existing at their latitudes of origin. The maximum occupancy density in the breeding tank was maintained under 0.5 fish/L. The water temperature was set at 27°C ($\pm$ 1°C) and fish were fed *ad libitum* with fine pellets from an automated feeder once a day, at a fixed time in the morning. This fish handling protocol complies with the European Directive 2010/63/EU for the protection of animals used for scientific purposes, as certified by the ESPCI Paris Ethics Committee.

1.4 OBJECTIVE AND OUTLINE OF THIS WORK

Collective movement studies tend to adopt two distinct approaches. The first, usually specific to biologists, is the field study, or study in an environment as close as possible to the actual living conditions of the organism. While this approach has

the advantage of being based on experimental "truth", it is nonetheless extremely difficult to propose quantitative measurements. In particular, tracking the positions of individuals within a group evolving in its natural environment poses obvious difficulties and requires a significant concentration of people and resources (Ballerini et al., 2008; Gómez-Nava et al., 2023). Furthermore, the conclusions reached by such studies are by definition difficult to generalize, since they concern a specific species and environment. Finally, the random nature of biological systems results in significant measurement noise, making field results sometimes difficult to interpret objectively. At the other end of the spectrum of collective motion studies are those carried out by physicists, generally adopting a numerical or theoretical approach. The advantages of these methods are numerous: for example, it is much simpler to obtain conclusions that can be generalized a priori to many species, or even to all types of collective motion. In a numerical or analytical model, it is possible to modify "environmental conditions" *ad infinitum*, and even to modify the nature of interactions between individuals.

The overall approach of this study is to propose an intermediate vision of collective motion, at the intersection of the two frameworks presented above. Our simple, controlled experimental setups enable us to study the nature, stability and emergence of collective motions and behaviors in a model organism. In this way, we place ourselves neither completely in the complexity of nature, nor in pure abstraction.

The main objective of this work is to improve our understanding of the collective motion of fish swimming under perturbed conditions, through direct experimental measurements and modelling. Our aim is to characterise the effects of environmental parameters on the interactions within a school of fish and their impact on the resulting collective states. We investigated two collective swimming scenarios: free swimming (without any flow) and forced swimming (with an incoming flow).

Chapter 2 examines the role of ambient light on the collective behaviour of free-swimming fish, using experiments on large schools of 50 individuals. It is shown that light controls the emergence of collective behaviour and the transition between polarisation and milling, depending on the intensity to which the group is exposed.

In Chapter 3 the issue of confinement is addressed, again in free swimming situation. The school is seen as a bistable system, where polarisation and milling states coexist. We observe experimentally that confinement, measured in fish per square meter, controls the transition from polarization to milling, and more particularly the statistics of the transition times between these two states.

Chapter 4 looks at the behaviour of rheotaxis (swimming against the current), comparing fish swimming alone and pairs of fish, considered as the minimum constitutive cell of a school. The experiments of forced swimming are carried out for different flow speeds and either in a lit or totally dark envrionnement. We show that

REFERENCES

Aoki, I. (1982). "A Simulation Study on the Schooling Mechanism in Fish." *Nippon Suisan Gakkaishi*. DOI: 10.2331/suisan.48.1081 (cit. on p. 6).

Arboleda-Estudillo, Y., M. Krieg, J. Stühmer, N. A. Licata, D. J. Muller, and C.-P. Heisenberg (2010). "Movement Directionality in Collective Migration of Germ Layer Progenitors." en. *Current Biology*. DOI: 10.1016/j.cub.2009.11.036 (cit. on p. 3).

Ashraf, I., H. Bradshaw, T.-T. T. Ha, J. Halloy, R. Godoy-Diana, and B. Thiria (2017). "Simple Phalanx Pattern Leads to Energy Saving in Cohesive Fish Schooling." *Proceedings of the National Academy of Sciences*. DOI: 10.1073/pnas.1706503114 (cit. on pp. 12, 13).

Ashraf, I., S. Van Wassenbergh, and S. Verma (2020). "Burst-and-Coast Swimming Is Not Always Energetically Beneficial in Fish (Hemigrammus Bleheri)." *Bioinspiration & biomimetics*. DOI: 10.1088/1748-3190/abb521 (cit. on p. 17).

Aurégan, T. (2023). "Bioinspired Propeller Propulsion : Reconfiguration and Intermittency." en. PhD thesis. Université Paris Cité (cit. on p. 17).

Bajec, I. L. and F. H. Heppner (2009). "Organized Flight in Birds." en. *Animal Behaviour*. DOI: 10.1016/j.anbehav.2009.07.007 (cit. on p. 2).

Ballerini, M et al. (2008). "Interaction Ruling Animal Collective Behavior Depends on Topological Rather than Metric Distance: Evidence from a Field Study." *Proceedings of the National Academy of Sciences of the United States of America*. DOI: 10.1073/pnas.0711437105 (cit. on pp. 6, 19).

Becco, C., N. Vandewalle, J. Delcourt, and P. Poncin (2006). "Experimental Evidences of a Structural and Dynamical Transition in Fish School." *Physica A: Statistical Mechanics and its Applications*. DOI: 10.1016/j.physa.2005.11.041 (cit. on p. 10).

Berdahl, A., C. J. Torney, C. C. Ioannou, J. J. Faria, and I. D. Couzin (2013). "Emergent Sensing of Complex Environments by Mobile Animal Groups." *Science*. DOI: 10.1126/science.1225883 (cit. on pp. 11, 16).

Berg, H. C. (2004). *E. Coli in Motion*. Springer (cit. on p. 17).

Bialek, W., A. Cavagna, I. Giardina, T. Mora, E. Silvestri, M. Viale, and A. M. Walczak (2012). "Statistical Mechanics for Natural Flocks of Birds." *Proceedings of the National Academy of Sciences of the United States of America*. DOI: 10.1073/pnas.1118633109 (cit. on p. 10).

Biancalani, T., L. Dyson, and A. J. McKane (2014). "Noise-Induced Bistable States and Their Mean Switching Time in Foraging Colonies." en. *Physical Review Letters*. DOI: 10.1103/PhysRevLett.112.038101 (cit. on p. 10).

Blake, R. W. (1983). *Fish Locomotion*. CUP Archive (cit. on p. 17).

Bleckmann, H. and R. Zelick (2009). "Lateral Line System of Fish." en. *Integrative Zoology*. DOI: 10.1111/j.1749-4877.2008.00131.x (cit. on p. 14).

Böhlke, J. (1955). "Studies on Fishes of the Family Characidae: No. 8. The Description of a New Hemigrammus from the Rio Negro of Brazil." *Transactions of the Kansas Academy of Science (1903-)*. DOI: 10.2307/3625765 (cit. on p. 16).

Bonabeau, E., G. Theraulaz, J.-L. Deneubourg, S. Aron, and S. Camazine (1997). "Self-Organization in Social Insects." *Trends in ecology & evolution*. DOI: 10.1016/S0169-5347(97)01048-3 (cit. on p. 8).

Bone, Q. and R. Moore (2008). *Biology of Fishes*. Taylor & Francis (cit. on p. 14).

Breder, C. M. (1959). "Studies on Social Groupings in Fishes." *Bulletin of the American Museum of Natural History* (cit. on p. 14).

— (1965). "Vortices and Fish Schools." *Zoologica* (cit. on p. 12).

Breder, C. M. (1926). "The Locomotion of Fishes." *Zoologica* (cit. on p. 17).

Buhl, J., D. J. T. Sumpter, I. D. Couzin, J. J. Hale, E. Despland, E. R. Miller, and S. J. Simpson (2006). "From Disorder to Order in Marching Locusts." en. *Science*. DOI: 10.1126/science.1125142 (cit. on pp. 2, 4).

Burgess, W. E. (2004). "CHECK LIST OF THE FRESHWATER FISHES OF SOUTH AND CENTRAL AMERICA." *Copeia*. DOI: 10.1643/0T-04-142 (cit. on p. 15).

Calovi, D. S., A. Litchinko, V. Lecheval, U. Lopez, A. Pérez Escudero, H. Chaté, C. Sire, and G. Theraulaz (2018). "Disentangling and Modeling Interactions in Fish with Burst-and-Coast Swimming Reveal Distinct Alignment and Attraction Behaviors." *PLoS Computational Biology*. DOI: 10.1371/journal.pcbi.1005933 (cit. on p. 13).

Calovi, D. S., U. Lopez, S. Ngo, C. Sire, H. Chaté, and G. Theraulaz (2014). "Swarming, Schooling, Milling: Phase Diagram of a Data-Driven Fish School Model." *New Journal of Physics*. DOI: 10.1088/1367-2630/16/1/015026 (cit. on p. 7).

Calovi, D. S., U. Lopez, P. Schuhmacher, H. Chaté, C. Sire, and G. Theraulaz (2015). "Collective Response to Perturbations in a Data-Driven Fish School Model." *Journal of the Royal Society Interface*. DOI: 10.1098/rsif.2014.1362 (cit. on pp. 7, 10).

Cambuí, D. S. and A. Rosas (2012). "Density Induced Transition in a School of Fish." en. *Physica A: Statistical Mechanics and its Applications*. DOI: 10.1016/j.physa.2012.03.009 (cit. on p. 10).

Chaté, H., F. Ginelli, G. Grégoire, F. Peruani, and F. Raynaud (2008). "Modeling Collective Motion: Variations on the Vicsek Model." *European Physical Journal B*. DOI: 10.1140/epjb/e2008-00275-9 (cit. on p. 5).

Collignon, B., A. Séguret, and J. Halloy (2016). "A Stochastic Vision-Based Model Inspired by Zebrafish Collective Behaviour in Heterogeneous Environments." *Royal Society Open Science*. DOI: 10.1098/rsos.150473 (cit. on p. 17).

Couzin, I. D. and N. R. Franks (2003). "Self-Organized Lane Formation and Optimized Traffic Flow in Army Ants." eng. *Proceedings. Biological Sciences*. DOI: 10.1098/rspb.2002.2210 (cit. on p. 3).

Couzin, I. D., J. Krause, R. James, G. D. Ruxton, and N. R. Franks (2002). "Collective Memory and Spatial Sorting in Animal Groups." *Journal of Theoretical Biology*. doi: 10.1006/jtbi.2002.3065 (cit. on pp. 6, 7, 9).

Cucker, F. and S. Smale (2007). "Emergent Behavior in Flocks." *IEEE Transactions on Automatic Control*. doi: 10.1109/TAC.2007.895842 (cit. on p. 5).

Domenici, P. (2001). "The Scaling of Locomotor Performance in Predator–Prey Encounters: From Fish to Killer Whales." *Comparative Biochemistry and Physiology Part A: Molecular & Integrative Physiology*. doi: 10.1016/S1095-6433(01)00465-2 (cit. on p. 17).

Domenici, P. and R. W. Blake (1997). "The Kinematics and Performance of Fish Fast-Start Swimming." *Journal of Experimental Biology*. doi: 10.1242/jeb.200.8.1165 (cit. on p. 17).

Drucker, E. G. (1996). "The Use of Gait Transition Speed in Comparative Studies of Fish Locomotion." *American Zoologist*. doi: 10.1093/icb/36.6.555 (cit. on p. 17).

Dyson, L., C. A. Yates, J. Buhl, and A. J. McKane (2015). "Onset of Collective Motion in Locusts Is Captured by a Minimal Model." en. *Physical Review E*. doi: 10.1103/PhysRevE.92.052708 (cit. on p. 2).

Faucher, K., E. Parmentier, C. Becco, N. Vandewalle, and P. Vandewalle (2010). "Fish Lateral System Is Required for Accurate Control of Shoaling Behaviour." *Animal Behaviour*. doi: 10.1016/j.anbehav.2009.12.020 (cit. on pp. 16, 18).

Filella, A., F. Nadal, C. Sire, E. Kanso, and C. Eloy (2018). "Model of Collective Fish Behavior with Hydrodynamic Interactions." *Physical Review Letters*. doi: 10.1103/PhysRevLett.120.198101 (cit. on p. 7).

Fish, FE (1999). "Energetics of Swimming and Flying in Formation." *Comments on Theoretical Biology* (cit. on p. 12).

Fish, F. E., J. F. Fegely, and C. J. Xanthopoulos (1991). "Burst-and-Coast Swimming in Schooling Fish (Notemigonus Crysoleucas) with Implications for Energy Economy." *Comparative Biochemistry and Physiology Part A: Physiology*. doi: 10.1016/0300-9629(91)90382-M (cit. on p. 17).

Fouloscopie (2019). *Ethologie, Physique et Psychologie Des Foules | EPISODE #3* (cit. on p. 2).

Gachelin, J., A. Rousselet, A. Lindner, and E. Clement (2014). "Collective Motion in an Active Suspension of Escherichia Coli Bacteria." en. *New Journal of Physics*. doi: 10.1088/1367-2630/16/2/025003 (cit. on p. 3).

Garcimartín, A., I. Zuriguel, J. M. Pastor, C. Martín-Gómez, and D. R. Parisi (2014). "Experimental Evidence of the "Faster Is Slower" Effect." *Transportation Research Procedia*. The Conference on Pedestrian and Evacuation Dynamics 2014 (PED 2014), 22-24 October 2014, Delft, The Netherlands. doi: 10.1016/j.trpro.2014.09.085 (cit. on p. 4).

Giannini, J. A. and J. G. Puckett (2020). "Testing a Thermodynamic Approach to Collective Animal Behavior in Laboratory Fish Schools." *Physical Review E*. doi: 10.1103/physreve.101.062605 (cit. on pp. 10, 16).

Gómez-Nava, L., R. T. Lange, P. P. Klamser, J. Lukas, L. Arias-Rodriguez, D. Bierbach, J. Krause, H. Sprekeler, and P. Romanczuk (2023). "Fish Shoals Resemble a Stochastic Excitable System Driven by Environmental Perturbations." en. *Nature Physics*. DOI: 10.1038/s41567-022-01916-1 (cit. on p. 19).

Harpaz, R. and E. Schneidman (2020). "Social Interactions Drive Efficient Foraging and Income Equality in Groups of Fish." en. *eLife*. DOI: 10.7554/eLife.56196 (cit. on p. 11).

Helbing, D., I. Farkas, and T. Vicsek (2000). "Simulating Dynamical Features of Escape Panic." en. *Nature*. DOI: 10.1038/35035023 (cit. on p. 4).

Hemelrijk, C. K. and H. Hildenbrandt (2012). "Schools of Fish and Flocks of Birds: Their Shape and Internal Structure by Self-Organization." *Interface Focus*. DOI: 10.1098/rsfs.2012.0025 (cit. on p. 2).

Hemmings, CC (1966). "Olfaction and Vision in Fish Schooling." *Journal of experimental biology*. DOI: 10.1242/jeb.45.3.449 (cit. on p. 17).

Herbert-Read, J. E., P. Romanczuk, S. Krause, D. Strömbom, P. Couillaud, P. Domenici, R. H. Kurvers, S. Marras, J. F. Steffensen, and A. D. Wilson (2016). "Proto-Cooperation: Group Hunting Sailfish Improve Hunting Success by Alternating Attacks on Grouping Prey." *Proceedings of the Royal Society B: Biological Sciences* (cit. on p. 11).

Ising, E. (1925). "Beitrag Zur Theorie Des Ferromagnetismus." *Zeitschrift für Physik*. DOI: 10.1007/BF02980577 (cit. on p. 3).

Jhawar, J., R. G. Morris, U. R. Amith-Kumar, M. Danny Raj, T. Rogers, H. Rajendran, and V. Guttal (2020). "Noise-Induced Schooling of Fish." *Nature Physics*. DOI: 10.1038/s41567-020-0787-y (cit. on p. 10).

Jiang, L., L. Giuggioli, A. Perna, R. Escobedo, V. Lecheval, C. Sire, Z. Han, and G. Theraulaz (2017). *Identifying Influential Neighbors in Animal Flocking*. DOI: 10.1371/journal.pcbi.1005822 (cit. on p. 16).

Klamser, P. P. and P. Romanczuk (2021). "Collective Predator Evasion: Putting the Criticality Hypothesis to the Test." *PLoS Computational Biology*. DOI: 10.1371/journal.pcbi.1008832 (cit. on pp. 10, 12).

Kramer, D. L. and R. L. McLaughlin (2001). "The Behavioral Ecology of Intermittent Locomotion." *American Zoologist* (cit. on pp. 17, 18).

Krause, J. (1993). "The Effect of'Schreckstoff'on the Shoaling Behaviour of the Minnow: A Test of Hamilton's Selfish Herd Theory." *Animal Behaviour*. DOI: 10.1006/anbe.1993.1119 (cit. on p. 15).

Küchler, I. L., N. Miekeley, and B. R. Forsberg (2000). "A Contribution to the Chemical Characterization of Rivers in the Rio Negro Basin, Brazil." en. *Journal of the Brazilian Chemical Society*. DOI: 10.1590/S0103-50532000000300015 (cit. on p. 15).

Kulpa, M., J. Bak-Coleman, and S. Coombs (2015). "The Lateral Line Is Necessary for Blind Cavefish Rheotaxis in Non-Uniform Flow." en. *Journal of Experimental Biology*. DOI: 10.1242/jeb.119537 (cit. on p. 15).

Li, G., I. Ashraf, B. François, D. Kolomenskiy, F. Lechenault, R. Godoy-Diana, and B. Thiria (2021). "Burst-and-Coast Swimmers Optimize Gait by Adapting Unique Intrinsic Cycle." *Communications Biology*. doi: 10.1038/s42003-020-01521-z (cit. on p. 17).

Li, G., D. Kolomenskiy, H. Liu, B. Thiria, and R. Godoy-Diana (2019). "On the Energetics and Stability of a Minimal Fish School." *PLoS ONE*. doi: 10.1371/journal.pone.0215265 (cit. on p. 13).

Li, L., M. Nagy, J. M. Graving, J. Bak-Coleman, G. Xie, and I. D. Couzin (2020). "Vortex Phase Matching as a Strategy for Schooling in Robots and in Fish." *Nature Communications*. doi: 10.1038/s41467-020-19086-0 (cit. on pp. 12, 13).

Liao, J. C. (2007). "A Review of Fish Swimming Mechanics and Behaviour in Altered Flows." *Philosophical Transactions of the Royal Society B: Biological Sciences*. doi: 10.1098/rstb.2007.2082 (cit. on p. 12).

Lorenz, J., H. Rauhut, F. Schweitzer, and D. Helbing (2011). "How Social Influence Can Undermine the Wisdom of Crowd Effect." *Proceedings of the National Academy of Sciences*. doi: 10.1073/pnas.1008636108 (cit. on p. 3).

Magurran, A. E., W. J. Oulton, and T. J. Pitcher (1985). "Vigilant Behaviour and Shoal Size in Minnows." en. *Zeitschrift für Tierpsychologie*. doi: 10.1111/j.1439-0310.1985.tb01386.x (cit. on p. 11).

Magurran, A. E. (1990). "The Adaptive Significance of Schooling as an Anti-Predator Defence in Fish." *Annales Zoologici Fennici* (cit. on p. 12).

Makris, N. C., P. Ratilal, D. T. Symonds, S. Jagannathan, S. Lee, and R. W. Nero (2006). "Fish Population and Behavior Revealed by Instantaneous Continental Shelf-Scale Imaging." *Science*. doi: 10.1126/science.1121756 (cit. on p. 11).

Marras, S., S. S. Killen, J. Lindström, D. J. McKenzie, J. F. Steffensen, and P. Domenici (2015). "Fish Swimming in Schools Save Energy Regardless of Their Spatial Position." *Behavioral Ecology and Sociobiology*. doi: 10.1007/s00265-014-1834-4 (cit. on p. 12).

McKee, A. A. (2020). "Sensing as It Relates to Behavior in Fishes." en. PhD thesis. UC Irvine (cit. on p. 15).

Méhes, E. and T. Vicsek (2014). "Collective Motion of Cells: From Experiments to Models." *Integrative Biology*. doi: 10.1039/c4ib00115j (cit. on p. 3).

Mekdara, P. J., M. A. Schwalbe, L. L. Coughlin, and E. D. Tytell (2018). "The Effects of Lateral Line Ablation and Regeneration in Schooling Giant Danios." *Journal of Experimental Biology*. doi: 10.1242/jeb.175166 (cit. on pp. 15, 16).

Mizumoto, N., S. Miyata, and S. C. Pratt (2019). "Inferring Collective Behaviour from a Fossilized Fish Shoal." *Proceedings of the Royal Society B: Biological Sciences*. doi: 10.1098/rspb.2019.0891 (cit. on p. 10).

Moussaïd, M. (2010). "Etude Expérimentale et Modélisation Des Déplacements Collectifs de Piétons." PhD thesis (cit. on p. 2).

Moussaïd, M., D. Helbing, and G. Theraulaz (2011). "How Simple Rules Determine Pedestrian Behavior and Crowd Disasters." *Proceedings of the National Academy of Sciences*. doi: 10.1073/pnas.1016507108 (cit. on p. 3).

Paoletti, P and L. Mahadevan (2014). "Intermittent Locomotion as an Optimal Control Strategy." *Proceedings of the Royal Society A: Mathematical, Physical and Engineering Sciences*. doi: 10.1098/rspa.2013.0535 (cit. on p. 17).

Parr, A. E. (1927). "A Contribution to the Theoretical Analysis of the Schooling Behaviour of Fishes." *Occ Pap Bingham Oceanogr Colln* (cit. on p. 14).

— (1931). "Sex Dimorphism and Schooling Behavior among Fishes." *The American Naturalist*. doi: 10.1086/280359 (cit. on p. 14).

Parrish, J. K., S. V. Viscido, and D. Grünbaum (2002). "Self-Organized Fish Schools: An Examination of Emergent Properties." *Biological Bulletin*. doi: 10.2307/1543482 (cit. on p. 2).

Partridge, B. L. and T. J. Pitcher (1979). "Evidence against a Hydrodynamic Function for Fish Schools." *Nature*. doi: 10.1038/279418a0 (cit. on p. 12).

— (1980). "The Sensory Basis of Fish Schools: Relative Roles of Lateral Line and Vision." *Journal of Comparative Physiology A*. doi: 10.1007/BF00657647 (cit. on p. 2).

Pavlov, D. S. and A. O. Kasumyan (2000). "Patterns and Mechanisms of Schooling Behavior in Fish: A Review." *Journal of Ichthyology* (cit. on pp. 2, 14, 17).

Pita, D., B. A. Moore, L. P. Tyrrell, and E. Fernández-Juricic (2015). "Vision in Two Cyprinid Fish: Implications for Collective Behavior." *PeerJ*. doi: 10.7717/peerj.1113 (cit. on p. 17).

Pitcher, T. J., G. Greenberg, and M. M Haraway (1998). "Shoaling and Schooling Behaviour in Fishes." *Comparative Psychology: A Handbook. New York: Garland* (cit. on p. 10).

Pitcher, T. J. (1986). "Functions of Shoaling Behaviour in Teleosts." *The Behaviour of Teleost Fishes*. doi: 10.1007/978-1-4684-8261-4_12 (cit. on p. 11).

Pitcher, T. J. and B. L. Partridge (1979). "Fish School Density and Volume." *Marine Biology* (cit. on p. 15).

Popper, A. N., A. D. Hawkins, O. Sand, and J. A. Sisneros (2019). "Examining the Hearing Abilities of Fishes." *The Journal of the Acoustical Society of America*. doi: 10.1121/1.5120185 (cit. on p. 15).

Poujade, M., E. Grasland-Mongrain, A. Hertzog, J. Jouanneau, P. Chavrier, B. Ladoux, A. Buguin, and P. Silberzan (2007). "Collective Migration of an Epithelial Monolayer in Response to a Model Wound." *Proceedings of the National Academy of Sciences*. doi: 10.1073/pnas.0705062104 (cit. on p. 3).

Puckett, J. G., A. R. Pokhrel, and J. A. Giannini (2018). "Collective Gradient Sensing in Fish Schools." *Scientific Reports*. doi: 10.1038/s41598-018-26037-9 (cit. on p. 16).

Romanczuk and Daniels (2022). "Phase Transitions and Criticality in the Collective Behavior of Animals – Self-organization and Biological Function." doi: 10.1142/9789811260438_0004 (cit. on p. 8).

Ryer, C. and B. Olla (1998). "Effect of Light on Juvenile Walleye Pollock Shoaling and Their Interaction with Predators." en. *Marine Ecology Progress Series*. doi: 10.3354/meps167215 (cit. on p. 10).

Schmitt, R. J. and S. W. Strand (1982). "Cooperative Foraging by Yellowtail, Seriola Lalandei (Carangidae), on Two Species of Fish Prey." *Copeia*. doi: 10.2307/1444679 (cit. on p. 11).

Shaw, E. (1962). "The Schooling of Fishes." *Scientific American*. doi: 10.1038/scientificamerican0662-128 (cit. on p. 2).

— (1978). "Schooling Fishes: The School, a Truly Egalitarian Form of Organization in Which All Members of the Group Are Alike in Influence, Offers Substantial Benefits to Its Participants." *American Scientist* (cit. on pp. 8, 10).

Spooner, G. M. (1931). "Some Observations on Schooling in Fish." *Journal of the Marine Biological Association of the United Kingdom*. doi: 10.1017/S0025315400050943 (cit. on p. 14).

Tailleur, J and ME Cates (2008). "Statistical Mechanics of Interacting Run-and-Tumble Bacteria." *Physical review letters*. doi: 10.1103/PhysRevLett.100.218103 (cit. on p. 17).

Tobalske, B. W. (2001). "Morphology, Velocity, and Intermittent Flight in Birds." *American Zoologist* (cit. on p. 17).

Tunstrøm, K., Y. Katz, C. C. Ioannou, C. Huepe, M. J. Lutz, and I. D. Couzin (2013). "Collective States, Multistability and Transitional Behavior in Schooling Fish." *PLoS Computational Biology*. doi: 10.1371/journal.pcbi.1002915 (cit. on p. 10).

Van Trump, W. J. and M. J. McHenry (2013). "The Lateral Line System Is Not Necessary for Rheotaxis in the Mexican Blind Cavefish (Astyanax Fasciatus)." *Integrative and Comparative Biology*. doi: 10.1093/icb/ict064 (cit. on p. 15).

Vicsek, T., A. Czirók, E. Ben-Jacob, I. Cohen, and O. Shochet (1995). "Novel Type of Phase Transition in a System of Self-Driven Particles." *Physical Review Letters*. doi: 10.1103/PhysRevLett.75.1226 (cit. on p. 3).

Vicsek, T. and A. Zafeiris (2012). "Collective Motion." *Physics Reports*. doi: 10.1016/j.physrep.2012.03.004 (cit. on pp. 2, 4).

Videler, J. J. and D. Weihs (1982). "Energetic Advantages of Burst-and-Coast Swimming of Fish at High Speeds." *The Journal of experimental biology*. doi: 10.1242/jeb.97.1.169 (cit. on p. 17).

Wang, W., R. Escobedo, S. Sanchez, C. Sire, Z. Han, and G. Theraulaz (2022). "The Impact of Individual Perceptual and Cognitive Factors on Collective States in a Data-Driven Fish School Model." en. *PLOS Computational Biology*. Ed. by N. Gov. doi: 10.1371/journal.pcbi.1009437 (cit. on p. 6).

Ward, A. J. W., J. E. Herbert-Read, D. J. T. Sumpter, and J. Krause (2011). "Fast and Accurate Decisions through Collective Vigilance in Fish Shoals." *Proceedings of the National Academy of Sciences*. doi: 10.1073/pnas.1007102108 (cit. on p. 11).

Webb, P. (1980). "Does Schooling Reduce Fast-Start Response Latencies in Teleosts?" en. *Comparative Biochemistry and Physiology Part A: Physiology*. doi: 10.1016/0300-9629(80)90230-3 (cit. on p. 12).

Weihs, D. (1973). "Hydromechanics of Fish Schooling." *Nature*. doi: 10.1038/241290a0 (cit. on pp. 12, 13, 17).

Wild, B., D. M. Dormagen, A. Zachariae, M. L. Smith, K. S. Traynor, D. Brockmann, I. D. Couzin, and T. Landgraf (2021). "Social Networks Predict the Life and Death of Honey Bees." *Nature communications*. doi: 10.1038/s41467-021-21212-5 (cit. on p. 8).

Zhang, H. P., A. Be'er, E.-L. Florin, and H. L. Swinney (2010). "Collective Motion and Density Fluctuations in Bacterial Colonies." en. *Proceedings of the National Academy of Sciences*. doi: 10.1073/pnas.1001651107 (cit. on p. 3).

Zheng, M., Y. Kashimori, O. Hoshino, K. Fujita, and T. Kambara (2005). "Behavior Pattern (Innate Action) of Individuals in Fish Schools Generating Efficient Collective Evasion from Predation." *Journal of Theoretical Biology*. doi: 10.1016/j.jtbi.2004.12.025 (cit. on p. 12).

2

ILLUMINANCE-TUNED COLLECTIVE MOTION

[...] and the melody of the song was the gray-green water and the little scuttling animals and the clouds of fish that flitted by and were gone.

— *The Pearl*, John Steinbeck (1947)

In this chapter, we report experimental investigations on the role of illumination on the collective dynamics of a large school (ca. 50 individuals) of *Hemigrammus rhodostomus*. The structure of the group is quantified while progressively altering the visual range of the fish through controlled cycles of ambient light intensity. We show that, at low light levels, the individuals within the group are unable to form a cohesive group, while at higher illuminance the degree of alignment of the school correlates with the light intensity. When increasing the illuminance, the school structure is successively characterized by a polarized state followed by a highly regular and stable rotational configuration (milling). Our study shows that vision is necessary to achieve cohesive collective motion for free swimming fish schools, while the short-range lateral line sensing is insufficient in this situation.

The results presented here have been published in Lafoux, B., Moscatelli, J., Godoy-Diana, R., & Thiria, B. (2023). Illuminance-tuned collective motion in fish. *Communications Biology*, 6(1), 585.

2.1 COLLECTIVE MOTION AND ILLUMINANCE

From a practical point of view, fish schooling involves, for each individual in a group, a knowledge of both position in space and kinematics of close neighbors (Calovi et al., 2018; Filella et al., 2018). In order to get this information, fish rely on vision, sensing of hydrodynamic disturbances and chemo-olfactory cues (Hemmings, 1966; Pavlov and Kasumyan, 2000). The role of each of these senses is not clearly elucidated today (Lopez et al., 2012), but it is generally accepted that vision and hydrodynamic sensing are the most predominant (Partridge and Pitcher, 1980; Pitcher and Partridge, 1979).

To sense hydrodynamic disturbances, fish use their lateral line system (Bleckmann, 2006). This ability has been suggested to be a factor in the formation of fish schools (Faucher et al., 2010). It is possible to impair the functioning of the lateral line of fish, resulting in a modified schooling behaviour (Faucher et al., 2010; Mekdara et al., 2021, 2018). However, this kind of invasive procedure may alter the behaviour of the fish in an unexpected manner.

Another way of quantifying the main sensory mechanisms for swimming interaction is to evaluate the role of vision. For instance, the ambient light level can modify the collective response of schooling fish in different situations (Giannini and Puckett, 2020; Puckett, Pokhrel, and Giannini, 2018). Recently, McKee, Soto, Chen, and McHenry (McKee et al., 2020) compared the role of the lateral line and vision in schooling fish. They suggested, based on experiments with 5 fish, that although both lateral line and vision are involved in the interaction between individuals, vision should be sufficient for schooling.

Previous studies (Partridge and Pitcher, 1980; Pitcher, Partridge, and Wardle, 1976) have also addressed the problem of vision with larger schools (20-30 fish), and showed that fish wearing opaque eye covers were able to maintain collective motion, using their lateral line system only. However, in these experiments, only one fish was blinded and placed back in a normal school, which limits the conclusions in terms of collective motion.

It has been found that fish reduce or completely suppress schooling behavior below a certain light threshold, that can vary across species (Ryer and Olla, 1998; Whitney, 1969). However, these experiments were conducted on 4 to 6 fish and therefore do not provide evidence for specific behaviors that may occur when increasing the number of individuals in the school. Furthermore, the question was tackled in terms of an abrupt limit between a cohesive and a non-cohesive state, without considering the effect of an increase in light level over a wide range once these thresholds are exceeded.

In this chapter, we go further in addressing the role of vision in the formation of large groups of fish, by altering the vision of all individuals at once. For that purpose, we chose to work with a species of highly cohesive fish, *Hemigrammus rhodostomus*, freely swimming in a large and shallow water tank. The available visual information is altered by modifying the illumination, either fixed in time or with two cycles of increasing then decreasing ramps. In addition to quantifying the role of vision, our study allows us to evaluate the role of the lateral line in a non-invasive way (typically, the response of fish in an experiment without light informs on their hydrodynamic sensing capabilities). Moreover, the

progressive nature of the light variation enables us to fully resolve the transition from non-cohesive to cohesive motion. In contrast with similar previous studies, we work on schools composed of a large number of individuals (around 50), allowing for a robust statistical analysis of the collective behavior parameters.

2.2 MATERIAL AND METHODS

2.2.1 *Free-swimming tank with controlled illumination*

The experimental setup consists of a large and shallow glass tank with a working area of 140 by 100 cm. This area is lit by visible light produced by a video projector (BenQ, 1920 $\times$ 1080 pixels) placed approximately 280 cm above the water surface (see Figure C.1). This device makes it simple to control the illumination in the tank, either fixed as a constant or varying over time: simple homogeneous images of different grey levels are projected, ranging from white (255, maximum light intensity) to black (0, no illumination). We measured with a luxmeter that the corresponding light intensity in the tank ranges from 0 to 900 lux ($\pm$3%). These levels of light intensity are comparable to those existing in the natural environment of origin of the tetra fish, as well as in their breeding conditions. For example, 900 lux corresponds to the illumination on a clear sunny day. In order to visualize the fish regardless of the visible light conditions, the tank was also back-lit from the bottom by a powerful custom-made infrared LED panel (200W, λ = 940 nm, LEDpoint). We ensured that the chosen infrared wavelength was large enough to be invisible to the fish (Carleton et al., 2020).

The entire setup is placed in an enclosure surrounded by opaque curtains, in order to avoid any light or visual disturbance due for example to the presence of the experimenter. The shallow water depth (h = 5 cm) induces swimming motion essentially in 2D without causing stress to the animals. The four side walls of the tank are covered with opaque, non-reflective plastic sheeting, to prevent visual interaction with the outside of the tank as much as possible, but also to limit the natural tendency of fish (like many other animals) to concentrate and move along the walls of the space allocated to them. Figure 2.2 shows a picture of the setup under a bright illumination.

2.2.2 *Data acquisition*

The fish schools are recorded over long periods of time (typically between 15 min and 1h), at a framerate ranging from 5 to 50 images per second, using a 4 Mpx Basler greyscale overhead camera. The frame rate is chosen to allow for long acquisition period without generating excessive data, while still being sufficient to accurately decompose the sometimes irregular movements of the fish, with their characteristic "burst and coast" motion (succession of propulsion and gliding phases): at 5 fps, a time step represents on average a displacement of 0.15 $\pm$ 0.02 BL. A filter letting only infrared light pass through (IR-

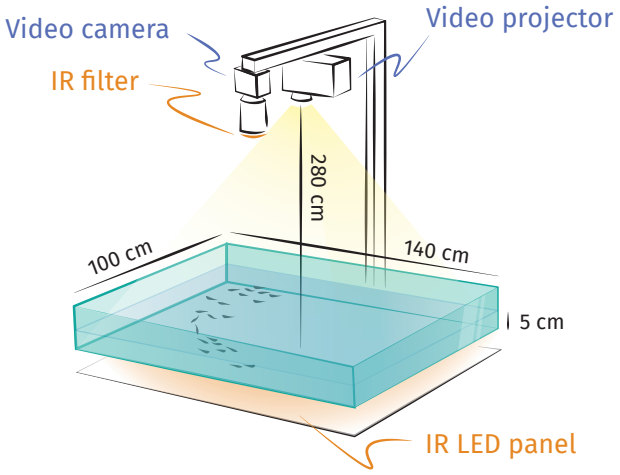

Figure 2.1: Groups of fish swim freely in a large, shallow tank where the light level can be adjusted using a video projector. The whole system is backlit by a custom-made infrared LED panel, and the fish's trajectories are filmed by a overhanging camera that records only infrared wavelengths at 5 frames per second (visible light is filtered so that its variations do not alter the lighting conditions of the videos).

transparent PMMA, thickness 3 mm, Lacrylic Shop) was placed in front of the camera lens to enhance the quality of the recorded images. A standard recording looks like the Figure 2.4, in which fish stand out clearly in dark against the brightly lit background.

2.2.3 *Experimental procedure*

In each experimental run, a group of fish was allowed to swim freely in the tank while the illuminance was varied. Two types of experiments were carried out :

- Experiments during which the light intensity was varied continuously over time
- Experiments with a constant illumination, as a control

For the continuous experiments, the light variation was slow enough that the experiment could be considered 'quasi-static'In this way, the fish were not stressed by sudden changes in light, and the structure of the school changed on a time scale shorter than the light variation. For each experiment, a group of fish is removed from the rearing tanks and placed in the swimming tank, which has previously been filled with clear water and brought to a temperature of 27°C using thermostats and pumps. The fish are initially kept in medium ambient light (the same as in the aquarium) for 15 minutes to allow them to acclimatize and to alleviate any stress caused by the change of environment. Both types of experiment lasted for 1 hour and were recorded at 5 frames per second.

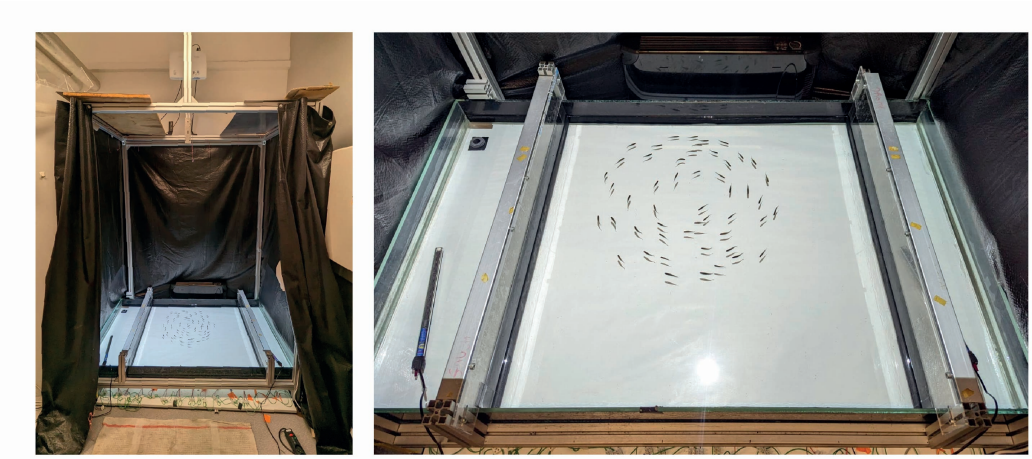

Figure 2.2: View of approximately 50 *Hemigrammus rhodostomus* in the free-swimming experimental setup. Here the swiming area is reduced to a 1:1 aspect ratio thanks to removable lateral walls.

Removable walls, covered with the same opaque material as the side walls, are placed on every side of the tank to create a uniform enclosure. Heaters are left on at the sides of the tank and an electric heater is started in the experimental enclosure. These precautions are taken to limit variations in water temperature to which the fish may be sensitive (Claireaux, Couturier, and Groison, 2006).

2.2.4 *Data processing*

The raw data obtained from the video recordings were processed according to the following pipeline, illustrated in Figure 2.3:

1. The background is first computed, as the maximum of 10 randomly selected frames in the total stack of 18 000 frames. The fish being darker than the background and moving constantly, this operation results in an image of the tank without any fish, that is then subtracted to every frame.
2. The resulting movie is processed with the python-based open-source tracking software FastTrack (Gallois and Candelier, 2021), that first binarizes the frames and filters the resulting pixel clusters according to their area, then reconstructs trajectories thanks to the Hungarian algorithm (Kuhn, 1955), with a dedicated algorithm to handle crossing events.
3. The data was finally exported and interpolated: missing positions were filled with a linear interpolation algorithm. The physical quantities we consider in our analysis are at the scale of the group, which means their are only weakly sensitive to potential switching of fish identities.

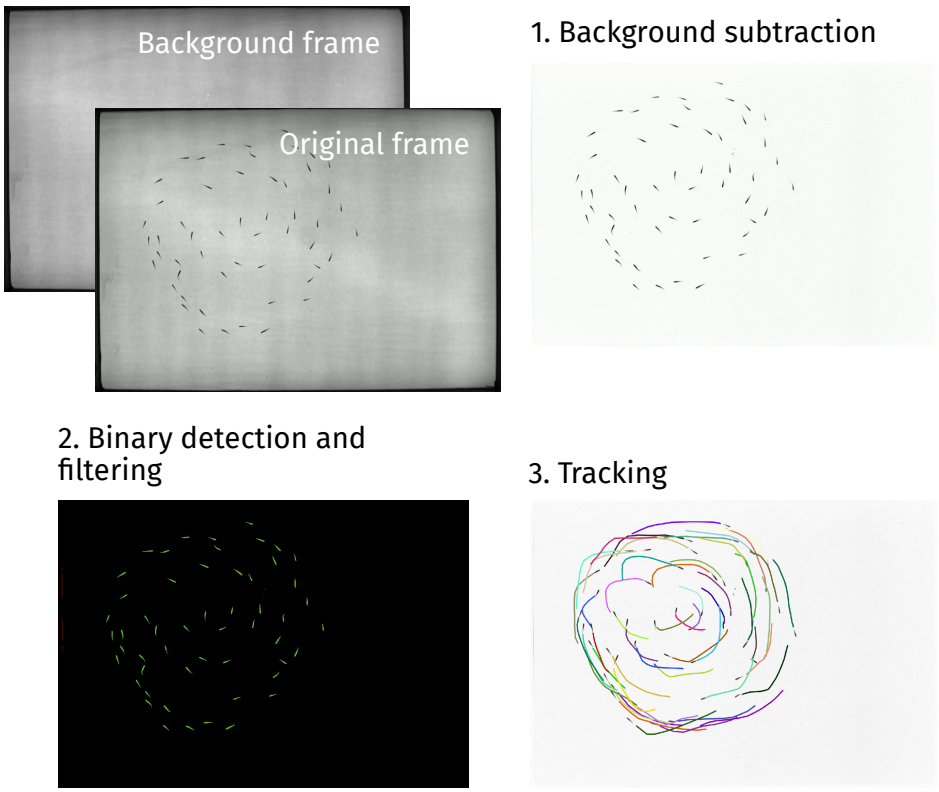

Figure 2.3: Data processing pipeline for a typical experiment on a school of 50 fish

2.3 ROLE OF ILLUMINATION ON THE STRUCTURE OF A FISH SCHOOL

2.3.1 *Physical quantities of interest*

In order to quantify the relationship between the organisation of fish schools and the level of illumination, we compute two physical quantities inspired by statistical order parameters that characterise the degree of order and cohesion within the group, in terms of alignment and rotation. The alignment (polarisation $\mathcal{P}$) and rotation (milling $\mathcal{M}$) order parameters are defined as follows:

$$\mathcal{P} = \left\langle \left| \frac{\mathbf{v}_i}{\|\mathbf{v}_i\|} \right| \right\rangle_{i \in 1..N} \tag{2.1}$$

$$\mathcal{M} = \left\langle \left| \frac{\mathbf{r}_i \times \mathbf{v}_i}{\|\mathbf{r}_i\| \|\mathbf{v}_i\|} \right| \right\rangle_{i \in 1..N,\ \|\mathbf{r}_i\| < L} \tag{2.2}$$

where $\mathbf{v}_i$ (resp. $\mathbf{r}_i$) is the instantaneous velocity vector (resp. the position with respect to the school instantaneous center of mass of the i-th fish) (see Figure 2.4). $\langle \cdot \rangle$ denotes the averaging operator over all fish in the school. These parameters both range from 0 to 1 and quantify how much the individuals within the school are aligned along the same direction ($\mathcal{P}$) or rotating around the center of mass of the group ($\mathcal{M}$). We use a slightly

modified expression of $\mathcal{M}$ to discard cases where the fish are spread over all the tank area and swim along the borders, artificially producing high values of the milling parameter $\mathcal{M}$, even when the group is not cohesive and no collective milling motion is observed in reality. $\mathcal{M}$ is thus defined in such a way that we only consider contributions from fish whose distance from the center of mass $\|\mathbf{r}_i\|$ is less than a threshold value L, chosen to be half the short length of the tank (L = 50 cm).

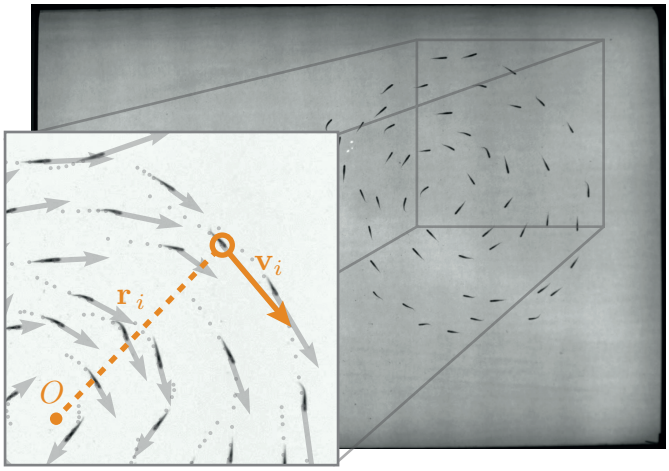

Figure 2.4: Snapshot of 53 fish swimming under an illuminance E of 810 lx. The group motion is captured at 5 fps with a high-resolution camera. From the videos, we reconstruct the individual trajectories of each animal (2D position and velocity at each time step). Zoom-in: 5 previous positions (1s-period, grey dots) and current velocity vectors from tracking data. For the i-th fish, we denote $\mathbf{v}_i$ the instantaneous velocity and $\mathbf{r}_i$ the position with respect to the school current center of mass O.

Additionally, we also quantify two intrinsic characteristic lengths of the fish school: the Nearest-Neighbour Distance (NN-D) and the Inter-Individual Distance (II-D). For a given individual, the NN-D is the distance to the closest fish and the II-D is the average distance to all the other fish. If we denote d_{ij} the distance between the i-th and the j-th fish:

$$\text{II-D} = \left\langle \langle d_{ij} \rangle_{j \in 1..N} \right\rangle_{i \in 1..N} \tag{2.3}$$

$$\text{NN-D} = \left\langle \min_{j \in 1..N} d_{ij} \right\rangle_{i \in 1..N} \tag{2.4}$$

2.3.2 *Experimental results for continuous light variations*

We perform a simple experiment in which groups of about $N = 50$ fish swim freely in the large tank while the illuminance E of their environment is controlled. Over the course of an hour, the ambient light is varied over a the full achievable range (from 0 lux to $E_{\max}$ = 900 lux). The light level is gradually increased and then decreased over a period of 15 minutes in a repeated pattern (2 up-down sequences, see the dashed line in Figure 2.5).

Variations of illumination strongly influence the values of the milling and polarization parameters (*Friedman test*, $\mathcal{M}$: $\chi^2(8) = 20.07$, $p = 1.21 \times 10^{-3}$, $\mathcal{P}$: $\chi^2(8) = 22.50$, $p = 4.2 \times 10^{-4}$). Sharp contrasts in behavior are observed, with 3 clearly identifiable phases. On Figure 2.5, we represent a time series of the values of $\mathcal{P}$, $\mathcal{M}$, and the normalized illuminance level $\bar{E} = E/E_{\max}$. When placed in very dark conditions ($\bar{E} < 0.05$), fish occupy the entire tank area and move without clear group organization: the average distance between individuals (II-D) is about 18 body lengths (BL) and fish are placed 1.6 ($\pm$0.2) BL away from their nearest neighbor (NN-D). Both the rotation parameter and the polarization are very low ($\mathcal{M} < 0.1$, $\mathcal{P} < 0.2$), showing the absence of significant cohesive motion (Figure 2.5.A). As the light gradually increases ($\bar{E} \in [0.05, 0.2]$), a short phase of strong alignment is visible (Figure 2.5.B and D), still with a weak but increasing value of the rotation parameter value. Further on, $\mathcal{M}$ keeps increasing linearly with illuminance, while the polarization drops ($\mathcal{P} < 0.2$) to eventually reach a plateau for $\bar{E} > 0.6$ where the behaviour in terms of both rotation and polarization does not change anymore. The school is highly structured, showing a very robust and stable rotational motion ($\mathcal{M} > 0.6$) with almost no interruption (Figure 2.5.C and E). The succession of these phases as a function of illumination is observed repeatedly with great statistical stability, whether the light is following an ascending or descending ramp.

Figure C.2 displays the averaged results obtained over 24 different cycles of the illuminance varying experiments (see Materials and Methods). The top graphic (Figure C.2.A) shows the evolutions of both $\mathcal{M}$ and $\mathcal{P}$ with respect to normalized illuminance level $\bar{E}$. The behaviour described for a single experiment in Figure 2.5 is found again in the average curves of Figure C.2.A: while the milling parameter increases monotonically with illuminance, the polarization parameter peaks rapidly and decreases afterwards to a plateau. Figure C.2.B shows the Nearest-Neighbor Distance (NN-D) and the Inter-Individual Distance (II-D) in Body Lengths (1 BL $\approx$ 3.9 cm). It is worth noting that in its averaged form, the II-D gives a good approximation of the characteristic size of the school. As can be observed, both characteristic lengths are large when there is no illumination: the average distance between the fish is about 20 BL and the distance to the nearest neighbor is 1.7 BL at the most. This case corresponds to a swarming behavior, without cohesion in the group, as confirmed by 2.5.A. The fish are distributed throughout the tank space and swim independently with respect to each other. These quantities rapidly decrease, showing that the individuals within the group get closer to each other as light intensity increases. II-D eventually saturates to a constant value above an illuminance threshold around E = 0.1. As can be observed, the average distance stabilizes around 8 BL, while the NN-D increases progressively before stabilizing around 1.5 BL after E = 0.5, which shows that, within a group of a given size (quantified by the II-D), a better quality of the visual information lets these highly cohesive fish reorganize, finding more regular patterns leaving more space between themselves and their nearest neighbor. It is known that fish can exhibit changes in their behavior in experiments over time (Shearer, 2000). We thus conducted an additional set of experiments at fixed illumination levels for one hour allowed to confirm the dynamical

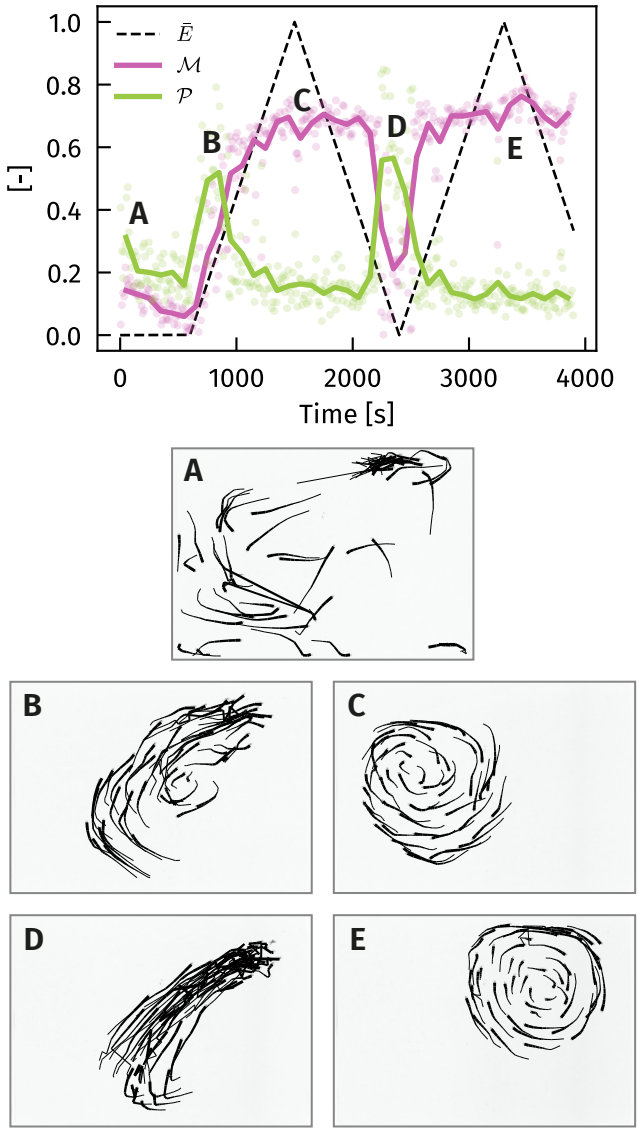

Figure 2.5: The structure of a fish school varies when the ambient light level is modified over time - **top** Time signal of the order parameters for a group of 53 fish experiencing a variation of normalized illuminance $\bar{E}$ (Dots : raw signal every 1 s. Lines : signal average with a rolling window of 60 s). $\mathcal{P}$ is the polarization parameter and $\mathcal{M}$ the milling parameter. After a 10 min adaptation period in the dark, the group is subjected to slow variations of illuminance, increasing then decreasing, between 0 $\pm$0.1 lx and $E_{\max}$ = 900 lx. **bottom** Trajectories snapshots at normalized illuminance $\bar{E}$ = {0, 0.22, 0.83, 0.10, 0.89} (black lines represent trajectories over the last 12 frames, *i.e* 2.4 s).

results and study the hypothesis that the variations of $\mathcal{M}$, $\mathcal{P}$, II-D, and NN-D observed here could be due to the time elapsed since the beginning of the experiment.

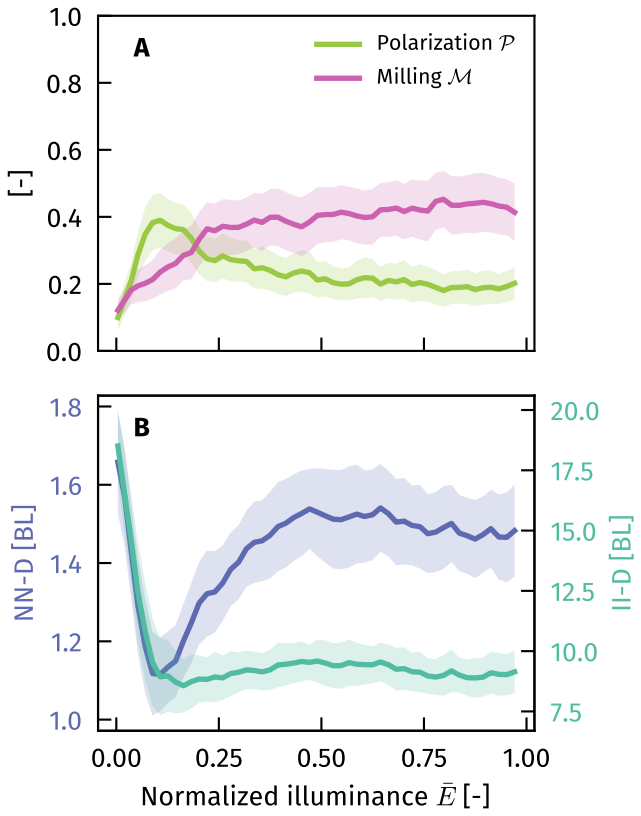

Figure 2.6: Fish school order parameters and distances with respect to light intensity. Solid lines show values averaged over every trials ($N = 6$) and every light ramps (either increasing or decreasing, 4 for each trial), which represents 24 replicates. (The shaded region is the 95% confidence interval for the mean). **A** Polarization and milling parameter. **B** Nearest-Neighbour Distance (NN-D) and Inter-Individual Distance (II-D) in Body Lengths. For a given individual, the NN-D is the distance to the closest fish and the II-D is the average distance to all the other fish. Values displayed here are averaged over all individuals in the school. (The scales for NN-D and II-D are different)

2.3.3 *Experimental results at fixed illuminance*

To control the accuracy of the results and evaluate any potential influence of the duration of the experiment on the behavior of the fish, another series of experiments was conducted with a consistent light intensity maintained for a prolonged period. In these experiments, approximately $N = 50$ fish swam for 60 minutes under a fixed light level, and their motion was recorded a rate of 5 frames per second, using the same experimental setup as for the continuous experiments. A total of 8 light levels were selected (with normalized intensities $\bar{E} = [0, 0.05, 0.10, 0.15, 0.3, 0.5, 0.75, 1]$), and 3 repetitions were performed for each level, in random order.

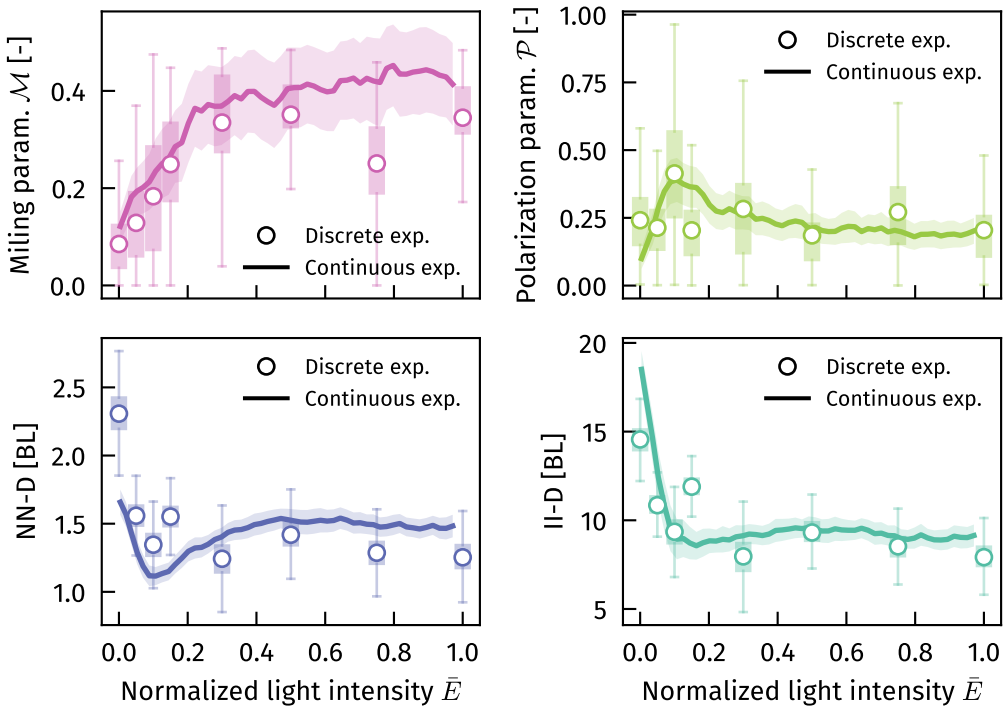

Figure 2.7: Comparison of experiments with continuous illuminance variation and experiments with constant illuminance for the milling and polarization parameters ($\mathcal{M}$ and $\mathcal{P}$, top), and NN-D and II-D (bottom). Continuous data are the same as in Figure C.2. The boxplots show the distribution over the replicates for each light level (dots represent the median of the distribution, and the error bars show the 95% confidence interval).

The results displayed in Figure 2.7 show a relatively good agreement between the two types of experiments. A comparable behaviour is observed in both cases: the average value of $\mathcal{M}$ increases with the light intensity before reaching a plateau at $\bar{E} \approx 0.4$, while the graph of $\mathcal{P}$ shows a peak at $\bar{E} = 0.1$. Both parameters still have values close to zero when the light is switched off. Inter-individual distance also exhibits comparable values. One difference is to be noted concerning NN-D, since the observation of a minimum at $\bar{E} = 0.1$ followed by a growth is no longer valid in the case of discrete experiments, even if the absolute values remain in the same range. Overall, this set of experiments with constant light intensity allows us to conclude that the dominant effect explaining the variation in behaviour observed here is mostly the changes in light intensity rather than any other external parameter, notably excluding the role of the duration of the experiments.

2.4 DISCUSSION AND PERSPECTIVES

2.4.1 *Interpretation of the experimental results*

The reading of both Figure 2.5 and Figure C.2 is here straightforward. In the absence of light, or with insufficient lighting, fish are unable to give rise to coherent and cohesive group dynamics. We also observed that above a certain threshold, the properties characterizing the collective dynamics do not statistically change with the degree of light intensity and tend to saturate to a constant value. This remark of course holds for the range of illuminance used for this work ($E \in$[0, 900] lx) and the global behaviour of the group might change with higher values of E. However, the range used in this work corresponds to lighting values in natural habitats for this kind of animals (Fraser and Metcalfe, 1997). This sheds light on the recent discussion on the respective roles of vision and lateral line sensing in the appearance of cohesive behaviors. Our observation in the absence of light suggests that lateral line sensing is not sufficient for the group to form a school in free swimming. Moreover, the quality of the visual cue seems to be paired with the capacity of the individuals to achieve collective swimming. It is worth noting again that the conclusions brought in this chapter are based on a large number of individuals constituting the group. This contrasts with most of past studies (Morrow, 1948; Steven, 1959; Torisawa et al., 2007) that characterized cohesion and collective dynamics under a changing illuminance using a reduced group of fish (less than 10 individuals), then mainly focusing on local interactions. Thus, this study constitutes the first experimental work examining vision-based global behavior of a large scale group of fish.

In addition, anticipating slightly onto Chapter 3, we note that the stable milling motion observed here with sufficient lighting may in fact be induced by the interaction with walls (Tunstrøm et al., 2013). Figure C.2A shows that the group polarization starts decreasing after exceeding the visual threshold. This decrease is coupled with the amplification of the milling parameter characterizing the group rotation around its center of mass. Thus, considering that fish tend to align with each other as their ability to see other individuals in the group is enhanced by a brighter environment, the milling behavior could be the consequence of being aligned in a confined space. Indeed, the alignment can be either quantified by the polarization or milling parameter, both having the same role in that particular geometry: while the polarization quantifies the alignment along lines, the milling parameters can be understood as a measure of an alignment along circles around the center of the group. The effect of confinement on this transition from polarization to milling is the subject of the following Chapter.

2.4.2 *Preliminary results on heterogeneous illuminance*

In the experiments detailed in this chapter, the illumination in the tank was uniformly adjusted. However, the question arises as to the influence of heterogeneous lighting on the schooling behaviour of fish. This question has been examined in various studies. It

is generally observed that the majority of fish display negative phototaxis, which means they move towards the darkest regions along the negative light gradient. Experiments on groups of golden shiners and *Hemigrammus r.* indicate that the effectiveness of phototaxis increases with an increase in the number of fish in the school (Berdahl et al., 2013). Additionally, other findings attempted to establish thermodynamic equivalents for fish schools weakly confined by dark circles of various sizes by calculating an equivalent of kinetic pressure (Giannini and Puckett, 2020).

This chapter compares the sensory mechanisms of vision and lateral line. One way to investigate this question further is to expose groups of fish to equivalent stimuli in isolation from one another. This can be achieved by studying the navigation of a school of fish in a jet: the fish are exposed to a liquid jet without light, or to a luminous "jet" projected into the tank, like the one in Figure 2.8. Such an experiment may reveal the relative effectiveness of vision and lateral line in the context of navigation.

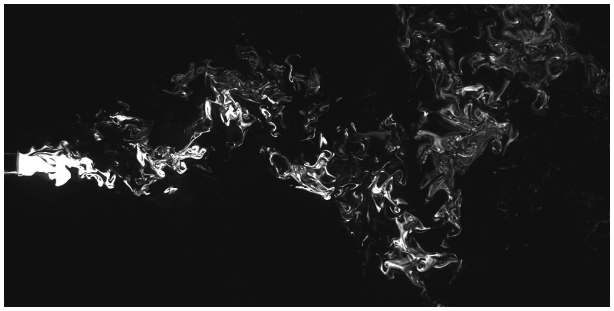

Figure 2.8: Example of turbulent jet image that could be used to compare the navigation ability of a school with mechanosensory cues from to lateral line and with vision (credit: E. Villermaux)

We conducted preliminary experiments in our setup, the results of which can be seen in Figure 2.9. Within a 100 $\times$ 100 cm square tank, groups of $N = 50$ fish swim under the same conditions as in the previous experiments. However, the illumination is now heterogeneous: a rectangular or toroidal shadow zone is included in the illumination (the illuminated zone is set at an intensity $\bar{E}$ = 1, the dark zone $\bar{E}$ = 0). The dark zone is not as dim as in the case of homogeneous illumination with $\bar{E} = 0$ since part of the light reflects, but the differences in lighting are sufficient to induce collective behaviour that are different from the homogeneous case. The key finding, evidenced in Figure 2.9, is that fish density is significantly greater in dark areas, which aligns with Hemigrammus natural tendency to prefer areas shaded from light. The presence of dark areas leads to a weak confinement of the group, as noted by Giannini and Puckett (2020). Specifically, the higher density presence can be attributed to lower average speeds in the dark regions.

While the previous situations are binary in terms of light intensity, we wanted to study the behaviour of schools of fish when other intensities are available in their environment. A supplementary test was conducted with two regions of varying intensities: the "dark" area, on the left in Figure 2.10, is set at $\bar{E} = 0$, whereas the "grey" region on the right is set at a marginally greater intensity ($\bar{E} = 0.3$). A slightly higher presence density is visually

observed in the darker zone, but further experiments would be needed to statistically confirm this effect.

Overall, these preliminary experiments confirm the existence of an interaction between heterogeneous lighting and collective behavior. They pave the way for more quantitative trials to analyze the respective roles of vision and lateral line in fish collective navigation.

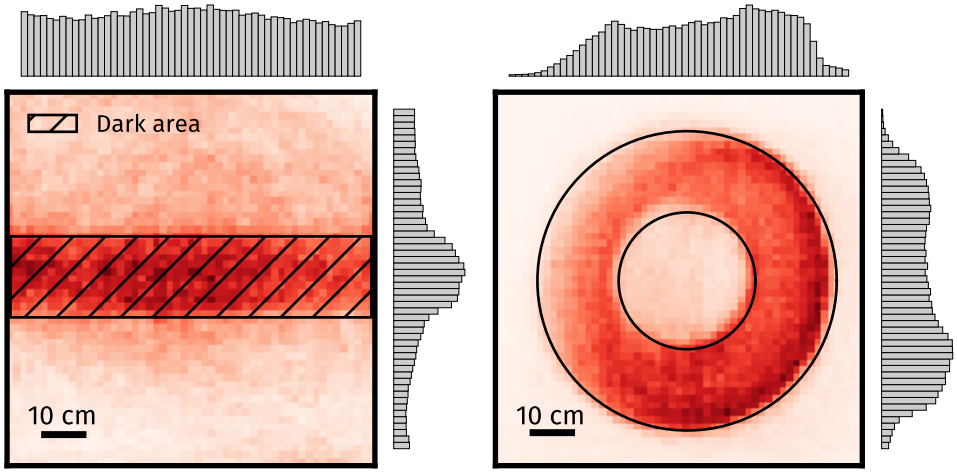

Figure 2.9: Spatial density of presence of 50 fish in heterogeneously lit tanks. The graphs on the right (resp. on the top) represent the distribution averaged in the left-right direction (resp. in the bottom-top direction).

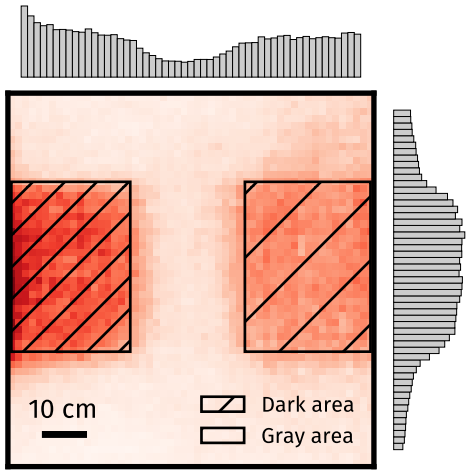

Figure 2.10: Spatial density of presence of 50 fish in an heterogeneously lit tank, with 3 different level of light intensity. Dark area corresponds to an area with normalized light intensity of $\bar{E} = 0$, while grey area corresponds to $\bar{E} = 0.3$. The graphs on the right (resp. on the top) represent the distribution averaged in the left-right direction (resp. in the bottom-top direction).

REFERENCES

Berdahl, A., C. J. Torney, C. C. Ioannou, J. J. Faria, and I. D. Couzin (2013). "Emergent Sensing of Complex Environments by Mobile Animal Groups." *Science*. doi: 10.1126/science.1225883 (cit. on p. 41).

Bleckmann, H. (2006). "The Lateral Line System of Fish." *Fish Physiology*. doi: 10.1016/S1546-5098(06)25010-6 (cit. on p. 30).

Calovi, D. S., A. Litchinko, V. Lecheval, U. Lopez, A. Pérez Escudero, H. Chaté, C. Sire, and G. Theraulaz (2018). "Disentangling and Modeling Interactions in Fish with Burst-and-Coast Swimming Reveal Distinct Alignment and Attraction Behaviors." *PLoS Computational Biology*. doi: 10.1371/journal.pcbi.1005933 (cit. on p. 30).

Carleton, K. L., D. Escobar-Camacho, S. M. Stieb, F. Cortesi, and N. Justin Marshall (2020). "Seeing the Rainbow: Mechanisms Underlying Spectral Sensitivity in Teleost Fishes." *Journal of Experimental Biology*. doi: 10.1242/jeb.193334 (cit. on p. 31).

Claireaux, G., C. Couturier, and A.-L. Groison (2006). "Effect of Temperature on Maximum Swimming Speed and Cost of Transport in Juvenile European Sea Bass (*Dicentrarchus Labrax*)." en. *Journal of Experimental Biology*. doi: 10.1242/jeb.02346 (cit. on p. 33).

Faucher, K., E. Parmentier, C. Becco, N. Vandewalle, and P. Vandewalle (2010). "Fish Lateral System Is Required for Accurate Control of Shoaling Behaviour." *Animal Behaviour*. doi: 10.1016/j.anbehav.2009.12.020 (cit. on p. 30).

Filella, A., F. Nadal, C. Sire, E. Kanso, and C. Eloy (2018). "Model of Collective Fish Behavior with Hydrodynamic Interactions." *Physical Review Letters*. doi: 10.1103/PhysRevLett.120.198101 (cit. on p. 30).

Fraser, N. H. C. and N. B. Metcalfe (1997). "The Costs of Becoming Nocturnal: Feeding Efficiency in Relation to Light Intensity in Juvenile Atlantic Salmon." en. *Functional Ecology*. doi: 10.1046/j.1365-2435.1997.00098.x (cit. on p. 40).

Gallois, B. and R. Candelier (2021). "FastTrack: An Open-Source Software for Tracking Varying Numbers of Deformable Objects." *PLoS Computational Biology*. doi: 10.1371/JOURNAL.PCBI.1008697 (cit. on p. 33).

Giannini, J. A. and J. G. Puckett (2020). "Testing a Thermodynamic Approach to Collective Animal Behavior in Laboratory Fish Schools." *Physical Review E*. doi: 10.1103/physreve.101.062605 (cit. on pp. 30, 41).

Hemmings, CC (1966). "Olfaction and Vision in Fish Schooling." *Journal of experimental biology*. doi: 10.1242/jeb.45.3.449 (cit. on p. 30).

Kuhn, H. W. (1955). "The Hungarian Method for the Assignment Problem." en. *Naval Research Logistics Quarterly*. doi: 10.1002/nav.3800020109 (cit. on p. 33).

Lopez, U., J. Gautrais, I. D. Couzin, and G. Theraulaz (2012). "From Behavioural Analyses to Models of Collective Motion in Fish Schools." *Interface Focus*. doi: 10.1098/rsfs.2012.0033 (cit. on p. 30).

McKee, A., A. P. Soto, P. Chen, and M. J. McHenry (2020). "The Sensory Basis of Schooling by Intermittent Swimming in the Rummy-Nose Tetra (Hemigrammus Rhodostomus): Schooling by Intermittent Swimming." *Proceedings of the Royal Society B: Biological Sciences*. DOI: 10.1098/rspb.2020.0568rspb20200568 (cit. on p. 30).

Mekdara, P. J., F. Nasimi, M. A. Schwalbe, and E. D. Tytell (2021). "Tail Beat Synchronization during Schooling Requires a Functional Posterior Lateral Line System in Giant Danios, Devario Aequipinnatus." *Integrative and Comparative Biology*. DOI: 10.1093/icb/icab071 (cit. on p. 30).

Mekdara, P. J., M. A. Schwalbe, L. L. Coughlin, and E. D. Tytell (2018). "The Effects of Lateral Line Ablation and Regeneration in Schooling Giant Danios." *Journal of Experimental Biology*. DOI: 10.1242/jeb.175166 (cit. on p. 30).

Morrow, J. E. (1948). "Schooling Behavior in Fishes." *The Quarterly Review of Biology*. DOI: 10.1086/396078 (cit. on p. 40).

Partridge, B. L. and T. J. Pitcher (1980). "The Sensory Basis of Fish Schools: Relative Roles of Lateral Line and Vision." *Journal of Comparative Physiology A*. DOI: 10.1007/BF00657647 (cit. on p. 30).

Pavlov, D. S. and A. O. Kasumyan (2000). "Patterns and Mechanisms of Schooling Behavior in Fish: A Review." *Journal of Ichthyology* (cit. on p. 30).

Pitcher, T. J., B. L. Partridge, and C. S. Wardle (1976). "A Blind Fish Can School." *Science*. DOI: 10.1126/science.982056 (cit. on p. 30).

Pitcher, T. J. and B. L. Partridge (1979). "Fish School Density and Volume." *Marine Biology* (cit. on p. 30).

Puckett, J. G., A. R. Pokhrel, and J. A. Giannini (2018). "Collective Gradient Sensing in Fish Schools." *Scientific Reports*. DOI: 10.1038/s41598-018-26037-9 (cit. on p. 30).

Ryer, C. and B. Olla (1998). "Effect of Light on Juvenile Walleye Pollock Shoaling and Their Interaction with Predators." en. *Marine Ecology Progress Series*. DOI: 10.3354/meps167215 (cit. on p. 30).

Shearer, K. D. (2000). "Experimental Design, Statistical Analysis and Modelling of Dietary Nutrient Requirement Studies for Fish: A Critical Review." en. *Aquaculture Nutrition* (cit. on p. 36).

Steven, D. M. (1959). "Studies on the Shoaling Behaviour of Fish." *Journal of Experimental Biology*. DOI: 10.1242/jeb.36.2.261 (cit. on p. 40).

Torisawa, S., T. Takagi, H. Fukuda, Y. Ishibashi, Y. Sawada, T. Okada, S. Miyashita, K. Suzuki, and T. Yamane (2007). "Schooling Behaviour and Retinomotor Response of Juvenile Pacific Bluefin Tuna Thunnus Orientalis under Different Light Intensities." *Journal of Fish Biology*. DOI: 10.1111/j.1095-8649.2007.01498.x (cit. on p. 40).

Tunstrøm, K., Y. Katz, C. C. Ioannou, C. Huepe, M. J. Lutz, and I. D. Couzin (2013). "Collective States, Multistability and Transitional Behavior in Schooling Fish." *PLoS Computational Biology*. DOI: 10.1371/journal.pcbi.1002915 (cit. on p. 40).

Whitney, R. R. (1969). "Schooling of Fishes Relative to Available Light." en. *Transactions of the American Fisheries Society*. DOI: 10.1577/1548-8659(1969)98[497:SOFRTA]2.0.CO;2 (cit. on p. 30).

3

INFLUENCE OF THE CONFINEMENT ON COLLECTIVE STATE TRANSITION AND STABILITY

Avec son impitoyable sens pratique, elle ne pouvait comprendre le commerce du colonel, lequel échangeait ses petits poissons contre des pièces d'or, puis transformait les pièces d'or en petits poissons

— Gabriel García Márquez, *Cent Ans de solitude* (1967)

We investigate in this chapter the impact of confinement density (i.e the number of individual in a group per unit area of available space) on transitions from polarized to milling state under controlled experimental conditions. We observe a continuous state transition controlled by confinement density. During this transition, the school exhibits a bistable state, wherein both polarization and milling states coexist, with the group randomly alternating between them. Importantly, the confinement density influences the statistics of this bistability, shaping the distribution of transition times between states. Our findings suggest that confinement plays a crucial role in state transitions of fish schools, and more generally they constitute a solid experimental benchmark for active matter models of macroscopic, self-propelled, confined agents.

3.1 STATE TRANSITION IN COLLECTIVE MOTION

Numerous physical parameters are able to trigger behavioral state transitions in groups of moving organisms by altering the nature or intensity of the inter-individual interactions (Jhawar et al., 2020). In the previous chapter, we showed experimentally that the level of illumination is a factor that can provoke the appearance of collective states as well as transitions between these states, by modifying the visual cues available to individuals. However, it is clear that in these experiments, the characteristic size of the group is similar to the size of the tank in which the fish swim, which leads to the question of the role of confinement in state transitions.

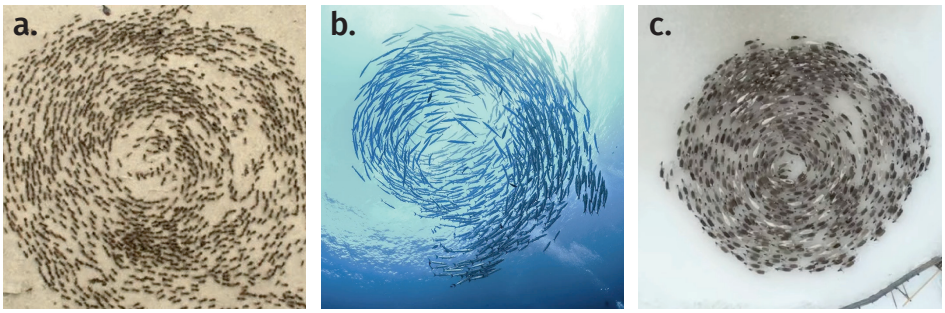

Figure 3.1: Examples of animal groups in milling configuration in the wild. **a.** A "death circle" of fire ants, **b.** A barracuda mill, **c.** A reindeer "vortex". The transition to milling state is widespread in nature and has been extensively described for a number of other species: marine worms (Franks et al., 2016), planktonic crustaceans (Ordemann, Balazsi, and Moss, 2003), sheeps...

The existing numerical models of self-propelled particles indicate that one of the key factors explaining these transitions is indeed the local density in the group (Biancalani, Dyson, and McKane, 2014; Dyson et al., 2015; Ordemann, Balazsi, and Moss, 2003; Vicsek et al., 1995). For fish schools specifically, studies have highlighted density-driven transitions, either experimentally (Becco et al., 2006; Tunstrøm et al., 2013) or with numerical simulations (Cambuí and Rosas, 2012). These studies focus on the role of the number of fish in a confined space, but also mention that the proximity to the walls of the swimming arena can be decisive in the apparition of certain type of transition, such as milling to polarization transition (Tunstrøm et al., 2013).

We can unify these observations by examining the issue of state transition from the perspective of group confinement -in the sense of how crowded the available area is- which covers two distinct factors: the number of individuals in the group,

and the surface of its arena. The impact of such confinement and the effect of boundaries have been previously studied for systems of non-living (Liu et al., 2020) or microscopic active matter (from bacteria (Beppu et al., 2017; Wioland, Lushi, and Goldstein, 2016) to cells (Méhes and Vicsek, 2014)), but seems to be a missing ingredient in our current understanding of state transitions for groups of live animals. In particular, we still lack knowledge on how the reduction of the space given to the group influences its collective behavior. The study by (Tunstrøm et al., 2013) indicates that the swimming area is non-significant in the state transitions between swarming, milling, and polarized states in groups of golden shiners. However, this conclusion was based on a single experiment carried out for a different swimming area. As of yet, no study has systematically investigated how confinement, both in terms of the number of individuals and the arena surface, impacts groups of animals on the move. Notably, the link between confinement and behavioral state transitions remains unsettled.

Here we report quantitative results on the collective dynamics of groups of rummy-nose tetras (*Hemigrammus rhodostomus*), a highly cohesive fresh water fish, under controlled experimental conditions. In first approximation, if one neglects the exact shape of the tank, the notion of confinement can be simply quantified by a "confinement density", which is the number of fish per unit area of the tank. Our analysis provides novel experimental evidence for a continuous state transition governed by confinement density. During this transition, the school is experiencing a bistable state, in which both polarization and milling states coexist; the group can fall randomly into one of these two states. Bouts of variable durations of either state intercede one another alternately over time. By measuring the distribution of transition times between states, we show that the statistics of this bistability is also directly influenced by the confinement density. Through these results, we show that the walls and the group size play a comparable role in the emergence of collective dynamics.

3.2 MATERIAL AND METHODS

3.2.1 *Experimental setup*

The experiment consists of recording the motion of free-swimming schools of *Hemigrammus rhodostomus* in a tank, using the same setup as described in the previous chapter, for different swimming areas S and school sizes N (number of individuals in the group). We systematically investigated the role of the confine-

ment density, or mean density, ρ, defined as the ratio of these two values $\rho = N/S$ in fish/m^2. The water depth in the tank is sufficiently shallow (6 cm) to constrain the trajectories in two dimensions. The average body length (BL) of the fish used here is 32 mm.

The swimming area S can be modified thanks to a system of movable partition walls. Three different surfaces are considered: 1, 0.5 and 0.25 m^2. We focus mainly on arenas with a square shape (aspect ratio AR = 1), but we also discuss the implications of a different aspect ratio. We studied 10 different group sizes ranging from 10 to 70 fish, resulting in densities between 10 and 120 fish/m^2. During the experiments, the tank is brightly lit from above with visible light (900 lux): as observed in Chapter 2, the milling state is predominant for a school of 50 fish under these lighting conditions.

3.2.2 *Data processing*

The acquisition frequency of the camera is 50 frames per second ($\Delta t = 0.02$ s). Using the open source particle tracking library Trackpy (Allan et al., 2021; Crocker and Grier, 1996), we extract the temporal signals of the two-dimensional positions $\mathbf{x}_i(t)$, from which we obtain velocities with a second order central differences method $\mathbf{v}_i(t) = [\mathbf{x}_i(t + \Delta t) - \mathbf{x}_i(t - \Delta t)]/2\Delta t$, where $i = 1, 2, ..., N$ is the fish label.

For each confinement density ρ, at least 2 different pairs of values of N and S corresponding to that density were tested (except for the two extreme density values 10 and 120 fish/m^2). We conducted at least 3 different trials of 15 min for every pair of values (swimming area, school size). In total, 76 distinct experiments have been conducted.

3.3 RESULTS

3.3.1 *Experimental results*

When first qualitatively examining the dynamics of the fish at any different combinations of number of fish N and tank surface S, we see that the group of tetras spontaneously and repeatedly alternate between milling and polarized states as can clearly be seen in Figure 3.2. The swarming state, where the school is disorganised and orientations are isotropic, ($\mathcal{M}$ and $\mathcal{P}$ both small) reported by previous studies in similar setups (Becco et al., 2006; Tunstrøm et al., 2013) is nearly not observed in our experimental conditions, and tends to only appear when the group

of fish is located in one of the corners of the observation tank. For this reason, we have chosen not to quantitatively study the swarming state in this case, and will consider only the milling and polarized states. This absence of swarming can be explained by the nature of the illumination to which the fish are subjected: we have observed in Chapter 2 that above a certain luminosity threshold, schools of *Hemigrammus rhodostomus* are almost exclusively in polarized or milling states, with swarming only occurring below this limit. The threshold, identified at 400 lux for a group of 50 fish swimming in a 1.40 m^2 tank, is largely exceeded here.

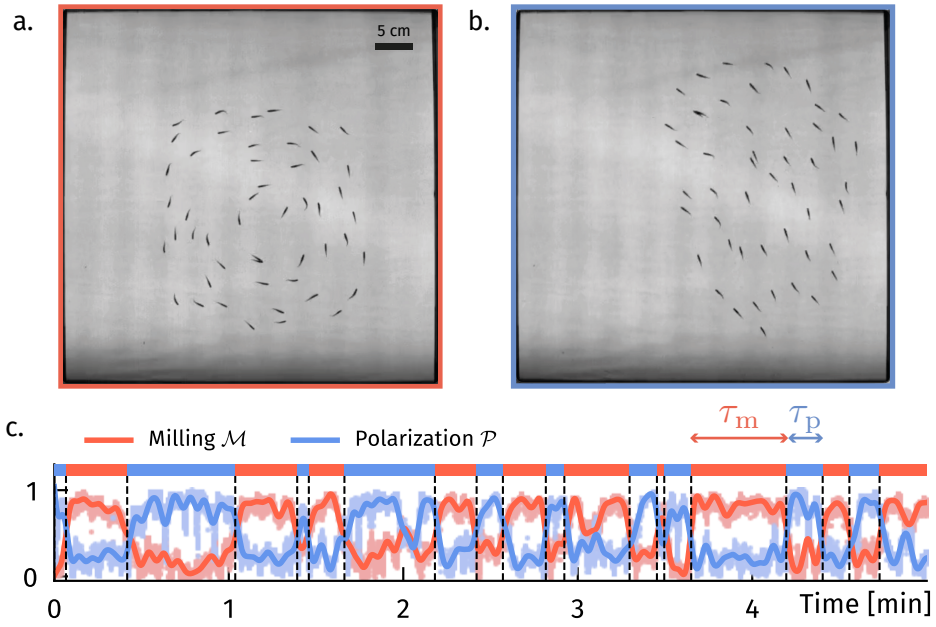

Figure 3.2: Example of an experimental result for $N = 50$ fish schooling in a square tank of swimming area $S = 1$ m^2. Snapshot of the school in (a.) milling configuration ($\mathcal{M} > 0.5$) and in (b.) polarized configuration ($\mathcal{P} > 0.5$). The photographs show the entire surface of the tank. (c.) The time signal of $\mathcal{M}$ and $\mathcal{P}$ shows clearly distinct periods of milling state followed by periods of polarized state of respective duration τ_m and τ_p. The colored bar on the top represents the current state of the school.

OBSERVATIONS At the smallest density values (10-20 fish/m^2), we observe that the school remains in a polarized state for almost the entire recording duration, with only short-lived (a few seconds) incursions to the milling state that quickly revert to the polarized state. This behavior is illustrated in Figure 3.3, for $S = 1$ m^2 and $N = 10$. As we further increase the confinement density by adding more

fish to the school or reducing the swimming area (typically for densities between 20 and 80 fish/m^2), the bistability can be more clearly observed, as milling bouts last for longer. The group state shows an increase in fluctuations, with frequent shifts observed between the polarized and milling states, although the proportion of time in the polarized state remains more significant than the time spent in the milling state for densities lower than 40 fish/m^2; as the density increases again, the milling state becomes more predominant (see Figure 3.3, for $S = 0.5$ m^2 for exemple). Finally, when approaching densities of 100 fish/m^2 and above, the groups mostly display a milling behaviour that lasts for long durations of time, still punctuated with occasional very short periods of polarization (typically less than a few seconds). This is shown by the panel corresponding to $S = 0.25$ m^2 and $N = 30$ in Figure 3.3. The complete set of results is shown on Figure 3.4 where all the experimental results for average time spent in either milling or polarized state are shown in a phase diagram with the parameters being N and S. From this figure, it is visible that milling state is concentrated in the lower right corner (high densities) while polarized state is seen in the upper right corner of the phase diagram (at lower densities).

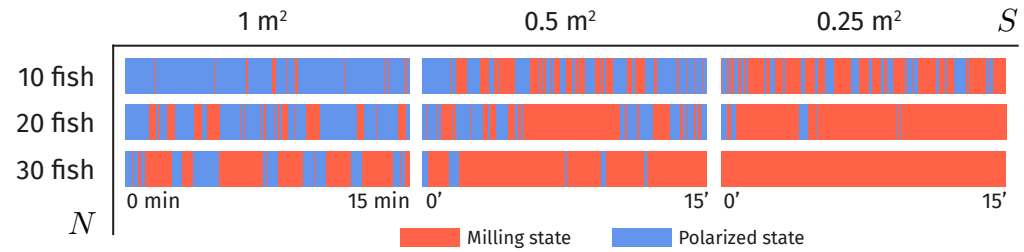

Figure 3.3: State transitions over 15 min experiments for various school sizes N and swimming area S.

This bistability of the school has been observed previously in experimental (Tunstrøm et al., 2013) and numerical studies (Strömbom et al., 2022), and is reminiscent of a simple dynamical system oscillating between two stable states. This leads us to define these two states objectively: we say that the school is in the milling state (resp. in the polarised state) when $\mathcal{M} > 0.5$ (resp. when $\mathcal{P} > 0.5$). The colored bar above the time signal in Figure 3.2c shows that the two states follow each other almost without interruption. Inspired by thermodynamics (Giannini and Puckett, 2020), the bistability of the fish group can be described by a potential landscape: transitions take place when the fluctuations of the system are greater than the corresponding potential barrier.

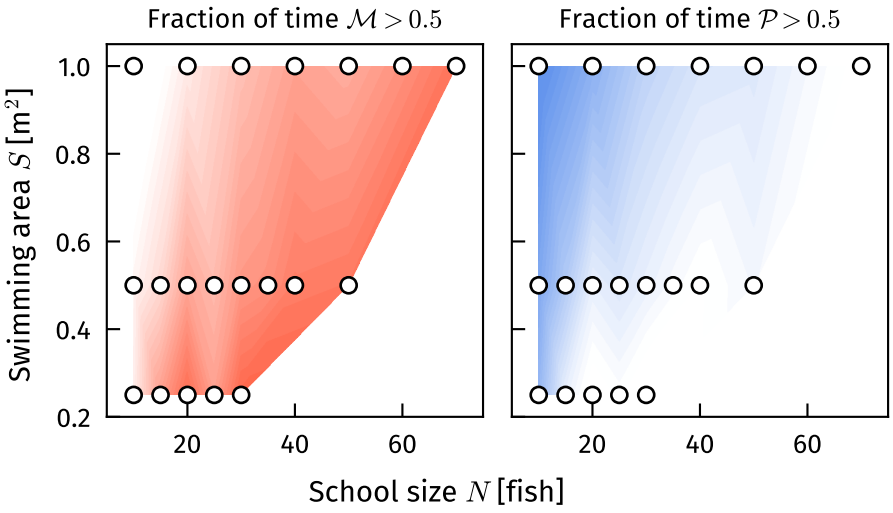

Figure 3.4: Phase diagram of the collective state transition in the parameter space (swimming area S, school size N). On the left (resp. on the left): fraction of experimental time spent in the milling state (resp. in the polarized state) by the school. Each dot represents at least 3 repeated experiments of 15 min each.

LOCAL DENSITY IN THE SCHOOL

From the trajectories $\mathbf{x}_i(t)$ obtained by tracking, we also extract a geometrical values to gain insight on the organization of the group, the group size D. If we denote d_{ij} the distance between the two fish labelled i and j respectively, with $(i, j) \in \{1..N\}^2$, the group size D is obtained by sorting the $N(N-1)/2$ unique distances d_{ij} and taking the average of the 8 largest. If the group is forming a disk (i.e in the milling state), D is a proxy of the diameter of this disk. In the polarized state, D can be understood as the major axis length of the smallest ellipse surrounding the group. Figure 3.5 shows the values of D with respect to the number of fish in the school N, for the 3 different swimming areas S. The first observation is that variations of S have no influence on the groupe size, and that the group size in-

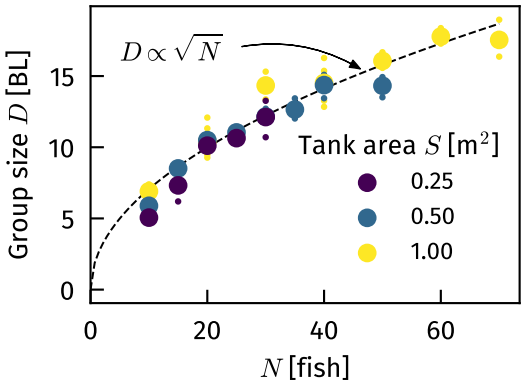

Figure 3.5: Group size (average of the 8 largest inter-individual distances, in Body Lengths, BL) with respect to the number of fish in the school N. The colors represent the size of the swimming area S.

creases slowly with N. We fit the experimental data with a square root function, tanks to a non-linear least squares method:

$$D = \sqrt{S_0 N} \tag{3.1}$$

with S_0 a constant fitting parameter homogeneous to a surface. The evolution of D is well captured by this fit, which suggests that whatever the experimental conditions, we can consider that the fish school maintains a constant local density. The best fitting parameter value is found to be $S_0 = 4.98$ BL^2: this surface can be interpreted as a minimal 'comfort' area kept by each individual around itself.

ROLE OF THE CONFINEMENT DENSITY In order to quantify the observed intermittency in states we first investigate it on the time scale of each experiment (15 minutes). Figure C.3 shows the time spent in either state plotted as a function of confinement density ρ. First, it corroborates the observations made on individual experiments, where time spent milling goes up with the density, and oppositely for time spent in the polarized state. Most strikingly Figure C.3 shows a clear collapse of the data of a total of 76 experiments with 20 different (N, S) combinations when plotted against the confinement density. For each confinement density (with the exception of 10 and 120 fish/m^{-2}), experiments with at least two (N, S) combinations were carried out, to ensure that they yielded equivalent results if the N/S ratio was the same. This collapse clearly highlights that the proportion of time spent by the group of Rummy-nose tetras in either state is solely a function of the confinement density, rather than of the number of fish alone, as suggested by previous studies on golden shiners (TUNSTRØM et al., 2013).

3.3.2 *Two-state model*

We introduce a simple two-state Markov process at the scale of the school to gain insight on the transition between the polarized and milling states. In this scenario, the school is considered as a bistable system; we denote α (resp. β) the rate of transition from the polarized to milling states (resp. from milling to polarized). The transition probability from polarized to milling (resp. milling to polarized) during a time δt is therefore $\delta t\alpha$ (resp. $\delta t\beta$). This probability is considered to depend only on the current state and is independant of the history of the system. In this case, the time between switching events (i.e the duration of the bout spent in either state) follows an exponential distribution with a rate parameter specific to that state.

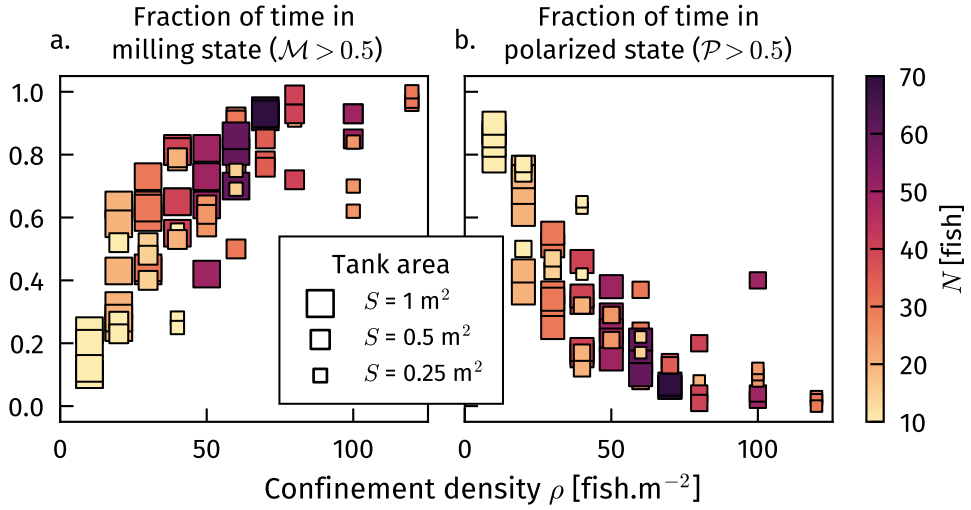

Figure 3.6: Fraction of time spend by fish schools in the milling state (a.) and in the polarized state (b.) over total experiment duration, with respect to confinement density, i.e the number of fish per unit area of the tank in fish.m^{-2}. The size of the markers indicates the area of the tank, while the colors show the number of fish in the school.

We have the following probability density functions for the duration of milling and polarized bouts:

$$\mu_{\mathrm{p}}(\tau_{\mathrm{p}} = \tau) = \alpha \exp(-\alpha\tau) \tag{3.2}$$

$$\mu_{\mathrm{m}}(\tau_{\mathrm{m}} = \tau) = \beta \exp(-\beta\tau) \tag{3.3}$$

We experimentally measured the distributions of the time spent in the milling and polarized states. The results, reported in Figure C.4a-b show an exemple of the empirical distribution of the durations between state transitions, for a confinement density at which fish spend approximately the same time in the milling and polarized states ($\rho = 30$ fish/m^2, for $N = 30$ and $S = 1$ m^2). At low densities, where transitions are frequent and the experimental statistics is therefore good, fitting an exponential distribution to the data shows good agreement. It should be noted that as density rises, and milling bouts become very long, the number of transitions falls sharply, and the number of bouts observed is much lower. For these high densities, the fit quality deteriorates, likely due to the insufficient statistics behind the experimental distribution. From the fit parameters we can directly obtain the mean time to transition for each state, with $\langle\tau_{\mathrm{m}}\rangle = \beta^{-1}$ and $\langle\tau_{\mathrm{p}}\rangle = \alpha^{-1}$. The good

agreement demonstrated by the distributions in Figure C.4a-b, which closely fit to an exponential distribution is the hallmark of a memoryless process and suggests that the school operates as a system near a pseudo-critical point (Gómez-Nava, Bon, and Peruani, 2022; Romanczuk and Daniels, 2022).

With this approach we extract α and β for every set of experiments, that is for all pairs of (N, S). The variations of the two rates are presented on Figure C.4c, with respect to the confinement density. We see that the stability of the milling state increases with density, while that of the polarised state decreases.

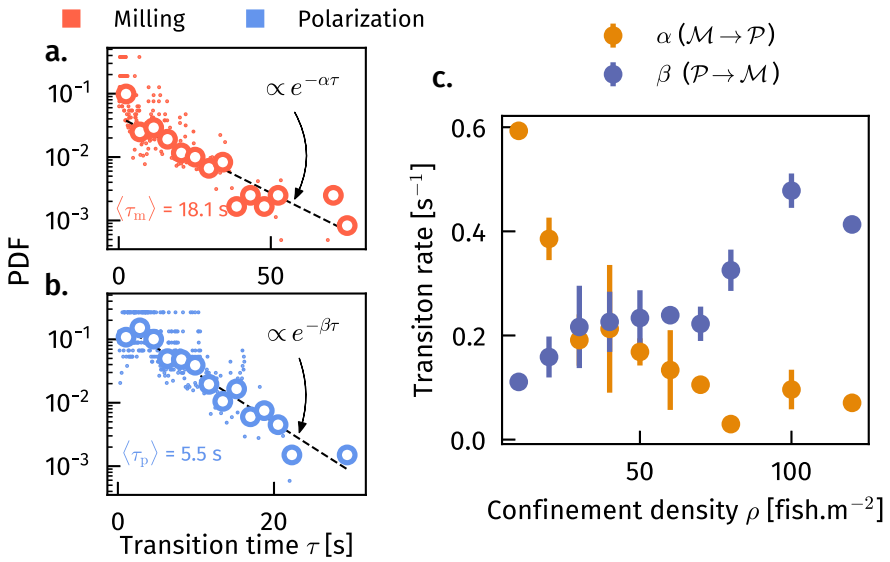

Figure 3.7: Loglog plot of the probability density function of the duration of milling state τ_m **(a.)** and polarized state τ_p **(b.)** for a confinement density $\rho = 30$ fish/m^2 ($N = 30$, $S = 1$ m^2, 6 replicates, 387 transition events). Small dots are generated by differentiating the complementary cumulative density function obtained from sorting the transition times, they do not depend on the binning. Large points are the histogram obtained by binning data into 15 linearly spaced time intervals. Dashed lines show the best exponential law fit with parameter $\alpha = \langle\tau_m\rangle^{-1}$ and $\beta = \langle\tau_p\rangle^{-1}$ (c) Transition rates with respect to confinement density. Error bars represent the standard deviation over all replicates of experiments at a given density.

3.3.3 *Influence of the aspect ratio of the tank*

The swimming area variations presented until now have been conducted using a constant unitary aspect ratio (AR), i.e with the tank retaining a square shape. However, because the interaction with the tank walls has been identified as a critical

parameter in the observed transition, it is possible that the aspect ratio also plays a significant role. To assess the influence of the aspect ratio, we conducted additional qualitative experiments with different AR values, specifically AR = {1, 2, 4, 10}. In this set of four additional experiments, the height of the tank remains fixed at 1 m, while the width is varied to 50, 25, and 10 cm. All other experimental parameters, such as frame rate, water depth, and ambient light intensity, were kept consistent with the conditions used in the initial experiments. This additional data set consists of one video recording of 10 minutes of schooling for each value of AR. Because of the proximity imposed on the fish in this setup, trajectory crossings are common and periods where fish are superimposed are regularly observed; therefore, tracking accuracy drops drastically and renders quantitative analysis with the tracking pipeline used for this study unreliable. However, a qualitative analysis of collective behaviour is still possible from the raw images.

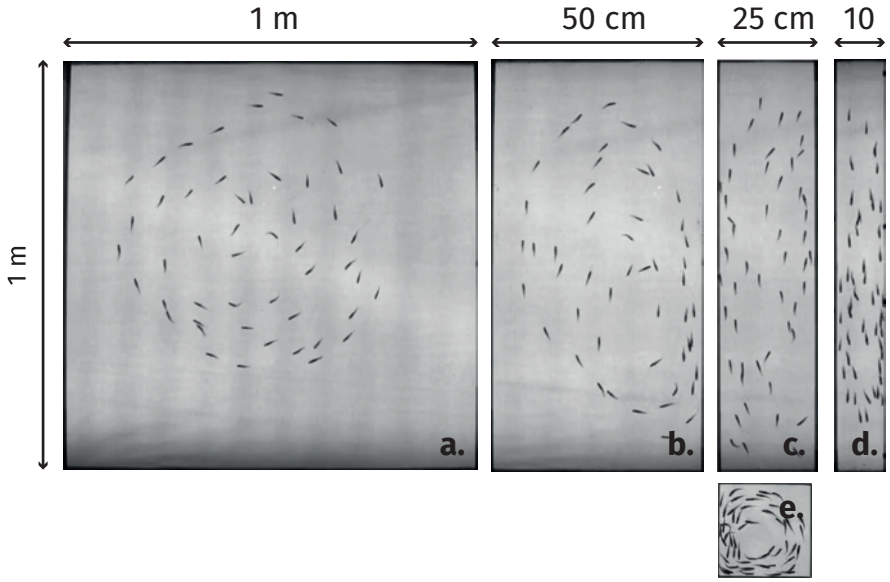

Figure 3.8: Effect of a variation of the aspect ratio AR of the tank, from $AR = 1$ to $AR = 10$. The height of the swimming area remains fixed at 1 m while its width changes: (**a.**) 1 m (**b.**) 0.50 m (**c.**) 0.25 m (**d.**) 0.1 m. Panel (**e.**) shows an experiment in a 0.2 m $\times$ 0.2 m ($AR = 1$). Note that the milling motion is totally suppressed for $AR > 2$.

As shown in Figure 3.8a-d, milling is clearly suppressed for elongated tanks with aspect ratios greater than 2. Starting from a situation where milling exists approximately 60% of the time in a square tank, we see a reduction in the time spent milling and a deformation of the vortex structure formed by the fish when we move to an aspect ratio of 2. Beyond AR = 2, the milling almost no longer exists

(no longer at all for $AR = 10$), and the fish move back and forth between the two ends of the tank, remaining aligned along its long side. We note that in this case the transition is exclusively due to geometric constraints, since at the confinement density considered here (respectively 100, 200, 500 fish/m^2 for $AR = 2$, 4, 10), we are well above the threshold after which we observe only milling in the case of a square tank. It is also interesting to point out that, starting from a situation where the milling is suppressed (for example the tank with an aspect ratio of 4), it is still possible to make the milling 'reappear' by reducing the aspect ratio, as demonstrated by an additional experiment carried out in a 20 $\times$ 20 cm square tank (see Figure 3.8e). We hypothesize that these observations explain the experimental results obtained by (Tunstrøm et al., 2013): they report that, when reducing the swimming area, higher confinement density does not lead to increased time spent milling. However, this reduction of area was conducted at an aspect ratio of approximately 2 (66 $\times$ 38 cm), which means that they might have observed the same phenomenon of geometrical suppression of milling that we describe here.

3.4 DISCUSSION

Although in this work, the confinement of the group of fish is carried out using simple walls, analogies can be drawn with systems in the wild. Confinement in cases of predation can take different forms: in some cases real boundaries are introduced, as with humpback whales caging off schools of fish, trapping them (Sharpe and Dill, 1997), in others the boundary may be effective like with dusky dolphins herding fish into 'prey balls' (Vaughn et al., 2011). Although these analogies are mostly qualitative, the parallel one can draw between geometric confinement and predation pressure opens an interesting avenue for research. Better understanding these similarities can help us break down complex behaviors observed in the wild.

The experiments reported here constitute the first quantitative laboratory study of the influence of confinement on the social behavior of live animals. Along with the works previously reported by (Lafoux et al., 2023), the results described above demonstrate that the collective states depend both on interactions between individuals and the environment of the fish group. Fundamentally, the coupling between the collective state and the surroundings is unsurprising, as the evolutionary pressure that has given rise to these states is likely highly environment-dependant.

In the case of confinement, we showed here that the nature of the bistability between polarization and milling of the group of *Hemigrammus rhodostomus* was controlled by confinement density. Whether it be the overall proportion of time spent in either state, or the statistical nature of bout durations, the intensity of the confinement seems to play a pivotal role. Furthermore, the qualitative investigation of different aspect ratios has shown that the boundary conditions can remove the bistability and select either state. These experimental results can be useful for future numerical models or the development of theory as an empirical benchmark to which these could be compared.

3.5 PERSPECTIVE

Since the shape of the tank appears significant in the behavioural state shift described in this section, it is reasonable to consider the impact of a circular tank on milling. Further experimentation was carried out in a circular tank with a diameter of 50 cm (S = 0.19 m^2) using a different fish species, zebrafish (*Danio rerio*) [1]. While zebrafish are less cohesive than rummy-nose tetras, they are similar in size and share a gregarious nature and a burst and coast swimming gait. In these experiments, the images were captured at 50 frames per second for a duration of one minute. The results presented here are exploratory and open the door to the question of the role of tank shape in confinement transitions.

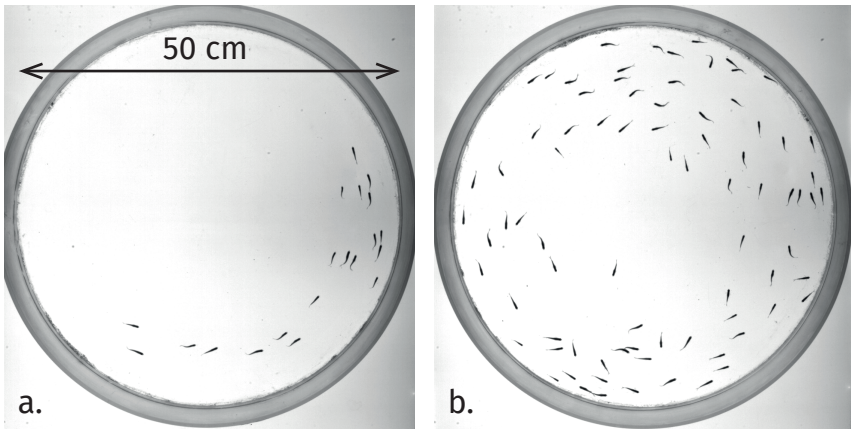

Figure 3.9: Images of experiments in a circular arena with 20 fish (a.) and 80 fish (b.)

Figure 3.10 displays the results of measurements for $\mathcal{M}$ and $\mathcal{P}$ parameters at various group sizes N, ranging from 5 to 80 fish (with one repetition per experi-

1 These experiments were carried out by Alicia Gimenez and Frederic Lechenault at PMMH in 2021, as part of an internship that was not directly related to this thesis

ment). The resulting confinement densities ρ varies from 30 to 400 fish/m^2 (see Figure 3.9 for an example of the typical experimental raw image). Similarly to the experiments conducted in rectangular tanks, we observed a reduction in the polarization parameter $\mathcal{P}$ as ρ increased. This reduction occurred from 0.5 at 30 fish/m^2 to approximately 0.05 for 400 fish/m^2. However, the milling parameter outcome differs for this geometry, as its value remains constant at around 0.65, irrespective of the confinement density. This difference of collective behavior can be explained by the discrete nature of the zebrafish trajectories, which move using a burst and coast gait. At the end of a each burst period, an individual selects an orientation angle. Experimentally, it can be shown that the distribution of these angles is a wrapped Gaussian centered around 0 (Calovi et al., 2018). However, when an individual is close to a wall with a curvature, like in this experiment, it is somehow 'trapped' by the edge of the tank because part of the accessible angle distribution is truncated. Thus, in fish swimming in burst and coast, the presence of a curved boundary favours the behaviour of alignment with the walls and therefore the emergence of milling.

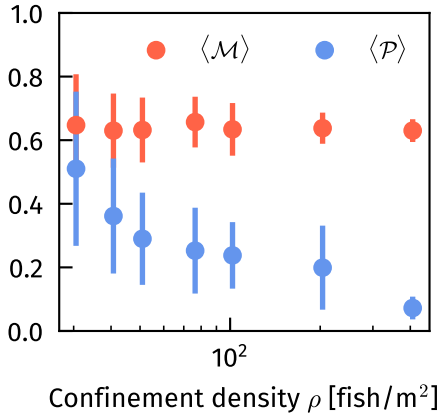

Figure 3.10: Average values of milling parameter $\mathcal{M}$ and polarization parameter $\mathcal{P}$ for experiments in a circular tank, with respect to confinement density ρ. The error bars show the standard deviation of the distributions of $\mathcal{M}$ and $\mathcal{P}$ for each experiment.

It should be noted, however, that the short duration of the additional experiments does not allow to conclude definitively about the role of a circular arena. Indeed, the behaviour described here could be more of a transition behaviour due to the stress of transferring the animals into the tank, since milling is not maintained in longer experiments. It would be necessary to carry out experiments in a controlled environment, with more repetitions. To investigate the role of confinement further, it may also be suitable to replicate the experiments presented in this chapter with a species of fish that swim continuously but have a morphology and behaviour similar to that of rummy-nose

tetras. The black neon Tertra (*Hyphessobrycon herbertaxelrodi*) exhibits potential as an appropriate model species for this purpose.

REFERENCES

Allan, D. B., T. Caswell, N. C. Keim, C. M. van der Wel, and R. W. Verweij (2021). "Soft-Matter/Trackpy: Trackpy v0. 5.0." *Zenodo repository* (cit. on p. 50).

Becco, C., N. Vandewalle, J. Delcourt, and P. Poncin (2006). "Experimental Evidences of a Structural and Dynamical Transition in Fish School." *Physica A: Statistical Mechanics and its Applications*. doi: 10.1016/j.physa.2005.11.041 (cit. on pp. 48, 50).

Beppu, K., Z. Izri, J. Gohya, K. Eto, M. Ichikawa, and Y. T. Maeda (2017). "Geometry-Driven Collective Ordering of Bacterial Vortices." en. *Soft Matter*. doi: 10.1039/C7SM00999B (cit. on p. 49).

Biancalani, T., L. Dyson, and A. J. McKane (2014). "Noise-Induced Bistable States and Their Mean Switching Time in Foraging Colonies." en. *Physical Review Letters*. doi: 10.1103/PhysRevLett.112.038101 (cit. on p. 48).

Calovi, D. S., A. Litchinko, V. Lecheval, U. Lopez, A. Pérez Escudero, H. Chaté, C. Sire, and G. Theraulaz (2018). "Disentangling and Modeling Interactions in Fish with Burst-and-Coast Swimming Reveal Distinct Alignment and Attraction Behaviors." *PLoS Computational Biology*. doi: 10.1371/journal.pcbi.1005933 (cit. on p. 60).

Cambuí, D. S. and A. Rosas (2012). "Density Induced Transition in a School of Fish." en. *Physica A: Statistical Mechanics and its Applications*. doi: 10.1016/j.physa.2012.03.009 (cit. on p. 48).

Crocker, J. C. and D. G. Grier (1996). "Methods of Digital Video Microscopy for Colloidal Studies." en. *Journal of Colloid and Interface Science*. doi: 10.1006/jcis.1996.0217 (cit. on p. 50).

Dyson, L., C. A. Yates, J. Buhl, and A. J. McKane (2015). "Onset of Collective Motion in Locusts Is Captured by a Minimal Model." en. *Physical Review E*. doi: 10.1103/PhysRevE.92.052708 (cit. on p. 48).

Franks, N. R., A. Worley, K. A. J. Grant, A. R. Gorman, V. Vizard, H. Plackett, C. Doran, M. L. Gamble, M. C. Stumpe, and A. B. Sendova-Franks (2016). "Social Behaviour and Collective Motion in Plant-Animal Worms." *Proceedings of the Royal Society B: Biological Sciences*. doi: 10.1098/rspb.2015.2946 (cit. on p. 48).

Giannini, J. A. and J. G. Puckett (2020). "Testing a Thermodynamic Approach to Collective Animal Behavior in Laboratory Fish Schools." *Physical Review E*. doi: 10.1103/physreve.101.062605 (cit. on p. 52).

Gómez-Nava, L., R. Bon, and F. Peruani (2022). "Intermittent Collective Motion in Sheep Results from Alternating the Role of Leader and Follower." en. *Nature Physics*. doi: 10.1038/s41567-022-01769-8 (cit. on p. 56).

Jhawar, J., R. G. Morris, U. R. Amith-Kumar, M. Danny Raj, T. Rogers, H. Rajendran, and V. Guttal (2020). "Noise-Induced Schooling of Fish." *Nature Physics*. doi: 10.1038/s41567-020-0787-y (cit. on p. 48).

Lafoux, B., J. Moscatelli, R. Godoy-Diana, and B. Thiria (2023). "Illuminance-Tuned Collective Motion in Fish." *Communications Biology*. doi: 10.1038/s42003-023-04861-8 (cit. on p. 58).

Liu, P. et al. (2020). "Oscillating Collective Motion of Active Rotors in Confinement." EN. *Proceedings of the National Academy of Sciences*. doi: 10.1073/pnas.1922633117 (cit. on p. 49).

Méhes, E. and T. Vicsek (2014). "Collective Motion of Cells: From Experiments to Models." *Integrative Biology*. doi: 10.1039/c4ib00115j (cit. on p. 49).

Ordemann, A., G. Balazsi, and F. Moss (2003). "Pattern Formation and Stochastic Motion of the Zooplankton Daphnia in a Light Field." en. *Physica A: Statistical Mechanics and its Applications*. Stochastic Systems: From Randomness to Complexity. doi: 10.1016/S0378-4371(03)00204-8 (cit. on p. 48).

Romanczuk and Daniels (2022). "Phase Transitions and Criticality in the Collective Behavior of Animals – Self-organization and Biological Function." doi: 10.1142/9789811260438_0004 (cit. on p. 56).

Sharpe, F. A. and L. M. Dill (1997). "The Behavior of Pacific Herring Schools in Response to Artificial Humpback Whale Bubbles." en. *Canadian Journal of Zoology*. doi: 10.1139/z97-093 (cit. on p. 58).

Strömbom, D., Stephanie Nickerson, Catherine Futterman, Alyssa DiFazio, Cameron Costello, and Kolbjørn Tunstrøm (2022). "Bistability and Switching Behavior in Moving Animal Groups." *Northeast journal of complex systems*. doi: 10.22191/nejcs/vol4/iss1/1 (cit. on p. 52).

Tunstrøm, K., Y. Katz, C. C. Ioannou, C. Huepe, M. J. Lutz, and I. D. Couzin (2013). "Collective States, Multistability and Transitional Behavior in Schooling Fish." *PLoS Computational Biology*. doi: 10.1371/journal.pcbi.1002915 (cit. on pp. 48–50, 52, 54, 58).

Vaughn, R. L., E. Muzi, J. L. Richardson, and B. Würsig (2011). "Dolphin Bait-Balling Behaviors in Relation to Prey Ball Escape Behaviors: Dolphin-Prey Ball Foraging Interactions." en. *Ethology*. doi: 10.1111/j.1439-0310.2011.01939.x (cit. on p. 58).

Vicsek, T., A. Czirók, E. Ben-Jacob, I. Cohen, and O. Shochet (1995). "Novel Type of Phase Transition in a System of Self-Driven Particles." *Physical Review Letters*. doi: 10.1103/PhysRevLett.75.1226 (cit. on p. 48).

Wioland, H, E Lushi, and R. E. Goldstein (2016). "Directed Collective Motion of Bacteria under Channel Confinement." en. *New Journal of Physics*. doi: 10.1088/1367-2630/18/7/075002 (cit. on p. 49).

4

COLLECTIVE RHEOTACTIC BEHAVIOR IN A MINIMAL SCHOOL

— Cependant le bateau fait une ombre
vert-bleue; paisible, clairvoyante, envahie de
glucoses où paissent
en bandes souples qui sinuent
ces poissons qui s'en vont comme le thème au
long du chant.

— Saint-John Perse, *Eloges* VII (1911)

This chapter examines the determinants of rheotaxic behaviour, *i.e* the ability to orient in the direction of a flow, using a swimming tunnel. In particular, we study the station-holding behaviour of fish subjected to different flow speeds. In order to identify the sensory mechanisms that enable this type of response to emerge, experiments were repeated in an illuminated tank and in a tank placed in total darkness. Little is known about the role of inter-individual interactions in this type of situation: to provide some insight on this issue, we compared fish swimming alone with 'minimal schools' of 2 fish.

4.1 INTRODUCTION

Rheotaxis refers to the ability of aquatic organisms to orient themselves in response to a flow. One refers to rheotaxis as negative if the animal moves preferentially in the opposite direction to the flow (if it is swimming against the current) and positive in the opposite case. In particular, negative rheotaxis is a behaviour common to numerous fish species and employed in diverse contexts, such as locating upstream sources of odours carried by currents, intercepting invertebrate drift during foraging, and conserving energy while avoiding downstream displacement (Coombs, Bak-Coleman, and Montgomery, 2020).

Typically, negative rheotaxis is manifested by station-holding behaviour, in which the fish (or group of fish) maintains a constant mean position in the laboratory reference frame (an external observer sees the animal as stationary). This behaviour is achieved by the interaction of different sensory mechanisms: the lateral line, especially for the slowest flow speeds (Bak-Coleman et al., 2013), and vision (Baker and Montgomery, 1999). In some cases it has also been suggested that the vestibular system (responsible for balance) and the sense of touch are also used by fish during rheotaxis (Baker and Montgomery, 1999; Lupandin, Kirillov, and Pavlov, 2003). Rheotactic behaviour is robust and is maintained in the absence of one or more of the sensory mechanisms mentioned above. For example, it has been shown experimentally that rheotaxis functions without visual cues, in complete darkness (Bak-Coleman et al., 2013). Similarly, fish whose lateral line has been chemically deactivated can maintain this type of behaviour (Baker and Montgomery, 1999).

Numerous studies have investigated the role of environmental disturbances on the rheotactic abilities of different fish species. For example, the turbulent or non-turbulent nature of the flow to which fish are exposed can, depending on the case, favour rheotaxis (Elder and Coombs, 2015) or have a destabilising effect (Tritico, Cotel, and Cote, 2010; Webb, Cotel, and Meadows, 2010). Most of these studies have focused on the behaviour of a single fish, although a few have measured the rheotactic performance of groups of animals (Pavlov, Lupandin, and Skorobogatov (2000)). However, no study to date has focused specifically on understanding the influence of collective behaviour on rheotaxis and station keeping. In this chapter, we compare the rheotactic performance of fish swimming alone and of fish pairs, considered as the minimum constitutive cell of a school.

4.2 MATERIAL AND METHODS

4.2.1 *Experimental setup*

The experimental apparatus is a modified Brett-type swimming tunnel (Enders and Scruton, 2006), in which one or more *Hemigrammus rhodostomus* can be subjected to a chosen flow velocity. The swim tunnel and its constituents are shown on Figure C.5. It consists of a large 50 x 80 cm glass tank filled with water at a controlled temperature (27°C $\pm$ 1°C). The tunnel itself consists in a secondary tank placed in this large tank. It is a closed-loop in transparent PMMA (plexiglass), with two linear sections and two turns. In the first section, the water is set in motion by a propeller rotating around a horizontal axis. The rotation is generated by a mechanical transmission system that transmits the rotation of a motor positioned vertically above the tank. This motor is a DC geared motor (RS Pro) capable of delivering up to 11W of mechanical power, with a nominal speed of 12 revolutions per second at 12V. 3D printed corner modules are placed between the two sections to minimise the curvature of the water path, allowing the flow to turn while reducing flow separation and turbulence in the test section. Thin guide walls are 3D printed vertically in these corner modules to laminarize the flow (wall thickness: 0.8mm, distance between walls 10mm). The swim channel, or test section, is located in the other linear section. It is enclosed upstream and downstream by two honeycombs blocks used to reduce the velocity gradients and the turbulence rate of the flow in the swimming area. Two fine meshes are placed in front of the honeycombs (HDPE, 0.5 mm mesh size) to prevent fish from escaping through.

Overall, the swim section has the following dimensions: 10 $\times$ 25 cm in the longitudinal plane, with a depth of 10 cm. A floor can be placed at any height to control the depth available to the fish. The entire swim tank is isolated by an upper wall with an access hatch to the swim section, allowing the operator to place the fish in this space. The flow in the channel has been extensively characterised using PIV measurements. Qualitatively, we found that the flow was unidirectional, without separation, and that the velocity was essentially in the longitudinal plane. The turbulence rate (ratio of velocity fluctuations to the average velocity) varies from 2.7 to 4.2 % depending on the prescribed flow velocity (see the dedicated section in Annexes for details on the calibration of the swim tunnel). By controlling the speed of the motor, the flow velocity can be varied from 2 cm/s to 23 cm/s (i.e. from 0.6 to 5.9 BL/s, 1 BL = 3.7 cm).

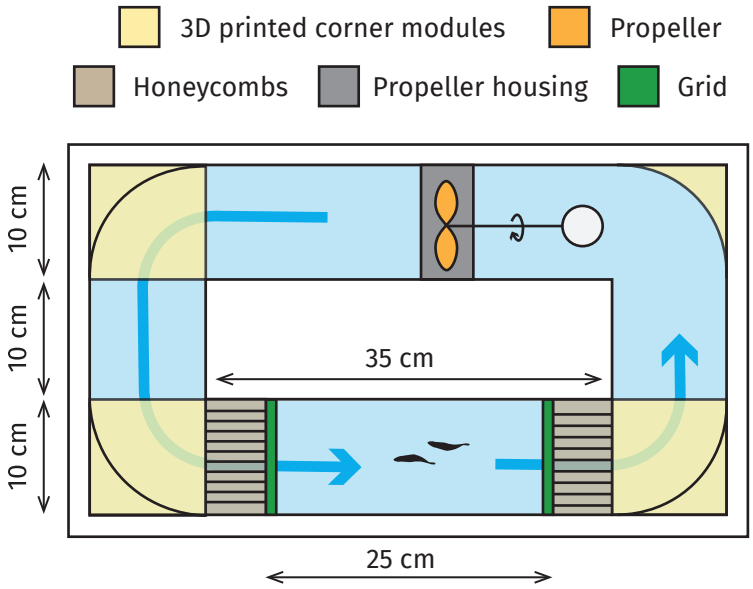

Figure 4.1: Schematic of the experimental setup (swim tunnel only, the large main tank is not represented). Tu blue arrows show the direction of the water current.

A 4 MPx camera (Basler ACa2000) was used to record the position and kinematics of the fish placed in the test section, placed approximately 1 m above the tank. It records 120 frames per second and is equipped with a fixed 35mm lens (Kowa, F1.4) sufficient to observe the entire longitudinal surface of the tunnel. The lighting for the camera is provided by a custom-made infrared LED panel (180W, 50 $\times$ 50 cm, 300 LEDs, LEDpoint) placed under the tank, allowing to obtain images with very good contrast without disturbing the fish with visible light, similar to the free-swimming experiment described in previous chapters. The entire experimental setup is surrounded by opaque walls. The sides are covered with sheets of opaque black plastic and the top with a rigid sheet of PMMA (plexiglass) that is only transparent to infrared light. In this way, no visible external light can enter the chamber, but the camera can record images thanks to infrared light. Inside the chamber, a strip of white LEDs controls the visible light to which the fish are exposed.

4.2.2 *Experimental procedure*

A typical experiments consists in recording forced swimming periods lasting from 10 to 30 seconds at 120 fps ($\mathrm{d}t$ = 8.3 $\times 10^{-3}$ s). We evaluate the role of different parameters on the kinematics and trajectories of the fish :

- The number of fish N is either 1 or 2
- The incoming flow velocity U is varied between 0.6 and 5.9 BL/s
- The visible light is either turned off or on

When the light is off, the swimming enclosure is completely dark. The light intensity measured in this case is below the sensitivity of the luxmeter (< 0.1 lux). If the light is switched on (12V voltage applied to the LED strip used for lighting), an ambient luminosity of 600 lux is measured.

Initially, before starting an experiment, N = 1 or 2 fish are selected at random from the rearing tanks. These fish are placed at rest in the swimming section without flow for 10 min, with medium light intensity (300 lux). During the experiment, the individuals are subjected to incident flows at 10 different velocities U randomly chosen between 0.6 and 5.9 BL/s. Only swimming events during which the fish swim continuously for at least 10 seconds are recorded. Acquisitions in which the fish explore the tank (particularly for incident velocities of less than 1 BL/s) or do not swim are discarded. After the experiment, the individuals studied are returned to a separate tank; they are only used for an experiment once a week at most. For all the experiments presented here, the floor of the swimming section was raised and the available depth was 5 cm. This depth is chosen to limit the crossing between fish or out-of-plane schooling during the two-fish experiments, making tracking and kinematic measurement impractical. However, this depth is still sufficient not to induce stress in the animals and is consistent with the usual values reported in the literature. At least 3 replicates of each experiment with a given triplet of parameters (N, U, light) is carried out, except for experiments with the lowest and highest values of U.

4.2.3 *Data processing*

CONTOUR EXTRACTION [1] A typical raw greyscale image acquired during experiments is represented on Figure 4.2. The fish shape is obtained by binarizing greyscale images, providing a fish silhouette. For each fish, we extract the contour which consists of M points in the 2D plane, that we denote x_n, y_n for $n = 1 \dots M$, describing

1 the codes developed for the data processing described in this section are open-source and made available on github

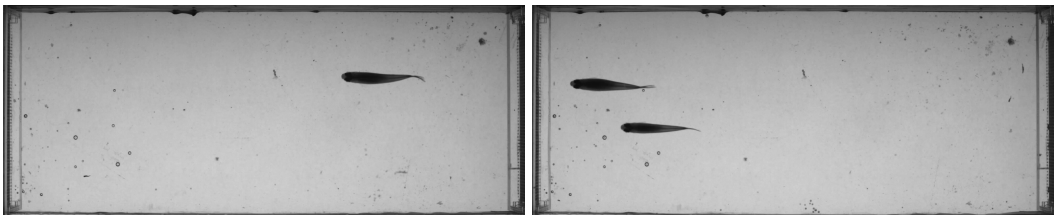

Figure 4.2: Examples of raw images obtained during swimming experiments. **left** N = 1 fish in the swimming section at U = 3.5 BL/s (light off). **right** N = 2 fish swimming at U = 2.4 BL/s (light on). The flow is going from left to right. Infrared illumination ensures a good image contrast and a similar lighting regardless of the ambient visible light intensity in the tank.

the boundaries of the black shape. Then, we compute the Fourier transform $S(k)$ of the signal $x_0 + iy_0, \ldots, x_M + iy_M$, which reads :

$$S(k) = \sum_{n=0}^{M-1} A_n e^{-i2\pi k \frac{n}{M}} \tag{4.1}$$

and keep only the first $M^\star$ Fourier coefficients A_n, with $M^\star = 16$. This method reduces the amount of data stored, smoothes the contour of the fish and obtains data whose size remain constant (unlike the initially extracted contour, that contains a variable number of points depending on the deformation of the fish's body). An exemple illustrating the extraction of the contour is shown on Figure 4.3.

MIDLINE EXTRACTION To accurately capture the kinematics of fish swimming, it is useful to know the position of the fish's centerline over time. The centerline is a curve running from the nose to the tail tip of an individual, passing through the centre of its body; it is used to describe the deformation of the fish's body over time.

In order to extract the position of the central line, we compute the Voronoi diagram (VORONOI, 1907) whose seeds are the contour points obtained previously. In this way, we define a set of regions in the plane such that each region contains all the points that are closer to one of the contour points than to any other point. In particular, the intersections of these Voronoi regions contained within the contour of the fish constitute a good approximation of the centerline (see Figure 4.4 for a visual explanation, and Figure 4.3 for an illustration of the method on experimental data). Finally, the midline is smoothed using the Savitzky–Golay convolution filter. An example of the extracted midline deformation over time is provided on Figure 4.5. This process is repeated for each time step of the experiment.

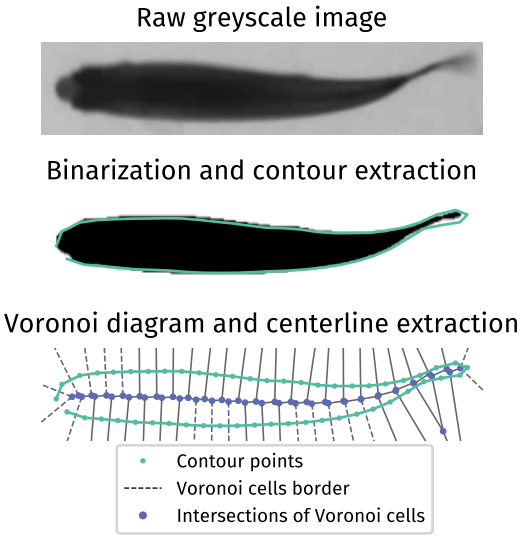

Figure 4.3: **top.** Raw experimental image of a fish in the swim tunnel. **middle.** Binarized black and white image and smoothed contour. **bottom.** Extraction of the midline points via the Voronoi diagram method: the midline is approximated by the intersections of the Voronoi cells that are inside the fish contour.

If the number of fish swimming in the experiment is $N = 2$, a tracking is also carried out, *i.e.* at each time step we check whether the identity of the fish has been preserved compared with the previous time step. Given the small number of individuals, this poses no particular technical issue: we simply assign to fish i the position $x(t + \mathrm{d}t)$, $y(t + \mathrm{d}t)$ that is closest to its position at time t.

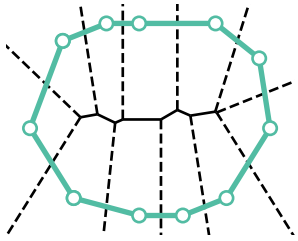

Figure 4.4: Example of the Voronoi diagram of a set of 2D points. The cyan dots are the seeds of the tilling, the black lines show the limits of the Voronoi cells (points that are closer from a given seed than to any other seed). Dashed lines represent borders that have infinite length.

4.2.4 *Measured quantities*

The points describing the contour and midline of each fish are extracted using the methods described above. From these physical quantities, we then compute derived kinematic measures that quantify the level of interaction between fish, the swim-

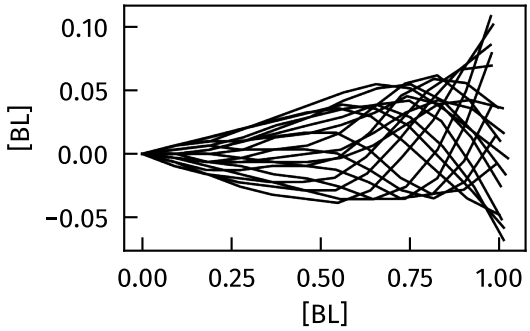

Figure 4.5: Midline deformation over time for a single fish swimming at 5.1 BL/s (no light). Each midline plotted is obtained from snapshots separated by 0.01 s in time. On this graph, the midlines are shifted so that the first point (nose of the fish) is always located in (0, 0).

ming efficiency and the rheotactic accuracy of the individuals (ability to maintain a stable position when swimming against a flow).

TAILBEAT To measure the characteristics of the tailbeat of each fish, we start by rectifying the positions of the points obtained for the midline with respect to the global orientation of the fish. If we consider a midline constituted of M points in 2D, the global orientation of the fish is considered to be the main direction of the first $M/3$ points of the midline (starting from the nose of the fish). By fitting a straight line to these first $M/3$ points, we find an orientation angle with the horizontal, that corresponds to the slope measured in this way. In this way, the displacement of each point along the midline can be broken down into two components: a transverse component (perpendicular to the overall orientation of the fish) and a longitudinal component (in the direction of the overall orientation of the fish). In the following, we will refer to the transverse component of the displacement of the tail tip as the "tail displacement". The tailbeat frequency and amplitude obtained from the tail displacement signal are proxies for the energy expenditure (cost of transport) of a fish (BAINBRIDGE, 1958; STEINHAUSEN, STEFFENSEN, and ANDERSEN, 2005).

The tail displacement signal is a complex numerical signal (see Figure 4.6 top panel), the frequency and amplitude (f_{tail} and A_{tail}) of which are not readily available using conventional methods (*e.g* the Fast Fourier Transform), due to the high noise and potentially time-varying frequency. To overcome these limitations, we use the Continuous Wavlet Transform (CWT): this method involves computing the convolution product of the signal with a set of Morlet wavelets (GROSSMANN and

MORLET, 1984) parameterised by their 'width' (*i.e.* their temporal frequency). This produces a spectrogram, that provides a robust estimate of the frequency and amplitude of the signal as a function of time, as well as an error estimate for these values. An example of CWT computed on an experimental signal is shown in Figure 4.6 (bottom panel).

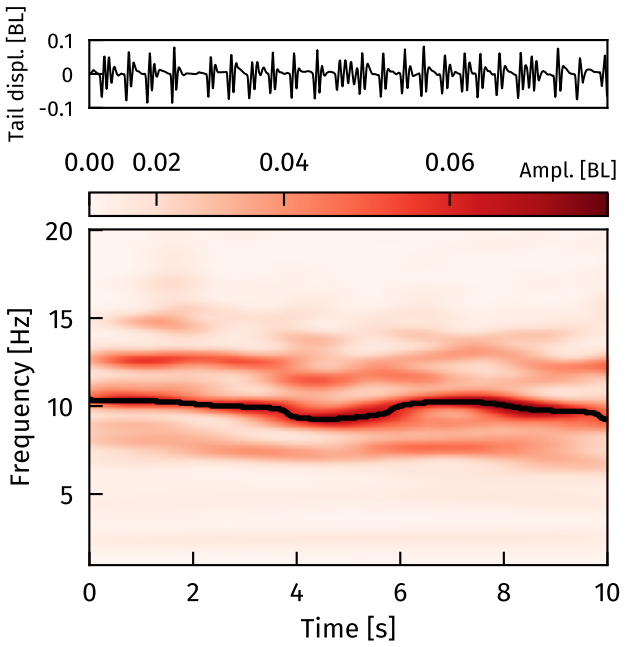

Figure 4.6: Illustration of the numerical method used to extract the tailbeat frequency and amplitude (experimental parameters here: U = 5.1 BL/s, no light). **top.** Raw signal of the tail tip displacement perpendicular to the fish global direction. **bottom.** Continuous Wavlet Transform (CWT) of the tail displacement signal. The black line in this graph follows the maximum amplitude of the CWT, providing both the tailbeat frequency and amplitude with respect to time.

POSITION We consider that the position of each fish is given by the position of the nose over time, $(x(t), y(t))$ its displacement with respect to its initial position $r(t)$ is thus:

$$r(t) = \sqrt{[x(t) - x(0)]^2 + [y(t) - y(0)]^2} \tag{4.2}$$

Figure 4.7 provides an exemple of a typical experimental timeseries of $x(t)$, $y(t)$ and $r(t)$. To assess the ability of the fish to maintain its average position when swimming, the amplitude of the variation in position of individuals (or positional

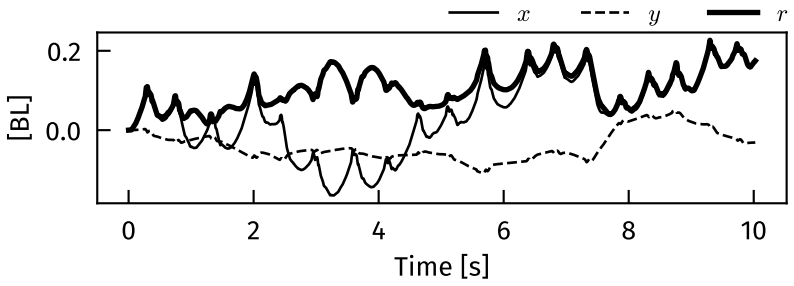

Figure 4.7: Timeseries of the displacement of a fish in the direction parallel to the incoming flow (x) and perpendicular to the flow (y). r represents the distance to the initial position ($r = \sqrt{x^2 = y^2}$)

variability) is evaluated using the standard deviation of r, denoted a. The expression for a is :

$$a = \sqrt{\frac{1}{N_T}\sum_{i=0}^{N_T}(r(i\,\mathrm{d}t) - \bar{r})^2} \tag{4.3}$$

where N_T is the number of time steps in the experiment and $\bar{r}$ is the average value of $r(t)$ over the duration of the experiment. Finally, for experiments with N = 2 fish, we also compute the distance d between individuals as a measurement of the level of interaction.

REMARK A metric commonly used to assess the intensity of rheotaxis behaviour is the rheotactic index RI (Bak-Coleman et al., 2013; Elder and Coombs, 2015) which is a measure derived from the angular deviation from the upstream direction. However, in the case of our experiments, this angular deviation remains mainly negligible, typically limited to angles of less than 5°, which makes this measure irrelevant here.

4.3 RESULTS

4.3.1 *General observations*

During the swimming experiments, we observe that the fish maintain or attempted to maintain a constant average position in the laboratory reference frame, oscillating around this position mostly in the streamwise direction x. The variations in position remain small in relation to the size of the tank (of the order of 1/10 to 1 BL, *i.e* approximately 3 to 30 mm). As shown in Figure 4.8, the variations in position are

negligible in comparison with the dimensions of the swimming tunnel, ruling out a priori the hypothesis that they would be influenced by the confinement of the walls. These streamwise position variations were strongly periodic, with a typical frequency of 2 Hz, due to intermittent swimming.

No favoured positioning was observed in the reference frame of the swimming section: the fish chose an average position close to the inlet or outlet of the tunnel with the same probability; generally, individuals did not touch the side walls and the upstream and downstream grids while swimming.

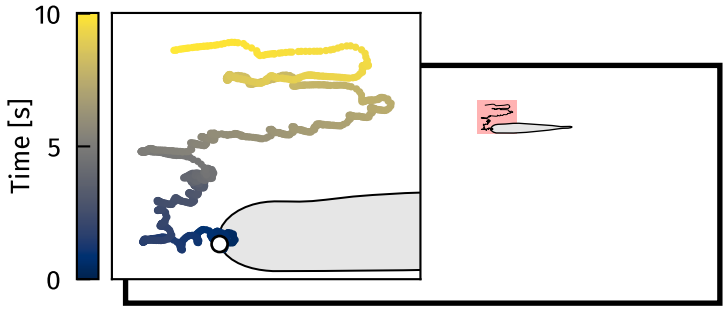

Figure 4.8: Temporal evolution of the position of a fish (the position of the nose is represented here, the fish body is shown by the gray silhouette) in the swim tunnel (U = 2.5 BL/s, light on). The black rectangle represents the swimming section limits, and the inset is a zoom on the red area. The flow in the swimming section is from left to right.

4.3.2 *Variations of the tailbeat kinematics*

Figure 4.9 (resp. Figure 4.10) shows the variations in the amplitude A_{tail} (resp. the frequency f_{tail}) of the fish tailbeat as a function of the incident flow velocity U. These quantities are computed using the methods described above, from the tail displacement signals, i.e. the transverse displacement of the tip of the tail (extreme point of the midline).

Overall, it can be seen that the amplitude is positively correlated with the flow speed: the greater the flow velocity, the larger the tailbeat amplitude. It varies from about 1% of the body length at low speeds to almost 10% at the highest speeds. For a fish swimming alone (N = 1, left panel) the tailbeat frequency is always higher when the fish is swimming in a lit environment compared to when it is swimming in an enclosure without light (Welch T-test, p = 1.54 $\times 10^{-4}$) and the positive correlation with speed is clear. For N = 2 (right panel) the fluctuations in the amplitude value are much greater. The amplitude remains greater in the illu-

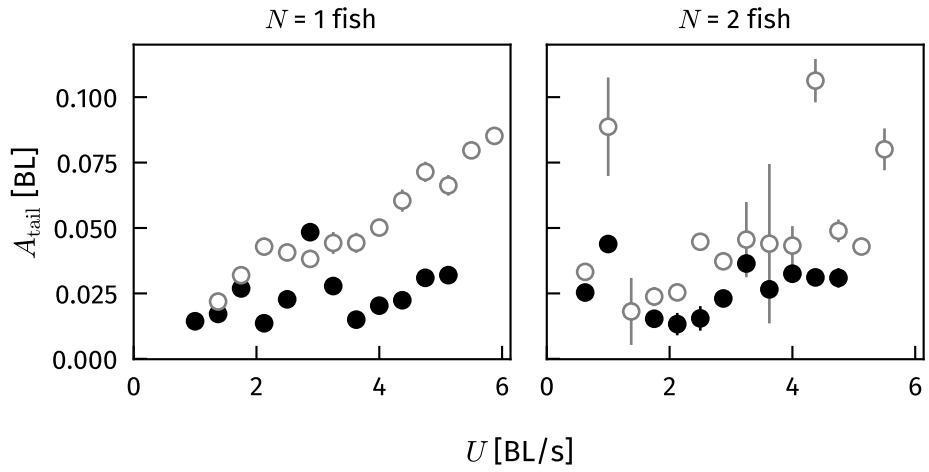

Figure 4.9: (●: light off - ○: light on) Tailbeat amplitude A_{tail} in fraction of the Body Length (BL) with respect to the incoming flow velocity U, for N = 1 (left) and N = 2 (right).

minated case, but with lower statistical significance (Welch T-test p = 1.27 $\times 10^{-3}$). On the other hand, the variations of the tailbeat amplitude A_{tail} with respect to U shows no clear trend for N = 2.

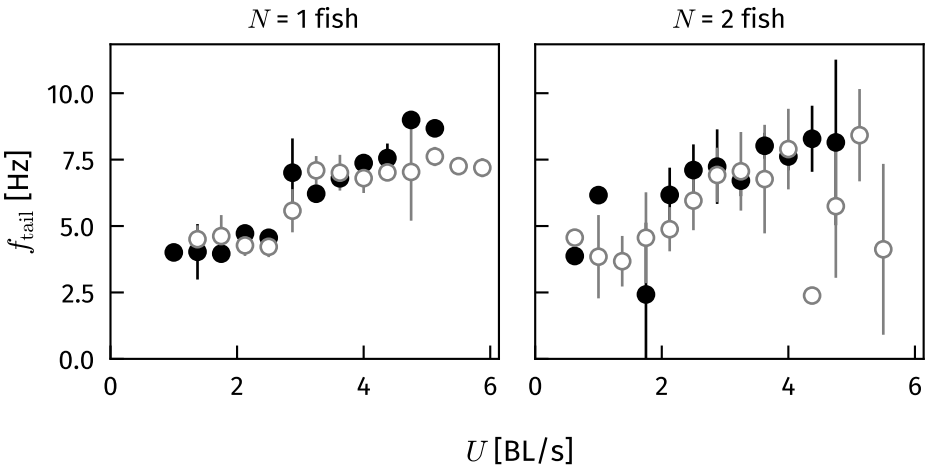

Figure 4.10: (●: light off - ○: light on) Tailbeat frequency in Hz with respect to the incoming flow velocity U, for N = 1 (left) and N = 2 (right).

Regarding the tailbeat frequency f_{tail}, as shown in Figure 4.10, a positive correlation with flow velocity U is also observed: the higher U, the more important is the frequency. f_{tail} varies from 4 Hz for the weakest flow velocities ($U \approx$ 1-2 BL/s) to 8-9 Hz for the strongest ones (6 BL/s). This is a classic observation that is verified in most aquatic species (Gazzola, Argentina, and Mahadevan, 2014; Herskin and Steffensen, 1998). However, it is noteworthy that, in our experiments, this re-

lationship does not seem to depend on either the number of individuals N or the illumination of the swimming channel.

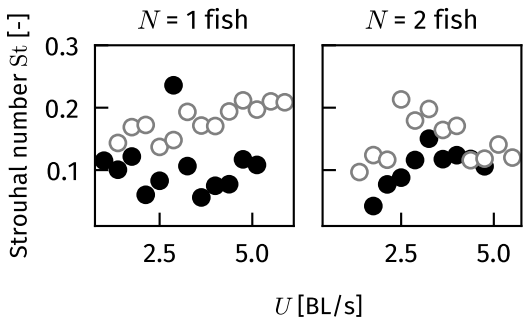

Figure 4.11: (● : light off - ○ : light on) Strouhal number of swimming fish with respect to flow speed U.

It may be noted that the Strouhal number St (TRIANTAFYLLOU, TRIANTAFYLLOU, and GOPALKRISHNAN, 1991), an dimensionless number linked to the arrangements of vortices in the wake of an oscillating body and defined by :

$$\mathrm{St} = \frac{f_{\mathrm{tail}} A_{\mathrm{tail}}}{U} \tag{4.4}$$

is relatively constant here, as can be seen from Figure 4.11. This observation is commonly made for animal locomotion, particularly aquatic oscillatory locomotion (ELOY, 2012), and confirms the quality of our measurements. The St values reported here are in the lower range of those reported in the literature (usually 0.2 < St < 0.3).

Tailbeat amplitude and frequency are indirect metrics of the fish cost of transport, i.e. their energy consumption necessary to maintain their position in the flow. These experimental results on swimming kinematics show that energy expenditure increases as flow velocity increases, and that the number of fish N or illuminance do not modify this trend.

4.3.3 *Rheotactic performance*

The rheotactic accuracy is measured as a function of the experimental parameters. In particular, the positional variability a, which corresponds to the standard deviation of the distance from the initial position r, is an indicator of this accuracy: the lower a is, the more precise the rheotaxis. Variations of a with respect to to the experimental parameters are shown in Figure C.6. Here, the data is divided into three categories according to the incident flow velocity U: low velocity (U > 2BL/s), cruising velocity (U between 2 and 4 BL/s) and high velocity (U > 4BL/s). We also assessed the impact of collective swimming by comparing the cases with one or two fish. In all cases, we observed that the precision was restricted to values between 0.1 and 0.5 BL on average. The distribution of data is wider for experiments

involving 2 fish.

Strikingly, for N = 1, the positional variability a decreases in the non-illuminated cases. This is true for cruising speeds (p = 0.043) and for high speeds (p = 0.0025), while the difference is statistically non-significant in the low speed cases. For N = 2, there is no statistically significant differences if the light is on or off in terms of positional variability.

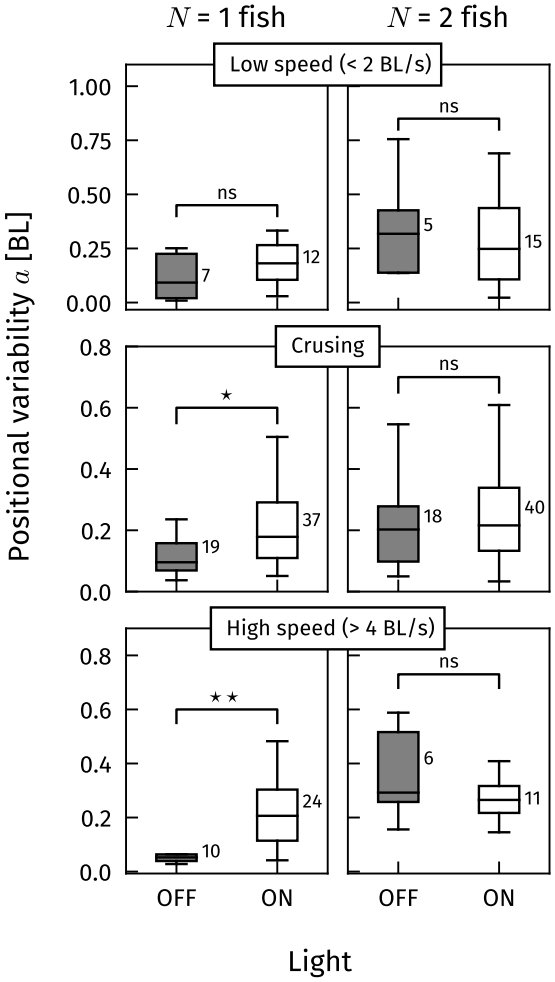

Figure 4.12: Positional variability a (standard deviation of the distance to initial position r) with respect to the lighting of the swimming tank, for three different flow velocity regimes. The left column (resp. the right column) show the data for N = 1 fish (resp. for N = 2 fish). p-values of the Welch T-Test for the means: (ns) non-significant, ($\star$) p < 0.05, ($\star\star$) p < 0.01. The numbers on the right of the boxplots are the sample size.

4.3.4 *Inter-fish distance*

For cases with two fish, the distance between individuals d is computed. The distributions of values for d are shown in Figure 4.13. We observe that with high statistical significance (p = 0.00134), the distance between fish is higher when the light is turned off. When the light is off, the fish swim at a typical distance d = 2.5 BL from each other, with distance values ranging from 1 to 6 BL. Conversely, in cases where the light is switched on, the fish pairs are found at much smaller distances and much less dispersed, of the order of 1 BL on average, and 2 BL at the maximum.

Figure 4.14 shows the decomposition of d in streamwise d_x and spanwise d_y contributions. This last graphs reveals that the variations of d are exclusively due to variations of the streamwise distance between fish, while the spanwise distance remains constant between lit or unlit conditions. This means that in non-illuminated cases, the fish are placed one behind the other and form a line in the streamwise direction.

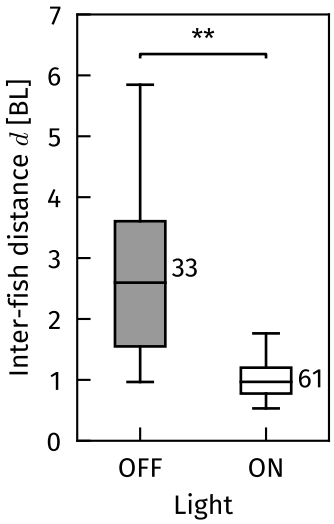

Figure 4.13: Distance between fish for experiments with N = 2, with respect to lighting conditions. p-values of the Welch T-Test for the means: ($\star\star$) p < 0.01.

4.4 DISCUSSION

The data presented in this Chapter sheds light on the emergence and accuracy of rheotactic behaviour for single fish or pairs of fish. Placed in total darkness, the fish studied have only their lateral line to assess the speed of the flow in which

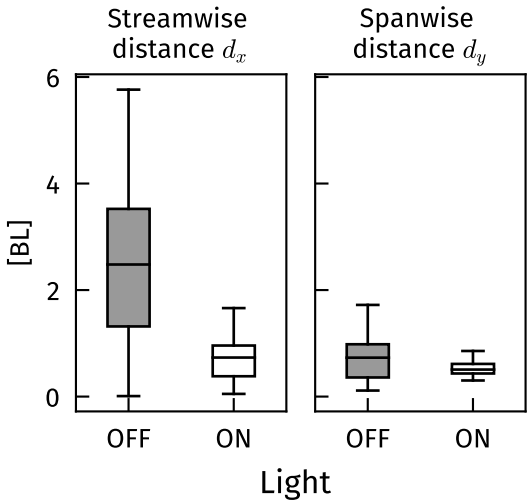

Figure 4.14: Decompostion of the distance d presented on Figure 4.13 in terms of streamwise d_x and spanwise d_y contributions, with respect to lighting conditions.

they are swimming, and adapt their gait accordingly to maintain a stable position. By limiting the amplitude of positional variation, the individuals are better able to use their lateral line to assess the average speed and structures in the flow. This may explain the low values of the positional variability a found in the unlit cases for solitary fish. This hypothesis is consistent with the observation in Figure 4.9 that the tail beat amplitude is reduced in the unlit case and for $N = 1$. Indeed, this behaviour potentially makes it possible to limit the disturbances generated by the individual itself on its environment, and therefore to improve hydrodynamic sensing. Elder and Coombs (2015) noted a different trend for similar experiments: their study reported greater position variability for fish with impaired vision (swimming in a dark environment) than for fish with visual cues. However, there is notable differences between this study and the present results, since the fish in Elder's study oscillate essentially in the span wise direction, and much more slowly (in order of magnitude: a few oscillations per minute).
The data concerning the distance d between fish suggests *a priori* a decrease in interaction between individuals for cases with no light, since d increases in these situations. However, the fact that the follower fish places itself behind the fish in front, without modifying the lateral distance, indicate that interaction may still occur via hydrodynamic sensing in the absence of visual information.

Overall, the data show no clear difference in terms of energy consumption (assessed indirectly via the kinematic quantities A_{tail} and f_{tail}) for solitary fish or pairs

of fish, whatever the lighting conditions. Additional direct measurements of cost of transport for schools of different sizes are reported in Appendix B.

4.5 PERSPECTIVES

To complete the results presented here, it might be useful to repeat the experiments with a larger number of fish in order to assess whether the trends observed for positional variability a are maintained for larger groups.

One of the pitfalls of this experiment is that the fish may be aware of the structure and size of the channel, as well as the presence of neighbours, even in unlit conditions. Indeed, the individuals always have the possibility of obtaining visual information during their transfer into the tank. To solve this problem, it is possible to use blind fish, such as *Astyanax mexicanus*. This tetra, native from eastern Mexico, is a fresh water fish that regroup multiple populations, some of which evolved to completely lose vision depending on their habitat (surface or caves).

Figure 4.15: Two forms of the *Astyanax mexicanus* species: surface-dwelling form with eyes (top) and blind, cave-dwelling form without eyes (bottom). The typical size of this fish is 7 to 8 cm for males and 8 to 9 cm for females. Credit: University of Maryland

REFERENCES

BAINBRIDGE, B. Y. R. (1958). "The Speed of Swimming of Fish as Related to Size and to the Frequency and Amplitude of the Tail Beat." *Journal of Experimental Biology* (cit. on p. 72).

BAK-COLEMAN, J., A. COURT, D. A. PALEY, and S. COOMBS (2013). "The Spatiotemporal Dynamics of Rheotactic Behavior Depends on Flow Speed and Available Sensory Information." en. *Journal of Experimental Biology*. DOI: 10.1242/jeb.090480 (cit. on pp. 66, 74).

BAKER, C. F. and J. C. MONTGOMERY (1999). "Lateral Line Mediated Rheotaxis in the Antarctic Fish Pagothenia Borchgrevinki." *Polar Biology*. DOI: 10.1007/s003000050366 (cit. on p. 66).

Coombs, S., J. Bak-Coleman, and J. Montgomery (2020). "Rheotaxis Revisited: A Multi-Behavioral and Multisensory Perspective on How Fish Orient to Flow." *Journal of Experimental Biology*. doi: 10.1242/jeb.223008 (cit. on p. 66).

Elder, J. and S. Coombs (2015). "The Influence of Turbulence on the Sensory Basis of Rheotaxis." en. *Journal of Comparative Physiology A*. doi: 10.1007/s00359-015-1014-7 (cit. on pp. 66, 74, 80).

Eloy, C. (2012). "Optimal Strouhal Number for Swimming Animals." *Journal of Fluids and Structures*. doi: 10.1016/j.jfluidstructs.2012.02.008 (cit. on p. 77).

Enders, E. C. and DA Scruton (2006). *Potential Application of Bioenergetics Models to Habitat Modeling and Importance of Appropriate Metabolic Rate Estimates with Special Consideration for Atlantic Salmon*. Science Branch, Fisheries and Oceans Canada (cit. on p. 67).

Gazzola, M., M. Argentina, and L. Mahadevan (2014). "Scaling Macroscopic Aquatic Locomotion." en. *Nature Physics*. doi: 10.1038/nphys3078 (cit. on p. 76).

Grossmann, A. and J. Morlet (1984). "Decomposition of Hardy Functions into Square Integrable Wavelets of Constant Shape." *SIAM journal on mathematical analysis*. doi: 10.1137/0515056 (cit. on p. 72).

Herskin, J. and J. F. Steffensen (1998). "Energy Savings in Sea Bass Swimming in a School: Measurements of Tail Beat Frequency and Oxygen Consumption at Different Swimming Speeds." en. *Journal of Fish Biology*. doi: 10.1111/j.1095-8649.1998.tb00986.x (cit. on p. 76).

Lupandin, AI, PI Kirillov, and DS Pavlov (2003). "Experimental Study of Feeding of the Dace Leuciscus Leuciscus at Different Current Velocities." *Journal of Ichthyology* (cit. on p. 66).

Pavlov, DS, AI Lupandin, and MA Skorobogatov (2000). "The Effects of Flow Turbulence on the Behavior and Distribution of Fish." *Journal of ichthyology* (cit. on p. 66).

Steinhausen, M. F., J. F. Steffensen, and N. G. Andersen (2005). "Tail Beat Frequency as a Predictor of Swimming Speed and Oxygen Consumption of Saithe (Pollachius Virens) and Whiting (Merlangius Merlangus) during Forced Swimming." en. *Marine Biology*. doi: 10.1007/s00227-005-0055-9 (cit. on p. 72).

Triantafyllou, M. S., G. S. Triantafyllou, and R. Gopalkrishnan (1991). "Wake Mechanics for Thrust Generation in Oscillating Foils." en. *Physics of Fluids A: Fluid Dynamics*. doi: 10.1063/1.858173 (cit. on p. 77).

Tritico, H. M., A. J. Cotel, and A. J. Cote (2010). "The Effects of Turbulent Eddies on the Stability and Critical Swimming Speed of Creek Chub (Semotilus Atromaculatus)." *Journal of Experimental Biology*. doi: 10.1242/jeb.041806 (cit. on p. 66).

Voronoi, G. (1907). "Nouvelles Applications Des Paramètres Continus à La Théorie Des Formes Quadratiques. Deuxième Memorie: Recherche Sur Les Parallélloèdres Primitifs." *Journal fur reine und angewandte Mathematik* (cit. on p. 70).

Webb, P. W., A. Cotel, and L. A. Meadows (2010). "Waves and Eddies: Effects on Fish Behavior and Habitat Distribution." In: *Fish Locomotion*. CRC Press (cit. on p. 66).

5

GENERAL CONCLUSION AND PERSPECTIVES

This thesis focused on collective motions in schools of fish. In particular, we attempted to shed light on how variations in environmental parameters can influence interactions between individuals within a group, and consequently the organisation of that group. Using simplified laboratory experiments, we varied these environmental parameters in a controlled manner and observed the motions of groups of fish in response to these perturbations. The model species chosen for these experiments is Hemigrammus rhodostomus, a small gregarious tropical fish.

We were able to show that light plays a major role in the emergence of collective motion: in the absence of lighting, schools of around 50 fish were unable to swim in a coordinated fashion. Conversely, as the light intensity gradually increases, the school goes through different behavioural phases, with an initially highly polarised organisation followed by a state of rotation (milling) that is stable over time above a light level threshold. The limits of the swimming range also play a part in determining the collective state observed for a group of interacting agents. In the case of schools of 10 to 70 fish, it has been shown that reducing the available swimming area and increasing the number of fish in the school have equivalent effects: the greater the confinement (measured by the density of fish per unit area), the greater the probability of moving from a polarised state to a rotating state. Finally, the behaviour of rheotaxis was studied, i.e. the aptitude of a fish or a group of fish to swim against the current. In particular, the ability to maintain a stable position for single fish and pairs of fish, considered as the minimum constitutive cell of a school, was measured during forced swimming experiments in a swim tunnel. The tests were repeated in illuminated and dark environments. The results suggest that flow sensing is used by fish in unlit conditions, but is not essential in lit conditions.

PERSPECTIVES One of the most promising avenues for extending the experimental results presented here is to carry out numerical simulations of self-propelled particles interacting with each other through a certain number of social rules, with the aim of reproducing the behaviour observed in fish. In particular, we know that light influences collective behaviour indirectly, by modifying the visual information available. However, we do not fully understand its role on viewing angle, viewing distance or the number of neighbours considered by each neighbour in its interaction rules. By modulating these parameters in a numerical simulation, we can relate light intensity and physiological characteristics indirectly. Such simulations can also confirm the results obtained concerning collective motion in confinement, to offer a generalisation beyond fish schools.

APPENDIX

This appendix is divided into two sections: Appendix A provides details on the design of the swim tunnel and the characterisation of the flow in the test section of this tunnel by PIV. Appendix B reports additional direct measurements of the cost of transport of schooling fish using respirometry.

A

SWIM TUNNEL DESIGN

A.1 CHARACTERISATION OF THE FLOW IN THE SWIM TUNNEL

This section presents the characterisation of the flow through the test section of the swim tunnel presented in Chapter 4.

SETUP AND METHODS The Particle Image Velocitmetry (PIV) method is used to measure this flow. The principle of PIV is the following: a flow is seeded with plastic particles (polyamide in our case) of small size (typically 10 to 100 microns in water). The fluid is illuminated by a thin laser sheet, whose light is reflected by the particles. The size of the particles ensures that they follow the flow without disturbing it, while preventing them from settling. By recording with a video camera the light reflections created by the particles over time, an image correlation algorithm can be used to reconstruct a time-dependent velocity field in the plane of the laser sheet.

In practice, the algorithm divides all the images into interrogation windows, in the present case of 32 pixels by 32 pixels. It compares two successive images by estimating, for each window, what is its most probable position in the next image. This produces a 2D velocity field, with a vector attached to each window. In our case, we obtain a field of 60 $\times$ 40 vectors, since the recorded images are 1920 $\times$ 1280 pixel in size. This procedure is repeated for each pair of frames, thus producing a time-dependant velocity vector field in 2D. We used the OpenPIV module in Python to process images and extract velocity fields.

The laser is positioned so as to illuminate a part of the horizontal plane of the test section (a 10 $\times$ 20 cm rectangle), at two different heights from the bottom floor of the section h (h = 5 cm, approximately in the middle of the height of the section, and h = 10 cm, almost at the top of the section). A camera positioned above the system records greyscale images at a rate of 120 frames per second.
The aim here is to calibrate the flow, *i.e*:

- establish the relationship between the average flow velocity in the section and the input voltage to the motor rotating the propeller responsible for setting the water in motion
- observe the flow structure to ensure that there is no excessive velocity gradient, that the turbulent intensity remains acceptable (typically less than 10%) and that there are no recirculation zones.

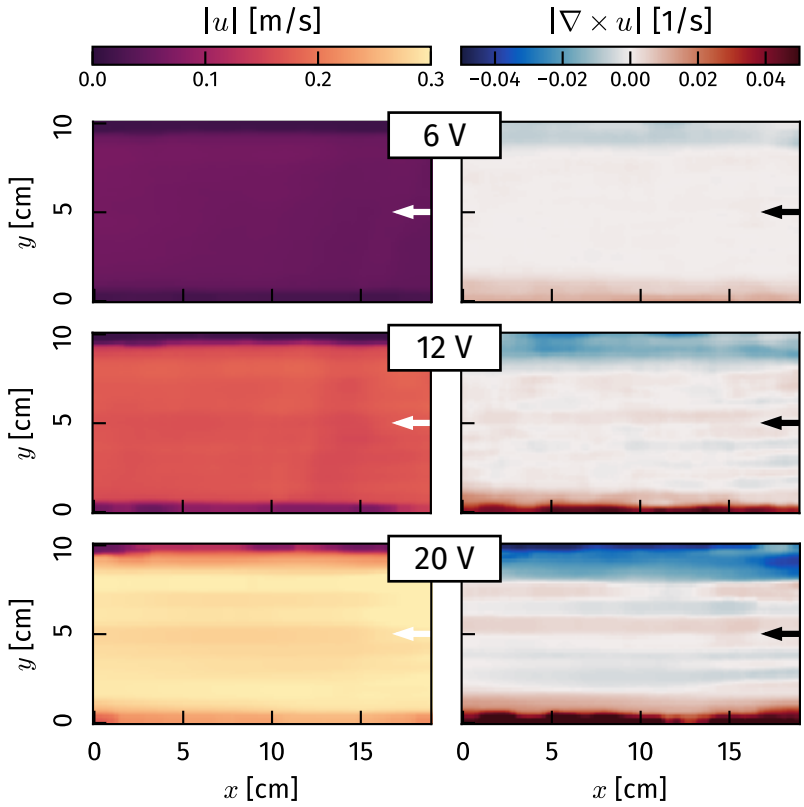

Figure A.1: Time-averaged flow in the test section, for different voltages input to the motor (6, 12, and 20 V), obtain with PIV measurements. The flow is going from right to left (arrows). **left.** Norm of the flow velocity $|u|$. **right.** Norm of the flow vorticity $|\nabla \times u|$.

In order to perform this calibration, PIV flow recordings are repeated for input voltages between 5 and 31 V, at the two chosen heights h, each recording lasting 60 s. In all the experiments, the floor used to reduce the depth available to the fish is left in place, to faithfully reproduce the experimental conditions of the forced swimming tests as described in Chapter 4. From the velocity fields u thereby obtained, we can also compute the vorticity field $|\nabla \times u|$, which provides local in-

formation about the intensity of the vortical structures in the flow.

Figure A.1 shows the velocity norm $|u|$ and the vorticity $|\nabla \times u|$, time-averaged over the whole duration of the recording (60 s), for h = 10 cm. The flow is going from right to left (arrows in Figure A.1). Firstly, we note that the velocity is highly homogeneous in the test section, particularly in the streamwise x direction. In the spanwise y direction, the walls cause a boundary layer to develop, resulting in a lower velocity near them. This boundary layer induces shear in this area of the flow, which results in higher vorticity values, especially as the mean velocity U increases. Figure A.2 shows the profil of the norm of the velocity in the y-direction, averaged over time and over the streamwise direction x.

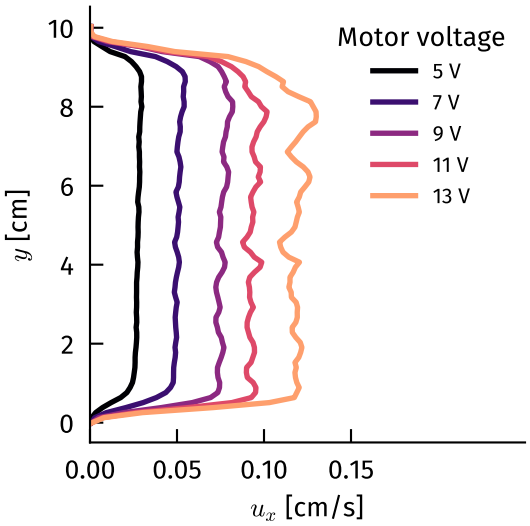

Figure A.2: Profil of the velocity in the streamwise direction u_x, for different voltage input to the motor driving the flow (color-coded), for h = 10 cm.

This graphs confirms the presence of a boundary layer, with zero velocity at the walls. It can also be seen that the profil is characterised by noise as the motor input voltage (and hence the average velocity of the flow) increases, with greater variations in central part of the velocity profil.

TURBULENT INTENSITY To assess the level of velocity fluctuations in the flow, we evaluate the turbulent intensity τ, defined as follows:

$$\tau = \frac{\sqrt{\frac{1}{3}(\tilde{u}_x + \tilde{u}_y + \tilde{u}_z)}}{U} \tag{A.1}$$

where $\bar{U}$ is the mean velocity of the flow, and $\tilde{u}_x = u_x - U$ (resp. $\tilde{u}_y = u_y - U$) is the velocity fluctuation in the streamwise (resp. spanwise) direction. Here we we

do not have access to the last velocity component u_z with the PIV, but we make the hypothesis that $u_z = u_y$ because of the symmetries of the channel geometry. The values of τ with respect to the input voltage are reported on Figure A.3. The overall trend observed is that of an increase in τ as the motor voltage increases. We note that τ remains limited to values below 7%, which is within the low range of the standards for swimming channels and water flumes.

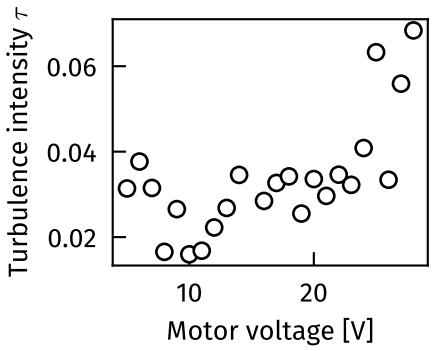

Figure A.3: Turbulent intensity in the test section of the swim tunnel, with respect to the input voltage of the motor.

VOLTAGE - FLOW SPEED RELATIONSHIP The main information that this calibration is designed to provide is the relationship between the input command (constant voltage) sent to the motor and the resulting mean flow velocity. This information is reported on Figure A.5, for both depths h = 5 and 10 cm. The data is well approximated by an affine function for the whole range of voltage input tested. The slope of the fit is slightly higher at h = 5 cm compared to h = 10 cm, which is probably due to the proximity to the upper lid of the swimming section in the case h = 10 cm.

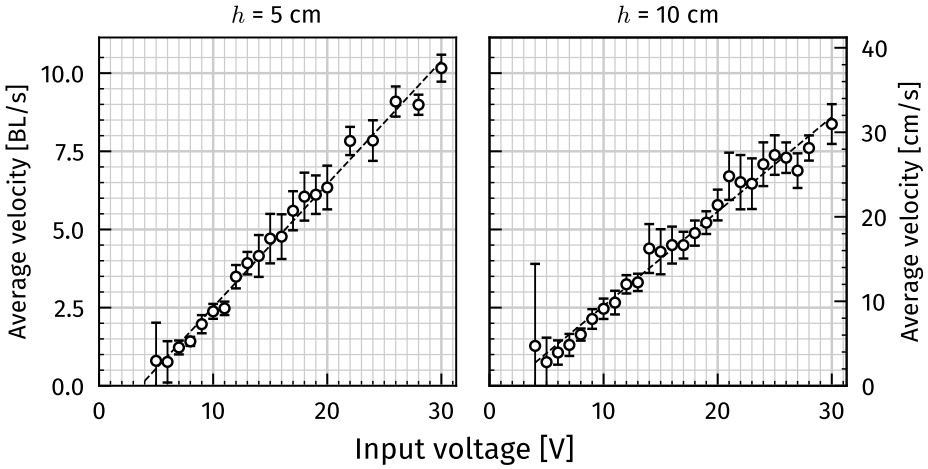

Figure A.4: Flow speed in the test section (in cm/s or in Body Lengths BL/s) with respect to the motor input voltage, for the different depth h (height at wich the laser sheet is placed).

A.2 GLOBAL VIEW OF THE SWIM TUNNEL EXPERIMENTAL SETUP

This last photograph (Figure A.5) shows the swimming channel as a whole, to help the reader visualise the experimental setup as a whole.

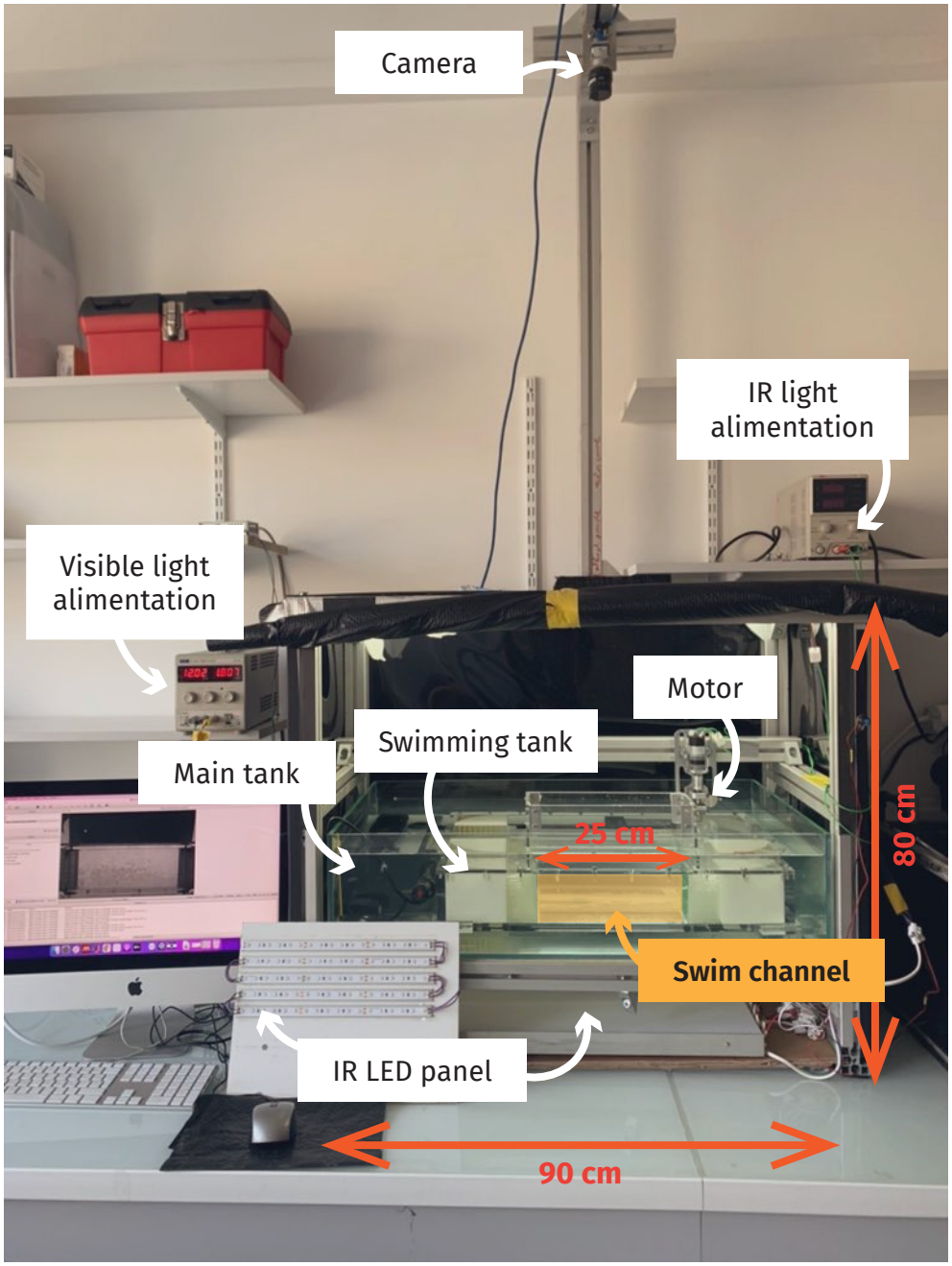

Figure A.5: Global view of the swim tunnel experimental setup

B

DIRECT MEASUREMENT OF THE COST OF TRANSPORT FOR DIFFERENT FISH SCHOOL SIZES BY RESPIROMETRY

As mentionned in Section 1.2, schooling of fish is considered to be a possible way for individuals to reduce their cost of transport (COT), i.e. the energetic cost associated with their displacements. Recent studies (Ashraf et al., 2017) have indirectly measured (via tailbeat frequency) a reduction of the COT for groups of *Hemigrammus rhodostomus* forced to swim in a swimming canal, as a function of the number of individuals in the school. However, there is no systematic study directly measuring the energy consumption of individuals as a function of the size N of the group. The only experimental means of directly measuring COT is to assess the metabolic rate of the school, i.e. the oxygen consumed per unit of time. This method is called respirometry.

In this section, we report experimental results on the measurement of metabolic rate of schools of sand smelts (*Atherina presbyter*, see Figure B.1) comprising N = 1 to 11 individuals in forced swimming, for different flow speeds. These experiments were carried out during a collaborative exchange in the summer of 2022 in Valentina di Santo's team (Stockholm University).

B.1 EXPERIMENTAL APPARATUS AND METHODS

SETUP AND MEASURED QUANTITIES In order to assess whether the number N of fish in a school subjected to a flow influences the average metabolic rate of the individuals, we use a swimming tank setup (Loligo systems), similar to that described in Section 4.2. The swimming tank itself is placed in a large buffer tank where the temperature, quality and salinity of the water is controlled. The dimensions of test section of the swimming tank in the vertical plane are 48 $\times$ 14 cm.

The upper lid of the tank is watertight and gastight, which allows for measurements of the dioxygen (O_2) concentration in the water contained in the tank, over time. For this measurement, we use a sensor consisting of an optical fiber probe, immersed in the flow where the group swims. The small size of the sensor (2 cm diameter, 4 cm height cylinder) limits the disturbance created in the flow. A sealed hole in the lid of the tank ensures that the watertightness of the swimming tank is

not compromised when the sensor is in place. The oxygen sensor measures the O_2 concentration c_{O_2} in mg of O_2 per liter of water, every second ($\mathrm{d}t$ = 1 s). Its measurement range is 0 to 45 mg/L, with a precison of 0.05 mg/L. Since the exact volume of water in the tank is V = 47.8 L, we get the quantity of O_2 consummed at time t in mg, $m_{O_2}(t)$, with:

$$m_{O_2}(t) = V\left(c_{O_2}(t) - c_{O_2}(0)\right) \tag{B.1}$$

where t = 0 is the starting time of the experiment. In the litterature, the metabolic rate is usually given in milligrams of O_2 consummed per kilograms of fish body mass, per hour ($mg_{O_2}/kg_{fish}/h$). We thus weight the fish used before each experiment to evaluate this quantity precisely (mass m ranging from m = 1.3 g to 3.1 g, average $\langle m \rangle$ = 2.1 g, standard deviation σ = 0.56 g, for 108 individuals).

MODEL ORGANISM For this study we used the sand smelt, which is a marine fish of the family *Atherinidae*. It is a common species originating from costal areas and estuaries in the north-eastern Atlantic, with a length that can reach up to 18 to 20 cm in the wild. The specimen used in this study are 6 to 7 cm long.

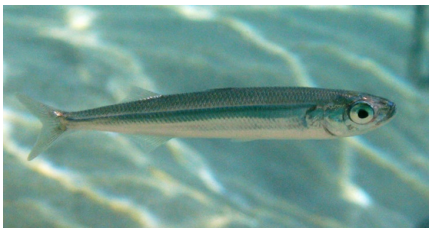

Figure B.1: A specimen of sand smelt (*Atherina presbyter*)

EXPERIMENTAL PROCEDURE AND PARAMETERS Similar to the setup described in Chapter 4, a DC motor rotates a propeller in the return section of the swim tunnel. This propeller sets the water in motion, generating flow speeds of 1 to 7 BL/s in the test section (1 BL = 6.4 cm $\pm$ 0.5 cm, measured on average over 10 individuals). The experimental parameters controlled in this experiment are the following:

- The flow speed U, from 1 to 7 BL/s, by steps of 1 BL/s
- The number of fish in the school N, ranging from 1 to 11 individuals. We selected 8 values for N (1, 2, 3, 4, 5, 7, 9, 11).

An experiment consists of letting N fish swim in the test section, for increasing flow speeds U, starting with U = 1 BL/s. For each speed, the school swims for 15 min at the set speed, then the flow is cut off for a recovery period of at least 5 min (5 to 7 min in practice). This procedure is repeated until the speed U = 7 BL/s is reached, or a fatigue behaviour is observed in at least one of the fish in the group

(typically the fish stops swimming and drifts into the flow). During this experiment, the oxygen concentration in the water is continuously monitored. An example of an experimental signal of the dioxygen consumption for N = 11 fish is shown on Figure B.2. For each pair of values (N, U), 3 replicates of the same experiment are carried out. In all cases, we ensure that the percentage of dissolved dioxygen in the water (the ratio between the measured concentration and the maximum concentration at 20°C, *i.e* 9.1 mg/L) is always greater than 90%, in order to prevent any risk of hypoxia for the fish.

After each experiment, the individuals are placed back in their rearing tank. The large number of the fish in this tank ($\sim$ 200 individuals) ensures that the animals are selected at random. Two successive experiments are carried out at least 24 hours apart.

EVALUATION OF THE METABOLIC RATE Figure B.3 (top panel) shows a time-series of the dioxygen consummed by this fish (here in mg/fish) for the different flow speeds (the recovery periods are removed from the signal). To measure the temporal rate of change of this quantity (metabolic rate MO_2), we assume that, for each swimming period of 15 min at a given flow speed U, the dioxygen consumption is an affine function of the time t. We thus extract the slope of this function with a standard least square method. The value of this slope (converted to the usual unit system) is the average metabolic rate (shown in Figure B.3, bottom panel). The values measured are typically ranging from 200 to 800 $mg_{O_2}/kg_{fish}/h$, which is consistent with previous similar studies (Chrétien et al., 2021).

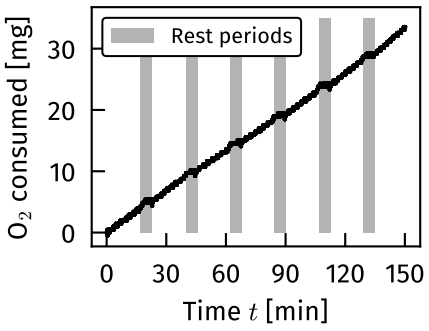

Figure B.2: Typical acquisition signal of the dioxygen consumption (in mg) in the swimming tank. Each rest period (in gray) last approximately 5 min. The flow velocity is increased from 1 to 7 BL/s by steps of 1 BL/s. Swimming periods last 15 min. Here N = 11 fish.

BACKGROUND RATE Measurements of the metabolic rate are affected by the background rate. This is a decrease in the concentration of dioxygen in the tank water, even in the absence of fish. This phenomenon is due to two factors: (1) the

presence of micro-organisms in the water, which can consume some of the available dioxygen, and (2) any leaks in the equipment, in particular the hole through which the dioxygen probe passes. The background rate also depends on the flow velocity U. To evaluate this background rate, we carry out an experiment similar to the swimming experiment, but in the absence of fish: we measure the time evolution of the dioxygen concentration in the water, for flow speeds U from 1 to 7 BL/s. The measurement period is 15 min for each U. A dioxygen depletion rate as a function of U is extracted from these measurements, with the method described in the previous paragraph; it is plotted in Figure B.4. It should be noted that these values are not negligible, as the typical consumption of a single fish is of the order of 1 mg_{O_2}/h, the background metabolic rate can thus correspond to the dioxygen consumption of approximately 1 to 5 fish depending on the value of U. These values of background rate are thus systematically subtracted from the measured values in each swimming experiment, for the corresponding value of U.

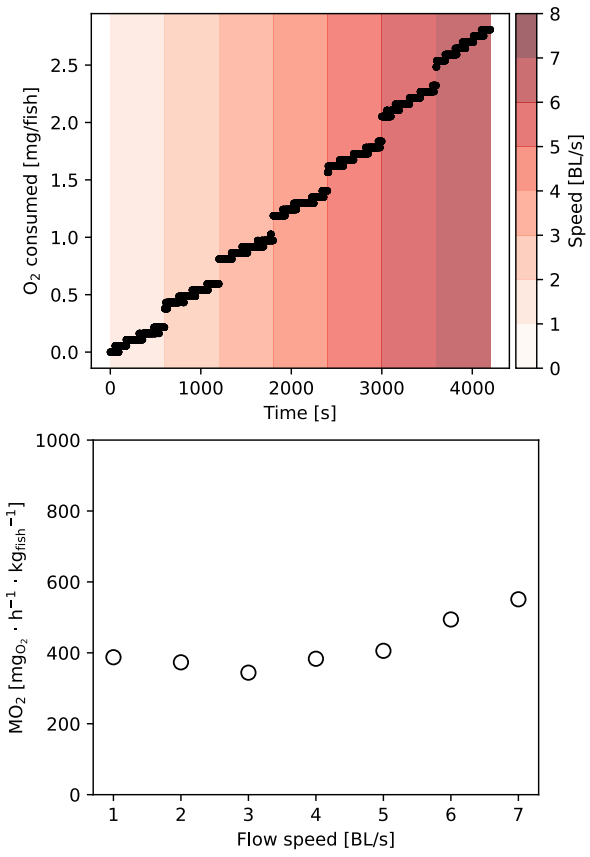

Figure B.3: **top.** Dioxygen consumption per individual in the tank for $N = 11$ fish as a function of time, for different flow speeds U represented by the colors. The recovery periods are removed from this time signal. **bottom.** Average metabolic rate with respect to U.

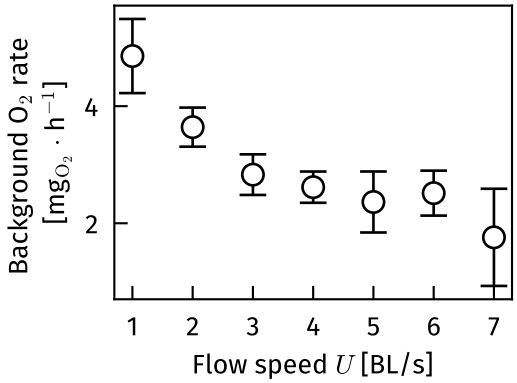

Figure B.4: Background metabolic rate (O_2 consumption rate in the absence of fish) in the swimming tank, with respect to the flow speed U. The errorbars show the standard deviation of the temporal signal.

B.2 EXPERIMENTAL RESULTS

Figure B.5 displays the experimental results averaged over all replicates and over all values of flow velocity U. It presents the dioxygen consumption rate in mg/h as a function of the number of fish (the background metabolic rate has been subtracted from these values). This rate ranges from approximately 1 to 12 mg_{O_2}/h for the different school sizes tested. It can be seen that the O_2 consumption rate depends linearly on the number of fish in the school N, as shown by the linear fit represented in the figure. This observation suggests *a priori* that the number of fish N has little or no influence on the average metabolic rate per individual, i.e. on the cost of transport of the fish.

We can examine the data further on Figure B.6. The graph on the left shows the metabolic rate MO_2 with respect to the number of fish N, for all the different flow speeds U. We can see that the value of MO_2 remains approximately in the order of 500 $mg_{O_2}/kg_{fish}/h$, irrespective of the number of fish in the school N, with little dependence on U. However, we note that for $N = 1$ (fish swimming alone), this value seems higher on average. This difference is particularly visible in the panel on the right on Figure B.5, which shows MO_2 as a function of N, averaged over all U values.

This increase is notably significant for the highest U values ($U > 4$ BL/s). These results seem to point to a possible energy-saving mechanism when fish swim in groups compared to when they swim alone. This effect is binary between swimming

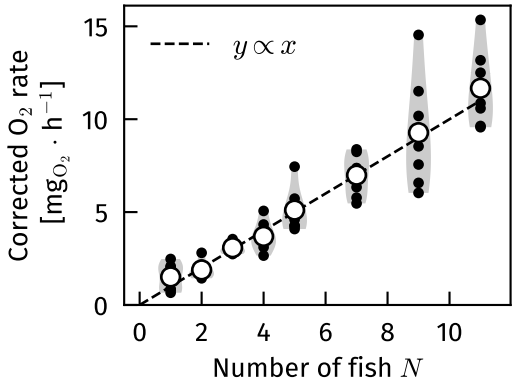

Figure B.5: Dioxygen consumption rate corrected from backgound rate, with respect to the number of fish in the group N. Each black dot (•) is the experimental data averaged over the 3 replicates of an experiment at a given flow speed U. White points (○) are the date averaged over the replicates and the different flow speeds U. The dashed line (- -) represents the best linear fit on the averaged data (r^2 = 0.993).

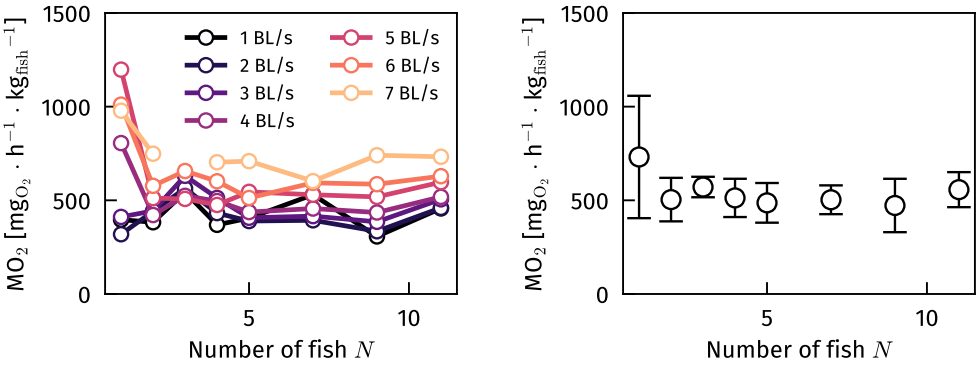

Figure B.6: Average metabolic rate MO_2 with respect to the number of fish in the school N. **left.** MO_2 for the different values of the flow speed U, color-coded. **right.** MO_2 averaged over all the different values of U. The errorbars show the standard deviation over the different U. All the data is averaged over the replicates.

alone and swimming in a group, and does not imply a decrease in COT as a function of N whatever the size of the group above 2.

Figure B.7 shows the respirometry data as a function of flow velocity U. The graph on the left confirms that at velocities U greater than 4 BL/s, the metabolic rate is much higher for N=1 than for any other number of fish (the increase is on average 75.4% for this range of flow velocities). In the graph on the right, where the data are averaged for all values of N, we find the classic U-shaped metabolism-speed curve phenomenon, previously reported in the literature (Di Santo, Kenaley, and

LAUDER, 2017), which confirms the relevance of the experiments carried out here. Indeed, a MO_2 curve as a function of speed is expected to have a quadratic shape, with a minimum reached at a positive speed, known as the optimum speed (speed at which the COT is minimal). Here we obtain an optimal swimming speed of 2 BL/s.

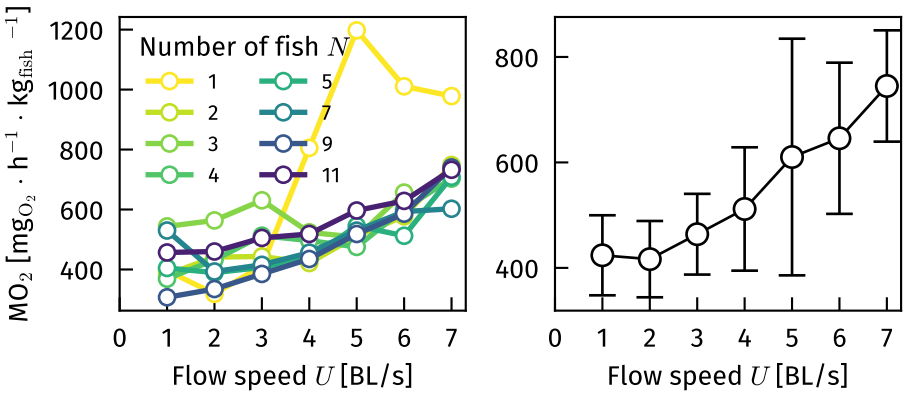

Figure B.7: Metabolism-speed curves: metabolic rate MO_2 with respect to flow speed U. **left.** MO_2 for the different values of the number of fish N, color-coded. **right.** MO_2 averaged over all the different values of N. The errorbars show the standard deviation over the different N. All the data is averaged over the replicates.

B.3 CONCLUSIONS AND PERSPECTIVES

In this appendix, a respirometry technique was used to measure the energetic cost of transport of groups of fish subjected to a flow, for different numbers of fish in the school. It was observed that this COT does not seem to be influenced by N, with the exception of the specific case of a fish swimming alone $N = 1$, which appears to have a higher COT than fish swimming in a group, whatever the number of fish in the group. These results are consistent with those reported for *Hemigrammus rhodostomus* (ASHRAF et al., 2017). Two hypotheses can be made to explain them: (1) there is a mechanism of interaction between individuals in a school, for example via the harvesting of vortices, in accordance with the Weihs hypothesis (WEIHS, 1973). However, this hypothesis should lead to a decrease in COT, not just for $N = 1$ compared with $N \leq 2$, but a decrease that becomes more significant as N increases, since more fish are interacting. (2) It is possible that the solitary swimming situation creates a stress response in the isolated individual, which would explain the increase in its metabolic rate.

In view of the dispersion of the measurement points for $N = 1$, the complexity of the measurements, the inherent noise associated with them and the limited

number of replicates carried out, it is however complicated to draw definitive conclusions. More experiments would be useful, as well as kinematic measurements of individuals in the school, which would make it possible to quantify both indirect markers of energy expenditure (tailbeat frequency and amplitude) and distances and organisation within the school. In this way, we would be more able to assess whether interactions between individuals do indeed lead to energy savings, and in which cases.

GENERAL SUMMARY

KEYWORDS Collective motion, fish schooling, confinement, sensory mechanisms, rheotaxis

This thesis is focused on collective motions in schools of fish. In particular, we attempted to shed light on how variations in environmental parameters can influence interactions between individuals within a group, and consequently the organisation of that group. Using simplified laboratory experiments, we varied these environmental parameters in a controlled manner and observed the motions of groups of fish in response to these perturbations. The model species chosen for these experiments is *Hemigrammus rhodostomus*, a small gregarious tropical fish.

We were able to show that light plays a major role in the emergence of collective motion: in the absence of lighting, schools of around 50 fish were unable to swim in a coordinated fashion. Conversely, as the light intensity gradually increases, the school goes through different behavioural phases, with an initially highly polarised organisation followed by a state of rotation (milling) that is stable over time above a light level threshold.

The limits of the swimming range also play a part in determining the collective state observed for a group of interacting agents. In the case of schools of 10 to 70 fish, it has been shown that reducing the available swimming area and increasing the number of fish in the school have equivalent effects: the greater the confinement (measured by the density of fish per unit area), the greater the probability of moving from a polarised state to a rotating state.

Finally, the behaviour of rheotaxis was studied, i.e. the aptitude of a fish or a group of fish to swim against the current. In particular, the ability to maintain a stable position for single fish and pairs of fish, considered as the minimum constitutive cell of a school, was measured during forced swimming experiments in a swim tunnel. The tests were repeated in illuminated and dark environments. The results suggest that flow sensing is used by fish in unlit conditions, but is not essential in lit conditions.

In summary, this research underscores the role of light and spatial constraints in shaping collective behaviors but also sheds light on the interplay between environmental factors and group dynamics in schools of fish. These insights contribute

to a deeper understanding of the mechanisms governing collective motion in complex biological systems.

RÉSUMÉ GÉNÉRAL

MOTS-CLÉS Mouvement collectif, bancs de poissons, confinement, mécanismes sensoriels, rhéotaxie

Cette thèse est consacrée à l'étude des mouvements collectifs au sein des bancs de poissons. Plus précisément, elle cherche à décrire la manière dont les variations des paramètres environnementaux peuvent influencer les interactions entre les individus au sein d'un groupe et, par conséquent, l'organisation de ce groupe. En utilisant des expériences simplifiées en laboratoire, nous avons fait varier ces paramètres environnementaux de manière contrôlée et observé les mouvements de groupes de poissons en réponse à ces perturbations. L'espèce modèle choisie pour ces expériences est *Hemigrammus rhodostomus*, un petit poisson tropical grégaire.

Nous avons pu démontrer que la lumière joue un rôle majeur dans l'émergence du mouvement collectif : en l'absence d'éclairage, des bancs d'environ 50 poissons sont incapables de nager de manière coordonnée. À l'inverse, à mesure que l'intensité lumineuse augmente progressivement, le banc passe par différentes phases comportementales, avec une organisation initialement fortement polarisée suivie d'un état de rotation (milling) stable au-dessus d'un seuil de luminosité.

Les limites de la zone de nage jouent également un rôle dans l'émergence de l'état collectif observé pour un groupe d'agents en interaction. Dans le cas de bancs de 10 à 70 poissons, nous montrons que la réduction de la surface de nage disponible et l'augmentation du nombre de poissons dans le banc ont des effets équivalents : plus le confinement est important (mesuré par la densité de poissons par unité de surface), plus la probabilité de passer d'un état polarisé à un état de rotation est élevée.

Enfin, le comportement de rhéotaxie a été étudié, c'est-à-dire l'aptitude d'un poisson ou d'un groupe de poissons à nager à contre-courant. En particulier, la capacité à maintenir une position stable pour un poisson seul et des paires de poissons, considérées comme la cellule constitutive minimale d'un banc, est mesurée lors d'expériences de nage forcée dans un canal de nage. Les tests sont répétés dans des environnements éclairés et sombres. Les résultats suggèrent que la dé-

tection de l'écoulement est utilisée par les poissons dans des conditions non éclairées, mais n'est pas essentielle dans des conditions éclairées.

En résumé, cette recherche met en lumière le rôle de la lumière et des contraintes spatiales dans la formation des comportements collectifs, mais éclaire également l'interaction entre les facteurs environnementaux et la dynamique de groupe au sein des bancs de poissons. Ces observations contribuent à une compréhension plus approfondie des mécanismes régissant le mouvement collectif dans des systèmes biologiques complexes.

C

RÉSUMÉ

Cette thèse est consacrée à l'étude des mouvements collectifs au sein des bancs de poissons. Plus précisément, elle cherche à décrire la manière dont les variations des paramètres environnementaux peuvent influencer les interactions entre les individus au sein d'un groupe et, par conséquent, l'organisation de ce groupe. En utilisant des expériences simplifiées en laboratoire, nous avons fait varier ces paramètres environnementaux de manière contrôlée et observé les mouvements de groupes de poissons en réponse à ces perturbations. L'espèce modèle choisie pour ces expériences est *Hemigrammus rhodostomus*, un petit poisson tropical. Ce poissons présente l'avantage d'être simple à élever et présente un comportement grégaire, ce qui en fait un organisme modèle de choix pour les études de mouvement collectif des poissons.

ECLAIREMENT ET NAGE COLLECTIVE

Le premier chapitre de ce travail porte sur le rôle de l'éclairement sur l'émergence des comportements collectifs dans les banc de poissons. Nous avons pu démontrer que la lumière joue un rôle majeur dans l'apparition de différents type de mouvement collectifs. Ces dernier sont quantifiés par deux paramètres d'ordre, appelés paramètre de polarisation $\mathcal{P}$ et paramètre de milling $\mathcal{M}$, définis de la manière suivante :

$$\mathcal{P} = \left\langle \left| \frac{\mathbf{v}_i}{\|\mathbf{v}_i\|} \right| \right\rangle_{i \in 1..N}$$

$$\mathcal{M} = \left\langle \left| \frac{\mathbf{r}_i \times \mathbf{v}_i}{\|\mathbf{r}_i\| \|\mathbf{v}_i\|} \right| \right\rangle_{i \in 1..N}$$

où $\mathbf{v}_i$ (resp. $\mathbf{r}_i$) est le vecteur vitesse instantané (resp. la position par rapport au centre de masse instantané du banc du i-ième poisson) (voir Figure 2.4). $\langle \cdot \rangle$ désigne l'opérateur de calcul de la moyenne sur tous les poissons du banc. Ces paramètres sont tous deux compris entre 0 et 1 et quantifient le degré d'alignement des individus du banc dans la même direction ($\mathcal{P}$) ou de rotation autour du centre de masse du groupe ($\mathcal{M}$).

Le dispositif expérimental se compose d'un grand réservoir en verre peu profond avec une zone de travail de 140 cm sur 100 cm. Cette zone est éclairée par la lumière visible produite par un vidéoprojecteur (voir Figure C.1). Ce dispositif permet de contrôler facilement l'illumination dans le réservoir, qu'elle soit constante ou variable dans le temps : des images homogènes simples de différents niveaux de gris sont projetées.

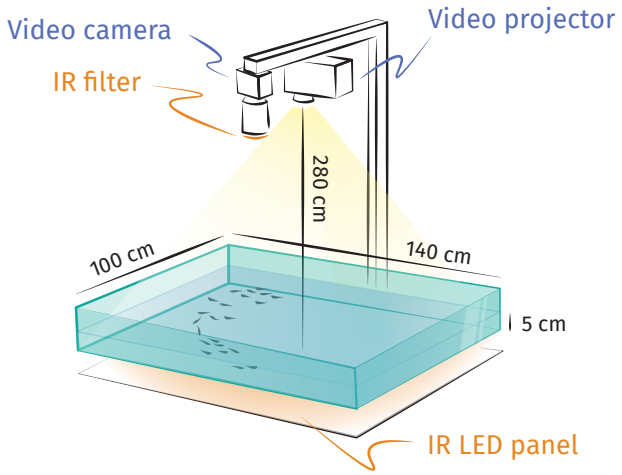

Figure C.1: Des groupes de poissons nagent librement dans un grand bassin peu profond dont le niveau de lumière peut être réglé à l'aide d'un vidéoprojecteur. L'ensemble est rétro-éclairé par un panneau LED infrarouge fabriqué sur mesure, et les trajectoires des poissons sont filmées par une caméra en surplomb.

En l'absence d'éclairage, des bancs d'environ 50 poissons sont incapables de nager de manière coordonnée. À l'inverse, à mesure que l'intensité lumineuse augmente progressivement, le banc passe par différentes phases comportementales, avec une organisation initialement fortement polarisée suivie d'un état de rotation (milling) stable au-dessus d'un seuil de luminosité (voir Figure C.2).

RÔLE DU CONFINEMENT SUR LA STABILITÉ DU MOUVEMENT COLLECTIF

Les limites de la zone de nage jouent également un rôle dans l'émergence de l'état collectif observé pour un groupe d'agents en interaction, que nous étudions dans le second chapitre. Dans le cas de bancs de 10 à 70 poissons, nous montrons que la réduction de la surface de nage disponible et l'augmentation du nombre de poissons dans le banc ont des effets équivalents : plus le confinement est important

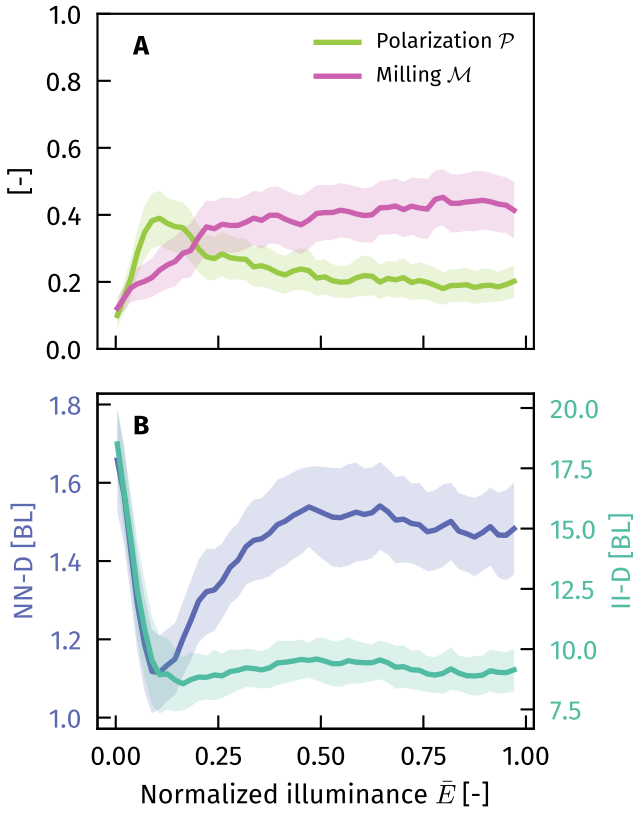

Figure C.2: Paramètres d'ordre des bancs de poissons et distances en fonction de l'intensité lumineuse. **B** Distance entre les plus proches voisins (NN-D) et distance interindividuelle (II-D) en longeur de poisson (Body Length BL). Pour un individu donné, la NN-D est la distance avec le poisson le plus proche et la II-D est la distance moyenne avec tous les autres poissons.

(mesuré par la densité de poissons par unité de surface), plus la probabilité de passer d'un état polarisé à un état de rotation est élevée (voir Figure C.3).

Nous introduisons un modèle simple basé sur un processus de Markov à deux états à l'échelle du banc, pour mieux comprendre la transition entre l'état polarisé et l'état de milling. Ici, le banc est considérée comme un système bistable. Les fonctions de densité de probabilité pour les durées des épisodes de milling et de polarisation nous permettent d'obtenir un estimation des taux α et β de transition de milling vers polarisation (et inversement) (voir Figure C.4)

RHÉOTAXIE DANS UN BANC MINIMAL

Enfin, le comportement de rhéotaxie a été étudié dans le dernier chapitre, c'est-à-dire l'aptitude d'un poisson ou d'un groupe de poissons à nager à contre-courant.

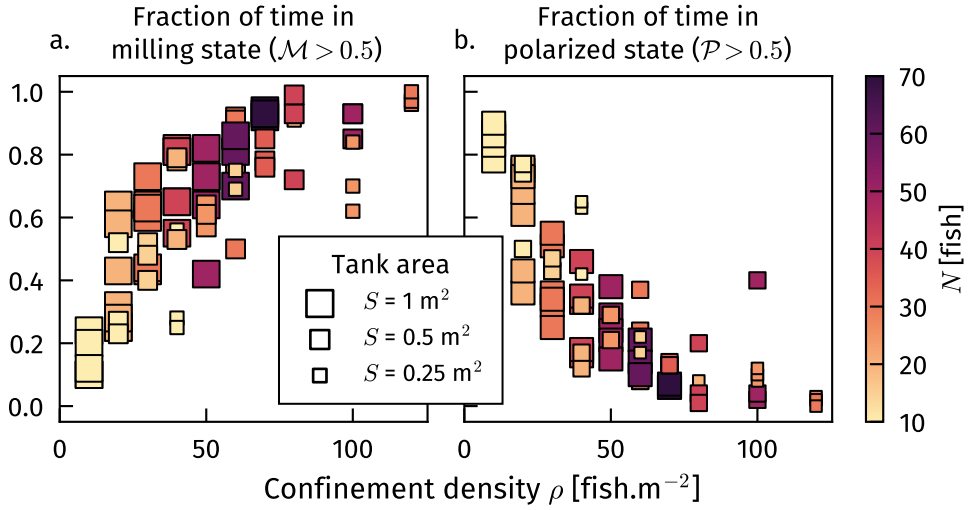

Figure C.3: Fraction du temps passé par les bancs de poissons dans l'état de milling (a.) et dans l'état polarisé (b.) sur la durée totale de l'expérience (15 min), en fonction de la densité de confinement, c'est-à-dire le nombre de poissons par unité de surface de l'aquarium en poissons/m^{-2}. La taille des marqueurs indique la surface de nage disponible, tandis que les couleurs indiquent le nombre de poissons dans le banc.

En particulier, la capacité à maintenir une position stable pour un poisson seul et des paires de poissons, considérées comme la cellule constitutive minimale d'un banc, est mesurée lors d'expériences de nage forcée dans un canal de nage, pour différentes vitesses d'écoulement (voir Figure C.5).

On mesure ici différentes grandeurs cinématiques: la précision rhéotactique ou variabilité positionnelle a, qui est l'écart-type écart-type de la distance à la position initiale lors de la nage, et la distance entre poissons pour les expériences avec deux poissons. Les tests sont répétés dans des environnements éclairés ou sombres.

On observe qu'à haute vitesse d'écoulement, les poissons seuls dans le noir sont plus précis dans leur positionnement que lorsque le canal est éclairé. En revanche, pour deux poissons, l'éclairement ne semble pas jouer de rôle sur la précision du positionnement Figure C.6.

Les résultats suggèrent que la détection de l'écoulement est utilisée par les poissons dans des conditions non éclairées, mais n'est pas essentielle dans des conditions éclairées.

En résumé, cette recherche met en lumière le rôle de la lumière et des contraintes spatiales dans la formation des comportements collectifs, mais éclaire

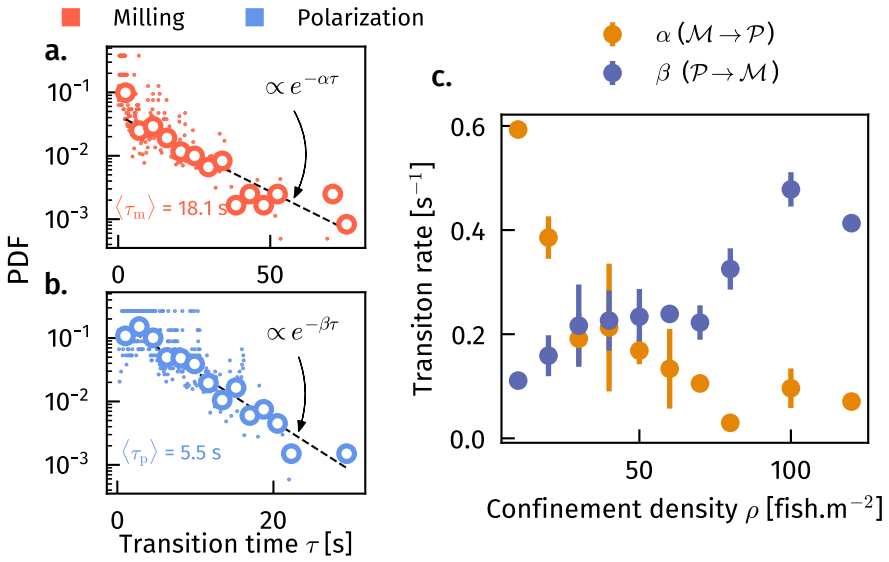

Figure C.4: Fonction de densité de probabilité de la durée de l'état de milling τ_m (**a.**) et de l'état polarisé τ_p (**b.**) pour une densité de confinement $\rho = 30$ poissons/m^2 ($N = 30$, $S = 1$ m^2, 6 réplications, 387 événements de transition). (**c.**) Taux de transition en fonction de la densité de confinement. Les barres d'erreur représentent l'écart-type sur toutes les répétitions d'expériences à une densité donnée.

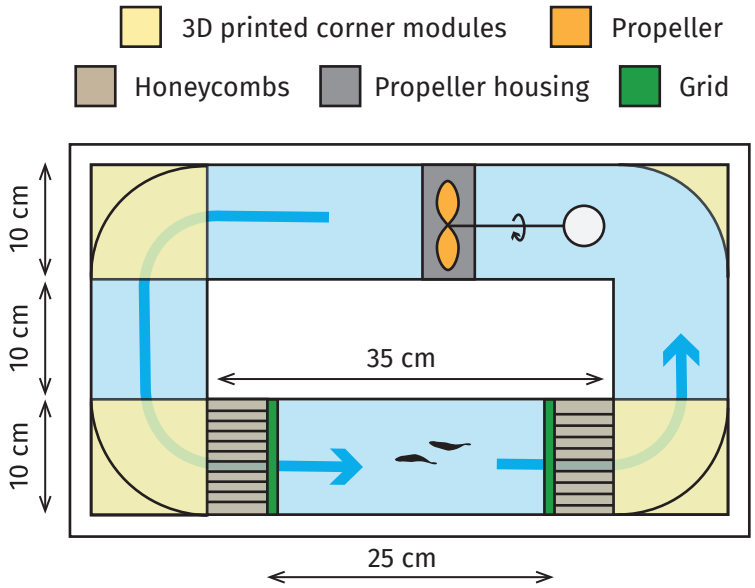

Figure C.5: Schéma du dispositif expérimental. Les flèches bleues indiquent la direction du courant d'eau.

également l'interaction entre les facteurs environnementaux et la dynamique de groupe au sein des bancs de poissons. Ces observations contribuent à une com-

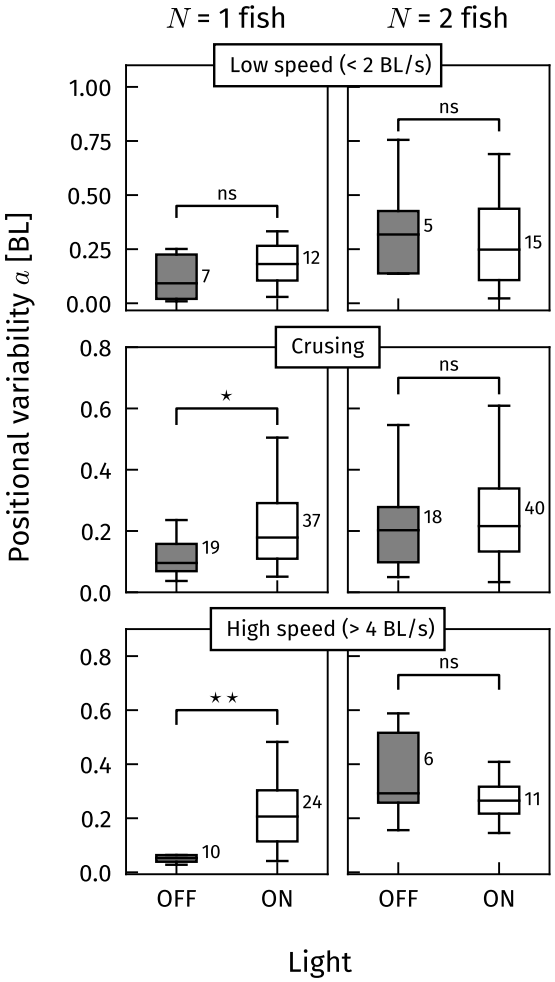

Figure C.6: Variabilité positionnelle a (écart-type de la distance à la position initiale) par rapport à l'éclairage de l'aquarium, pour trois régimes de vitesse d'écoulement différents. La colonne de gauche (resp. la colonne de droite) montre les données pour N = 1 poisson (resp. pour N = 2 poissons).

préhension plus approfondie des mécanismes régissant le mouvement collectif dans des systèmes biologiques complexes.

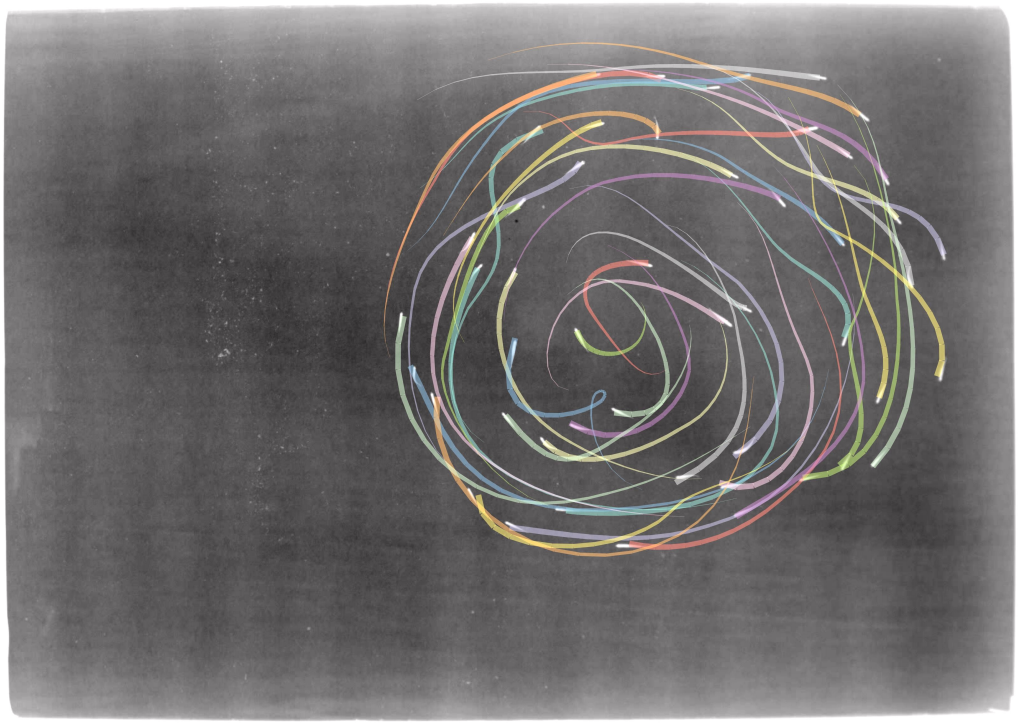

COLOPHON

ILLUSTRATIONS

- Frontpage — M.C. Escher, *Water - Strens New Year's Greeting Card (Fish)*, 1956
- Chapter 1 — The Garden of Earthly Delights (detail), 1490-1500, Hieronymus Bosch, Museo Nacional del Prado, Madrid (Espagne)
- Chapter 2 — Triptych of the Temptation of St. Anthony (detail), 1501, Hieronymus Bosch, Museu Nacional de Arte Antiga, Lisbonne (Portugal)
- Chapter 3 — Triptych of the Temptation of St. Anthony, *Ibidem*
- Chapter 4 — The Garden of Earthly Delights, *Ibidem*

This document was typeset using LaTeX and the typographical module `classicthesis` developed by André Miede `https://bitbucket.org/amiede/classicthesis/`.

Final Version as of November 27, 2023